Vrije Universiteit Brussel

FACULTY OF ENGINEERING
Departement of Electrical Engineering and Energy Technology

Performance Analysis of Pedal Electric Cycles: an Objective and Subjective Approach

Thesis submitted in fulfilment of the requirements for the award of the degree of Doctor in Engineering by

Jan Cappelle

April 2008

Promotor: prof. dr. ir. Philippe Lataire

Jury

- Prof. J. Tiberghien, chairman, Vrije Universiteit Brussel, Belgium
- Prof. R. Pintelon, vice-chairman, Vrije Universiteit Brussel, Belgium
- Prof. Ph. Lataire, advisor, Vrije Universiteit Brussel, Belgium
- Prof. J. Van Mierlo, secretary, Vrije Universiteit Brussel, Belgium
- Prof. A. Van den Bossche, UGent, Belgium
- Prof. C. Macharis, Vrije Universiteit Brussel, Belgium
- Dr. P. Van den Bossche, Erasmushogeschool, Belgium
- Dr. K. Gössel, Heinzmann GmbH, Germany
- Dr. J. De Brabanter, Katholieke Hogeschool Sint-Lieven, Belgium

Dankwoord
–Acknowledgments–

Dankwoorden bij proefschriften van doctoraten, het blijft iets curieus...
En ik begrijp steeds beter waarom. Het neerschrijven van de resultaten van jarenlang wetenschappelijk onderzoek, betekent ook het afsluiten van een periode uit het leven van een mens. Bij mij betekent dit onder andere het einde van de schizofrenie van twee werkplekken en het wegvallen van een zwaard van Damocles. Maar het doet eveneens beseffen bij hoeveel personen je in het krijt komt te staan gedurende zo'n doctoraatsperiode.
In de eerste plaats vermeld ik graag prof. Philippe Lataire, die het promotorschap van een docerende en uithuizige doctorandus op zich durfde te nemen en van wie ik hoop een beetje van zijn ongelooflijke technische bagage en zijn jongensachtige interesse in techniek te zullen blijven meedragen.
Bijzondere dank gaat uit naar wijlen prof. Gaston Maggetto, wiens gedrevenheid voor elektrische voertuigen op de EVS-congressen ook voor mij (en zelfs zonder das) veel deuren opende.
Veel dank ook aan de ETEC-juryleden professor Van Mierlo en professor Van den Bossche die ook na de (verzuilde) associatievorming in Vlaanderen alle medewerking bleven verlenen aan mijn onderzoek. De wereldwijde EVS-congressen waren dankzij hun connecties binnen de wereld van elektrische voertuigen steeds fantastische belevenissen.
Met jurylid Dr. Gössel had ik dan weer een heel inspirerend gesprek net voor het finaliseren van het onderzoek. Hem moet ik ook bijzonder danken omdat hij meermaals naar Brussel wilde afzakken om dit werk te beoordelen. Uiteraard dank ik ook de overige leden van de jury, omdat ze bereid werden gevonden dit werk naar waarde te schatten.
Bij het ontwerp en de realisatie van de testbank waren de bijdragen van Frédéric Dalle, Nico Smets, Dimitri Goethals en vooral Jean-Marc Timmermans onder de praktische supervisie van Etienne Vandenhaute onmisbaar. Voor de organisatie van de uitleendienst waren de inspanningen van Elisabeth Leloup en Francis Heymans van onschatbare waarde.
Veel dank gaat ook uit naar de collega's van het departement industrieel ingenieur

van KaHo Sint-Lieven die me de kans boden dit doctoraat te behalen. Hierbij wil ik vooral Luc Peelman bedanken voor de urenlange discussies, jurylid Jos De Brabanter voor het helpen zoeken naar een geschikte regressietechniek en Bart Huyck voor zijn bijdrage bij het loggen van de fietssnelheden. Bedankt ook aan Jean-Marc Timmermans en Wouter Vandersypen die in hun vrije tijd aan de tekst hielpen sleutelen.

Het schrijven van dit werk was echter compleet onmogelijk geweest zonder de warmte en liefde van mijn vrouw Ann, voor wie geen inspanning te veel was om dit werk op de rails te houden. En voor Douwe en Noah: jullie papa zal nu weer wat minder achter de *comtupoeter* zitten. Beloofd!

Gent, april 2008
Jan Cappelle

Table of Contents

List of Figures

List of Tables

List of Acronyms

AWD	All Wheel Drive
Ah	Ampère hours
BDC	Brushless Direct Current
BMI	Body Mass Index
BR	Battery Range
cc	cubic centimeter
CITELEC	Association of European Cities interested in Electric Vehicles
d	Distribution of a quantity
DC	direct current
DOD	Depth Of Discharge
EBD	Electronic Bike Development
EMC	ElectroMagnetic Compatibility
E-PAC	Electrically Power Assisted Cycle
ETA	Efficiency
ETEC	ElektroTEChniek en EnergieTEChniek
E-Tour	Electric Two-wheelers On Urban Roads
EU-25	European Union of 25 member states
IEEE	Institute of Electrical and Electronics Engineers
ISLENET	Network of European Island Authorities promoting sustainable energy
FLY	Swiss Flyer F6
FWD	Front Wheel Drive
GUI	Graphical User Interface
HEI	Human Energy Input
IOx	x^{th} model of the Sparta ION
LEV	Light Electric Vehicle
LS-SVM	Least Squares Support Vector Machines
m	Average value of a quantity
MAe	Low (economic) Motor Assistance
MAn	Normal Motor Assistance
MAp	High (power) Motor Assistance
MER	l'Avenir pre-scoot Merida

NiMh	Nickel Metal Hydride
NiCd	Nickel Cadmium
n.a.	Not Available
PAS	Yamaha Power Assist easy
POD	Power-On-Demand
prEN	preliminary European Norm
PVC	PolyVinyl Chloride
RBF	Radial Basic Function
RMSE	Root Mean Squared Error
rpm	rotations per minute
SA	Slope-Ability or Climbing-ability
SAx	Sachs Elo-bike touring in gear x
SubVI	Sub Virtual Instrument
TIA	Time Interval Analyser
TTL	Transistor-Transistor-Logic
UD	User-Dependent performance parameters
UI	User-Independent performance parameters
VXI	VME eXtensions for Instrumentation
XI	Assistance factor
ZA	Zero Assistance

List of Symbols

Nederlandse samenvatting
–Summary in Dutch–

De prestatieanalyse van elektrische fietsen: subjectief en objectief benaderd

1 Inleiding

Elektrische geassisteerde fietsen of pedelecs zijn relatief nieuw in het mobiliteitslandschap. Het betreft fietsen uitgerust met een elektrische hulpmotor, die enkel vermogen levert als de fietser trapt. Twee- of meerwielers met trapondersteuning worden in Europa als fiets geklasseerd als ze aan de volgende voorwaarden voldoen:
De elektrische motor heeft een nominaal continu vermogen van maximaal $250W$ *waarvan de aandrijfkracht geleidelijk vermindert en ten slotte wordt onderbroken wanneer het voertuig een snelheid van* $25km/h$ *bereikt, of eerder, indien de bestuurder ophoudt met trappen[22].*

2 Een subjectieve benadering van de prestatieanalyse

De bevindingen van een uitleendienst voor elektrische fietsen

Binnen het kader van een Europees onderszoeksproject werden vanaf november 2000 tot april 2003 door de vakgroep $ETEC$ van de *Vrije Universiteit Brussel* elektrische fietsen ter beschikking gesteld van meer dan 250 personen gedurende meerdere weken. Op die manier werden gegevens verzameld omtrent de producttevredenheid, de eisen die de klant stelt aan elektrische fietsen, het marktpotentieel,... Daaruit is vooral gebleken dat de elektrische fiets geen simpel alternatief is voor gewone fietsen, maar wel degelijk een nieuw transportmiddel dat uitstekend geschikt blijkt voor afstanden tussen de 5 en $15km$. De elektrische fiets werd door de proefpersonen zowel gebruikt voor woon-werk verkeer, als voor boodschappen en ontspanning. De meeste klachten kwamen er over het gewicht ($\pm 30kg$), de hoge kostprijs ($\pm$ €1700), de autonomie van de batterijen en de vele technische problemen met de testfietsen. De fietsinfrastructuur in Brussel (waar de meeste testpersonen vandaan kwamen) dient echter serieus te worden aangepast om het elektrisch (en conventioneel) fietsen comfortabeler te maken. Uit de testen bleek ook dat de appreciatie van elektrische fiet-

sen sterk afhangt van de plaats (stad/platteland) waar de fiets gebruikt werd en de voorgeschiedenis (al of niet frequent fietsen) van de testpersonen.

De markt voor elektrische fietsen in Vlaanderen

Aangezien 82% van de Vlamingen hun fiets koopt bij de gespecialiseerde fietshandel [29], is een bevraging van de fietsenhandelaars over hun ervaring met elektrische fietsen een goede manier om een zicht te krijgen op de Vlaamse pedelec markt. In december 2005 werd naar 468 Vlaamse fietsenhandelaars een elektronische enquête gestuurd. Iets meer dan honderd van hen waren bereid aan dit onderzoek mee te werken. Daarnaast werden ook nog eens 110 websites van fietsenhandelaars bezocht op zoek naar info over elektrisch fietsen.
Ongeveer 85% van de fietsenhandelaars in Vlaanderen biedt volgens de bevraging elektrische fietsen aan. Er blijken maar liefst 31 verschillende merken op de markt te zijn, waarvan Electronic Bike Developments, Sparta en Batavus de drie meest voorkomende merken waren in 2005. Gemiddeld gezien verkocht de fietsenhandelaar 13 pedelecs in 2005, tegenover ongeveer 400 conventionele fietsen. De prijzen voor deze fietsen variëren van €695 tot €3600. De fietsenhandelaar ziet ook de batterijradius, het grote gewicht en de hoge kost van de fietsen als de belangrijkste nadelen. Weinig van hen bleken inspanningen te doen om de elektrische fietsen actief te promoten.

3 Een objectieve benadering van de prestatieanalyse

De bouw van een testbank voor elektrische fietsen

Om een objectief beeld te krijgen van de prestaties van elektrische fietsen werd een testopstelling gebouwd aan de *Vrije Universiteit Brussel*. Deze testopstelling (zie figuur 4.3) is een verlengde loopband, aangedreven door een snelheidsgestuurde inductiemotor. Hiermee kan een snelheid opgelegd worden aan een elektrische fiets die zich op de loopband bevindt.
Op de plaats van het zadel wordt een stroomgestuurde gelijkstroommotor geplaatst. Deze motor drijft een riemschijf aan die op de pedaalas van de fiets wordt gemonteerd. Op deze manier kan een koppel worden opgedrongen ter hoogte van de pedalen. De riemschijf bevat een koppel- en snelheidsensor.
De fiets wordt verhinderd voorwaarts te bewegen door een kabel met een krachtsensor. Het meten van een elektrische fiets bestaat erin na te gaan welke trekkracht wordt ontwikkeld bij een opgelegde snelheid en een opgelegd koppel. Deze trekkracht hangt niet alleen af van de fietser (hier vervangen door de gelijkstroommotor) maar ook van de bijdrage van de assistentiemotor. Indien in elk werkingspunt 2 metingen verricht worden, één met de assistentiemotor ingeschakeld en één met de assistentiemotor uitgeschakeld, kan men door het verschil in gemeten trekkracht de bijdrage van de motor gaan kwantificeren.

Prestatieanalyse aan de hand van testbank metingen

Aan de hand van de beschreven metingen is het mogelijk om modellen te gaan maken voor het gedrag van de elektrische fiets op de testbank en op de weg.

- *Het trekkracht model* geeft de trekkracht weer in functie van de snelheid en het koppel. Indien meerdere assistentieniveaus beschikbaar zijn, kan men per fiets voor elk van deze niveaus een trekkrachtmodel opstellen.
- *Het klimcapaciteit model* geeft de maximale helling weer die de fietser kan overwinnen in functie van de snelheid en het koppel. Deze modellen zijn herschaalde versies van de vorige, maar hebben een betere fysische interpreteerbaarheid.
- *Het vereiste fietserkoppel model* geeft het koppel weer dat de fietser moet leveren om een bepaalde snelheid en een bepaalde trekkracht te ontwikkelen. Ook hier kan er per assistentieniveau een koppelmodel worden opgesteld.
- *Het rendement model* modelleert de mechanische verliezen. Het toont het rendement van de fiets in elk (niet-geassisteerd) werkingspunt in functie van snelheid en fietserkoppel.
- *Het assistentiefactor model* geeft in elk werkingspunt weer wat de verhouding is tussen de netto trekkrachtbijdrage van de elektrische motor tot de totale beschikbaar trekkracht.

Verschillende vormen van regressieanalyse werden uitgeprobeerd om deze modellen op te stellen voor het ganse werkingsgebied van de fiets, vertrekkend van een beperkt aantal testbankmetingen. De LS-SVM regressiemethode leek hiervoor uitermate geschikt.

Prestatiecurven

De prestatieanalyse kan in de eerste plaats gebeuren op basis van grafische voorstellingen van de beschreven modellen. Zo geven figuren die $3D$-oppervlakken weergeven van verschillende assistentieniveaus van de trekkracht (figuur 9.1), de klimcapaciteit (figuur 9.7) of het vereist fietserkoppel (figuur 9.4) reeds een goed beeld van het gedrag van de elektrische fiets. Door $2D$-figuren (contourplots, doorsneden bij constante snelheden of constante koppels) van deze oppervlakken te analyseren kan nog beter ingezoomd worden op de toegepaste controlestrategie.

Prestatieparameters

Naast de visuele prestatieanalyse worden ook een aantal parameters gedefinieerd die bepaalde eigenschappen van de fiets in een enkel getal proberen weer te geven. Er worden 2 soorten parameters gedefinieerd:

- **De gebruiksonafhankelijke parameters** zijn parameters die enkel bepaald worden door de elektrische fiets zelf. Hierbij horen de volgende parameters:

  - Het $100W$ *rendement* is het mechanisch rendement van de fiets uitgemiddeld over alle werkingspunten waarvoor de fietser $100W$ dient te leveren.
  - De $75W$ *assistentiefactor* is het gemiddelde van de assistentiefactor over alle werkingspunten waarvoor de fietser $75W$ dient te leveren. De assistentiefactor heeft de relatieve nettobijdrage van de motor tot het tractievermogen.
  - De $100W$ *klimcapaciteit* is het gemiddelde van de klimcapaciteit over alle werkingspunten waarvoor de fietser $100W$ dient te leveren.

- **De gebruikersafhankelijke parameters** zijn parameters die zowel door de fiets zelf worden bepaald als door de manier waarop hij gebruikt wordt door de fietser. Daarvoor dient een representatieve rit van de gebruiker opgegeven te worden. Deze rit kan eventueel gelogd worden met een zelfontworpen logsysteem. De gebruikte parameters zijn:

  - Het *rit rendement* is het mechanisch rendement van de fiets uitgemiddeld over alle werkingspunten waarin de fiets verkeert tijdens het afleggen van de vooropgestelde rit.
  - De *rit assistentiefactor* is het gemiddelde van de assistentiefactor over alle werkingspunten waarin de fiets verkeert tijdens het afleggen van de rit.
  - De *benodigde menselijke energie tijdens de rit* is de totale energie die door de fietser dient geleverd te worden voor het afleggen van de rit.
  - De *benodigde motor energie tijdens de rit* is de totale energie die geleverd wordt door de motor tijdens het afleggen van de rit.
  - De *rit batterijradius* is de afstand die met een gegeven batterij kan afgelegd worden tijdens het (meermaals) uitvoeren van de rit met de elektrische fiets.

Een grafische gebruikersinterface voor het verwerken van de testbankmetingen

Omdat het verwerken van de testbankmetingen nogal wat datamanipulaties vraagt, werd een grafische gebruikersinterface in Matlab ontwikkeld die deze manipulaties automatiseert. Deze interface bestaat uit 5 delen.

1. *Models_Creation.m* creëert vanuit de gegeven metingen alle gevraagde LS-SVM modellen en slaat ze op in een *pedelec.mat*-file.

2. *Performance_Plots.m* maakt het mogelijk om alle soorten grafische $3D$ en $2D$ voorstellingen van deze modellen op te roepen.

3. *DriveCycle.m* kan vertrekkend vanuit de gegevens van de logger van een fietsrit, een testcyclus opstellen en analyseren.

4. *Performance_Parameters.m* berekent aan de hand van de LS-SVM modellen en een testcyclus de verschillende gebruikersonafhankelijke en gebruikersafhankelijke prestatieparameters.

5. *Comparison.m* maakt een vergelijking tussen de metingen op verschillende elektrische fietsen mogelijk.

Testresultaten

Zes verschillende elektrische fietsen werden reeds op de testbank geplaatst. De metingen worden weergegeven in tabel 13.2. De beschreven prestatieanalyse slaagt erin de verschillen in controlestrategie van de constructeurs aan te tonen. Ook het prestatieverschil van de fietsen bij verschillend gebruik kan mooi in kaart worden gebracht.

English summary

Performance analysis of pedal electric cycles: a subjective and objective approach

1 Introduction

Pedelecs or Electrically Power Assist Cycles (EPACs) are a relatively new means of transportation. It are bicycles equipped with an electric motor only providing assistance. These cycles are classified as bicycles in Europe, if they meet the following specifications:
The electric motor has a maximum continuous rated power of $250W$*, of which the output is progressively reduced and finally cut off as the vehicle reaches a speed of* $25km/h$*, or sooner, if the cyclist stops pedalling [22].*

2 A subjective approach

A lending service for pedelecs

A lending service for pedelecs was organised by the group $ETEC$ of the *Vrije Universiteit Brussel* in the framework of an European research project. During the period november 2000 - april 2003 more than 250 persons tested a pedelec for several weeks. In this way a lot of information was gathered about the product satisfaction, the user's needs and the market potential of pedelecs.
One of the findings was that the electric bicycle is certainly not a simple alternative for normal bikes, but a new mobility means, especially suited for distances between 5 and $15km$. The pedelecs were used for commuting, shopping as well as leisure. Most complaints were about the weight ($\pm 30kg$), the high purchase price ($\pm$ €1700), the battery range and the many technical problems with the testbikes. The cycling infrastructure in Brussels (where most of the test persons lived) has to be improved seriously to make (electric) cycling more attractive. Moreover the apprecation of pedelecs was highly dependent on the region (city/countryside) and the cycling history of their user.

The pedelec market in Flanders

More than 80% of the Flemish bicycle consumers buy their bicycles in specialized dealer shops [29]. An inquiry for those bicycle dealers might give a good insight in the Flemish pedelec market. In december 2005, an electronic questionnaire was sent to 468 Flemish dealers. More than hundred of them wanted to participate in this research. Also 110 websites of Flemish dealers were checked for pedelec related information.
About 85% of the dealers are offering pedelecs. At least 31 different brands were found, of which Electronic Bike Development, Sparta and Batavus were most frequently found in 2005. An average dealer sold 13 pedelecs and about 400 conventional bicycles during 2005. Prices of pedelecs are varying from €695 until €3600. Also the dealers mentioned the battery range, the weight and the high purchase price as the more important disadvantages. Few of the dealers were actively promoting the electric bicycle.

3 An objective approach

The development of a test bench for pedelecs

The objective performance of a pedelec is analysed by means of test bench designed and constructed at the *Vrije Universiteit Brussel*. This test bench (figure 4.3) is an extended treadmill, driven by a speed-controlled induction machine. In this way, a speed may be imposed to a bicycle that is situated on the treadmill.
A current-controlled DC-machine is used as a 'dummy cyclist' and is placed at the place of the saddle. This motor drives the pedal axis via a belt and pulley system. So, a torque can be imposed to the pedal axis. At the pedal axis there is also a speed and torque sensor installed.
The pedelec is kept from forward motion by a cable with a load cell. Measuring the traction force on this load cell for different speeds and (dummy) cyclist's torques is an interesting tool to analyse the pedelec's performance. After all, the traction force does not only depend on the cyclist's efforts, but also on the added motor power from the assistance motor. With the difference in traction force in measurements with and without this assistance motor, for the same speed and cyclist torque, one can quantify the contribution of the motor power to the traction power.

Performance analysis

From the above mentioned measurements, different models are made to analyse the behaviour of the pedelec on the test bench.

- *The traction force model* gives the traction force as a function of speed and cyclist torque. If more than one assistance level for the pedelec is available, one can make a traction force model for all these assistance levels.

- *The climbing-ability model* gives the maximum slope that can be overcome at a certain speed and cyclist torque. These models are rescaled versions of the former ones, but have a better understandable physical interpretation.
- *The required cyclist torque model* gives the cyclist torque that is required to get a certain speed and to realise a certain traction force. Also in this case, one model per assistance level is required.
- *The efficiency model* shows the efficiency of the bicycle transmission in every (non-assisted) point of operation as a function of speed and cyclist torque.
- *The assistance factor model* shows the relation between the net motor contribution to the traction force and the total available traction force.

Different ways for regression modelling were tried out, to model the behaviour of the pedelec over the whole operation area, starting from a limited number of test bench measurements. The LS-SVM regression method seemed to be very well suited for this work.

The performance plots

The performance analysis may be based in the first place on graphical representations of the described models. So, $3D$-plots of the different assistance levels of the traction force (figure 9.1), the climbing-ability (figure 9.7) or the required cyclist torque (figure 9.4) already gives a good idea of the behaviour of the pedelec. By analyzing $2D$-plots like contourplots, and slices of constant speed and torque, the control strategy can be studied in more detail.

The performance parameters

Next to the visual performance analysis, also some parameters are defined to catch different qualities of the pedelecs in a single value. Two groups of parameters are used:

- **The user independent parameters** are parameters that are only determined by the pedelec itself. There are three different ones defined:
  - The $100W$ *efficiency* is the mechanical efficiency of the bicycle, averaged out over all points of operation where the required power input of the cyclist is $100W$.
  - The $75W$ *assistance factor* is the average of the assistance factor over all points of operation where the required power input of the cyclist is $75W$. The assistance factor gives the relative net contribution of the motor to the traction power.

  - The $100W$ *climbing-ability* is the average of the climbing-abilities over all points of operation where the required power input of the cyclist is $100W$.

- **The user-independent parameters** are parameters that are determined by the pedelec itself as well as by the way it is used by the cyclist. Therefore a representative drive cycle of the user is required. This cycle may be obtained by a developed speed log system. The applied parameters are:

  - The *drive cycle efficiency* is the mechanical efficiency of the bicycle, averaged out over all points of operation of the bicycle during the postulated drive cycle.
  - The *drive cycle assistance factor* is the average of the assistance factor over all points of operation of the pedelec during the drive cycle.
  - The *human energy need during the drive cycle* is the total amount of energy that has to be delivered by the cyclist during the drive cycle.
  - The *motor energy need during the drive cycle* is the total amount of energy that is delivered by the motor during the drive cycle.
  - The *drive cycle battery range* is the distance that can be covered with a given battery while (multiple) executing the drive cycle with the pedelec.

A graphical user interface for the test bench measurements

Because the data processing of the test bench measurements requires a lot of manipulations, a graphical user interface is developed to automate these manipulations. This interface consists in 5 different parts

1. *Models_Creation.m* creates all defined LS-SVM models starting from a given pedelec measurement set. These models are saved as a *pedelec.mat*-file.

2. *Performance_Plots.m* enables the visualisation of all kinds of $3D$ and $2D$ plots of these models.

3. *DriveCycle.m* starts from the measurements of the logger to create and analyse a drive cycle.

4. *Performance_Parameters.m* calculates the defined user-dependent and user-independent performance parameters for a given pedelec and a given drive cycle.

5. *Comparison.m* compares the performance parameters of different pedelecs.

Test results

Six different pedelecs were already tested with the test bench. The measurement results are given in table 13.2. The applied performance analysis uncovers the different control strategies of the manufacturers. Also the performance difference of the pedelecs by a different way of use is well charted.

0

Introduction

0.1 Introduction

Mobility is an important factor for the sense of well-being of people: A European citizen covers a distance of about 14000km a year. 73% of this distance is covered by car [1]. This fact and the increase of cars in the EU-25 to an average of 472 cars per 1000 inhabitants in 2004 prove that the car is commonly seen as the favorite means of transport [2]. However, in the last decennia the drawbacks of this succes were becoming clearer and are bringing a growing consciousness of the need for a diverser and cleaner mobility.

The conventional bicycle could be a solution for a number of these drawbacks. It has been an efficient means of transport well appreciated for short distances but the limitation of the human power might have been a restriction to massive daily use. People have been trying to overcome this power limitation in different ways. One of the solutions is to equip the bicycle with an electric motor.

Electrical bicycles are already widely available in today's market. They appear in many different forms and their motors are controlled in many different ways. The 'Electrically Power Assisted Cycle' (E-PACs) or 'PEDal ELEctric Cycle' (pedelecs) seems to be one of the most suitable concepts for the European countries. Pedelecs are bicycles equipped with an electrical motor that only assists when the cyclist is pedalling. The market potential of these pedelecs and their technical performances will be investigated in this work.

0.2 Outline

This book is divided in two major parts: the findings of a market analysis for pedelecs in Flanders and the description of an objective method to analyse the performance of a pedelec.
These two parts are preceded by an introduction on electric bicycles. *Chapter 1* starts with a justification for the adding of motor power to a human powered vehicle, followed by a brief history of the electric bicycle, the name giving of electric bicycles and the different ways that are used to classify them. The technical working principle of and the legislation for pedelecs conclude the introduction.
Part I of this book explains how the subjective performance of pedelecs is analysed by a double market research: the point of view of the pedelec users as well as the bicycle dealers are investigated. *Chapter 2* reports about the experiences of a lending service for pedelecs and shows the daily user's appreciation. The pedelec market in Flanders is outlined in *Chapter 3* by means of information that is received from the bicycle dealers.
Part II reports about the development of a test method to characterize, in an objective way, the performance of pedelecs. A general description of what is meant by performance analysis is given in *Chapter 4*. *Chapter 5* describes the design and realisation of the test application required for the intended performance analysis. The way this testbench is used and the measurements that are taken are given in *Chapter 6*. The testbench measurements are used to create models that describe the behaviour of the pedelec. Therefore the non-parametric LS-SVM regression analysis is used. This method is explained in *Chapter 7*. The different regression models that are used to analyse the pedelec's performance are given in *Chapter 8*. The performance analysis itself is based on the creation of a number of performance plots (*Chapter 9*) as well as the calculation of a number of performance parameters (*Chapter 10*). The discussion about a standard drive cycle for the testing of pedelecs is started in *Chapter 11*. Because the complete performance analysis of a pedelec requires a lot of measurement data manipulation, *Chapter 12* presents a handy graphical user interface to automate these manipulations. The results of the performance analysis of different pedelecs are discussed in *Chapter 13*. Finally, part II is ended by some suggestions for further research in *Chapter 15*.

1 Electric Bicycles

1.1 The electric bicycle concept

For ages people have been looking for a way to amplify or replace the human force for their displacements. This research yielded a large variety of means of transport: steps, roller skates, (recumbent) bicycles, segways, motorbikes, cars, airplanes,..., and also electric bicycles. Each of these are developed in many different appearances, for many different aims, but none of them has been able to replace all the others. Also the addition of an electric motor to a conventional bicycle will not lead to the perfect means of transportation. The introduction of the electric bicycle might even surprise people. Why should one keep on searching for an adaptation of a vehicle that is (partly) propelled by human force while there are completely autonomous vehicles available?
Today, the benefits of cycling (as well for the cyclist as for the society) are sufficiently known [3]:

- cycling is a flexible way of moving, perfectly suited for a city environment
- considering the purchase price and the ease of use, it is suited for a wide range of people
- there is no insurance or driving license required
- cycling does not produce noise
- cycling does not pollute the air
- cycling keeps the cyclist in good physical condition
- ...

Although many people are convinced of these benefits, still too many reasons can be found for keeping away from cycling (see section 2.4). The human power limit is

certainly one of them. The combination of human and external power may erase this excuse and might result in an interesting hybrid means of transportation. In this way the cyclist gets the choice to cycle faster with the same effort or to reach the same speed with less effort.

1.2 The history of electric bicycles

Figure 1.1: Steam bicycle from Michaux/Perraux[4].

The principle of the electric bicycle is not very new. Its history is closely related to that of the conventional bicycle and the motorcycle.
The principle of today's conventional bicycles (the so-called 'pneumatic tired safety bikes') dates from the 1890's[5]. Before Gottlieb Daimler builds the first motorcycle in 1885, there are already some experiments with a hybrid drive for bicycles. One of them is the steam bicycle from Michaux/Perraux that is shown in figure 1.1. Although this hybrid bicycle is rather a step towards the fully motorized motorcycle than a considered choice, it might be seen as the first 'power-assisted' bicycle.
In the next decades the will to get rid of the pedals dominates the research. The reasons for the presence of pedals in the models with combustion engine only have to be looked for in the still imperfect technology of the engines in those days: people still want to be able to cycle home when the engine fails (A fear that is also recognized by today's potential pedelec buyers as shown in chapter 2). Because the early day's combustion engines present some danger for the cyclist, many applications are submitted to patent bicycles with an electric motor. In some cases the electric motor has to be started by a second person controlling the starting resistors.
In the early 1900's, the improved combustion technology eclipses the electric alternative. The only feats worth mentioning before the second world war are the electric bicycle developed by a subsidiary of Philips and the development of the first rear wheel hub motor with possibility of recuperation braking in England [6].
The years after the second world war are characterised by the research in the 'auto'-mobile technology. Bicycles in general are degraded to the transportation of the poorer people. This is seized by the French constructor of carburetors 'Vélosolex S.I.F.A.C'. They develop a popular assisted bicycle with a small combustion engine

driving the front wheel with a friction roller that is presented in figure 1.2 [7].[1]

Figure 1.2: The solex combustion assisted bicycle with friction wheel

In 1985 the Dutch cycle manufacturer Sparta develops the 'Spartamet', a bicycle with an auxiliary $30cc$ combustion hub motor from the German motor manufacturer Sachs [8]. Today this bicycle is still available as the 'Saxonette'.
The electrically assisted bicycle or pedelec as it is known today dates from the late 80's. The first one is called Rivolt, but is not really successful because of the many technical imperfections. Yamaha comes in 1995 with the PAS system, which is seen as the first sales success for pedelecs [9]. These PAS bicycles are especially promoted as bicycles for people having problems to ride a common bicycle. Ever since plenty of bicycle manufacturers come out with their own electric version (see 3.2). Nowadays the image of 'bicycle for disabled persons' is never far away. But the younger designs (e.g. hidden motor and battery) and lighter models of the last years may people make aware that there might be a difference between 'reducing the human effort' and 'amplifying the human force'. However, the legal limits for this amplification are discussed in section 1.5. Today, all bicycle sales are raising [10],[11]. The electric assisted bicycles are following this trend[12].

1.3 Classification of electric two-wheelers

Nowadays a lot of names are circulating to describe electric vehicles. In the case of small vehicles the term LEV (Light Electric Vehicles) is often used. Electric two-wheelers are a subcategory of the LEVs, but their naming is not always unambiguous. A two-wheeler is called 'electric' from the moment it is equipped with an electrical motor. But there are many ways to use the motor in the drive system. The classification of electric two-wheelers can be based on different criteria. The most commonly used classification criteria are illustrated in this section.

[1] In 2005 the french firm Mopex restart the production under the brand name Black 'n roll proving that assisted two-wheelers have market potential.

1.3.1 The relationship between motor power and human power

Electric two-wheelers may be propelled by human as well as electric power. The possibility of riding without pedalling is an often used classification criterion by legislators[13].

Light Electric Scooters

Light Electric Scooters are two-wheelers with an electric drive system: an electric motor supplied by a (rechargeable) battery delivers all the traction. The amount of power is controlled by a twist-grip. There is no possibility to add human power by pedalling. These scooters are mainly popular in the USA and the Asian countries, but also have growing sales numbers in the EU. They come in two general types:

- Light Stand Up Scooters carry the rider standing upon a deck.
- Light Sit Down Scooters have a seat for the rider.

E-bikes

E-bikes are electric two-wheelers equipped with an electric motor drive and pedals. The amount of motor power is more or less independently adjustable from the human power input. There is so-called power-on-demand (POD) without pedalling available by using a kind of twist-grip.
In Europe, the legislator classifies these vehicles as mopeds, because they are able to drive without human power (see section 1.5).

Pedelecs

Pedelecs or Pedal Electric Cycles (also called Electrically Power Assisted Bicycles, E-PACs, E-PABS, Power Assists, PABs...) also have an electric motor, but the delivered motor power depends on the cyclist's effort. If the cyclist does not pedal, the motor will not assist. The electric drive automatically provides additional power while pedalling. The amount of motor power depends on the measurements of one or more sensors, the control strategy and the behaviour of the pedelec system itself. The performance analysis in this book is focussed on this type of electric two-wheelers. They will be referred to as 'pedelecs' in the rest of the text.
If their rated motor power is limited at 250W and the maximum assisted speed stays beneath 25 km/h, the European law still classifies them as bicycles. This has the advantage of being free of driving license and insurance. In most member states even a helmet is not mandatory.

1.3.2 The ease of assembly

One can also classify electric bikes according to their ease of assembly. Next to the ready-made electric two-wheelers also electric 'power kits' are available. These

kits can be mounted on conventional bikes to give them additional motor power. The cheapest ones are equipped with a motor with a friction roller unit that can drive the front or rear wheel, but also hub motor types are available (BionX, E-motor,Heinzmann,...). Both power-assist and power-on-demand operation are available on the market.

1.3.3 The location of the motor

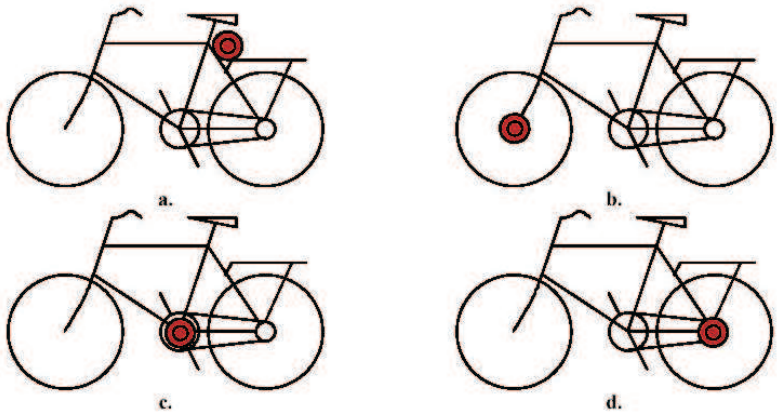

Figure 1.3: Applied mounting places for the electric motor

Another distinction can be made by the location of the motor. Four possibilities will be considered.

- The mounting of the motor *on the carrier* (figure 1.3a) behind the saddle initially seemed a cheap solution, but has proofed impractical. Only prototypes and self-built examples were found in this configuration.

- Introducing *Front wheel* traction (FWD) is another possibility (figure 1.3b). Some mountainbike manufacturers state the advantages of the introduction of a front wheel drive for bicycles: the cyclist should have a greater control over wet roots and slippery rocks and it would be easier to climb slopes[14]. It may be one of the easiest options for the implementation of power kits because the front wheel is free of brackets and gear apparatus. Although the common cyclist may experience this as a less comfortable for driving.

- *Rear wheel hub motors* easily fit on existing frames and platforms (figure 1.3d). They use a space that is otherwise not used and reduce the visibility of the auxiliary device. This explains why there seems to be a nearly universal intuitive acceptance of hub motors by consumers[15].

- Another often used location for the motor is near *the bottom bracket* (figure 1.3c). The space at this location is rather limited, so ingenious mechanical constructions have been developed. This motor location increases the stability of the bicycle because the center of mass is moved to the middle of the bicycle. Also the flexibility is better because the gear shifting is available for both motor and cyclist power. However, there are also some disadvantages for this configuration. A small amount of motor power is already lost in the transmission of the bicycle and there is more chain and sprocket wear required.

1.4 The pedelec working principle

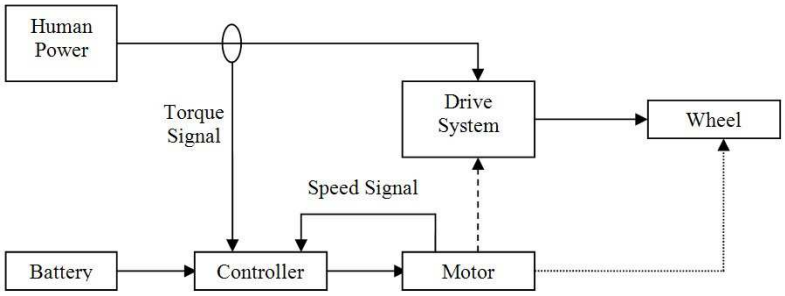

Figure 1.4: The pedelec working principle

The pedelec is an electric two-wheeler with a hybrid drive system. Its working principle is shown in figure 1.4. The traction is partly coming from the *human power* input and partly coming from an electric *motor*. The most popular motor type for pedelecs is the brushless DC motor. The motor may be directly (dotted line) or indirectly (dashed line) driving the wheel. The motor is supplied by rechargeable *batteries*. Lead-Acid, Lithium-Ion, NiMh and NiCd are commonly used battery types for pedelecs.
The amount of motor power is continuously determined by a *controller*. The controller output is based on the measurement signals of a *speed and/or torque sensor*. Sometimes (not on the figure) the cyclist has the opportunity to influence the controller output (and thus the motor power output) by switching between different assistance levels. There is often a built-in protection against motor overheating that is also steered by the controller. Another task of the controller is to organise the (intelligent) recharging of the batteries.
This book will proof that the behaviour of the controller influences the performance as well as the appreciation of the pedelec to a large extent.

1.5 Legislation

The ease of use and market potential of a pedelec are quite influenced by the way they are treated by the legislator. If they are classified as motorcycles, a helmet, driving license and insurance are obliged in most countries. If they are seen as bicycles (some of) these conditions may be called off. In this section the evolution of and the current EU regulations specifically concerning pedelecs are considered. Conventional bicycle standards or pure electric motorcycle standards are discussed in reference [17]. For legislation in other countries references [18] and [19] might help.

1.5.1 EU Directive 92/61/EEC

In 1992, the EU comes out with directive [2] 92/61/EEC that applies to 'all two or three-wheel motor vehicles, twin-wheeled or otherwise, intended to travel on the road, and to the components or separate technical units of such vehicles' [16]. This directive did not mention E-PACs or pedelecs. Motor vehicles were supposed to have a combustion engine. Only for the light quadricycles, the possibility of an electric motor was discussed. It is important to notice that a directive is binding on the Member States as regards the objective to be achieved but leaves it to the national authorities to decide on how the agreed Community objective is to be incorporated into their domestic legal systems [20].
This freedom results in different interpretations in the member states.

1.5.2 EU Member states regulations until November 9th, 2003

In anticipation of a stricter EU regulation, every member state creates his own regulation/toleration concerning pedelecs. Differences are found in vehicle classification, maximum rated motor power, assisted speed limit, helmet and insurances obligations and age limits. Table 1.1 sums up the regulations of most EU member states that were applicable until November 9^{th}, 2003.

1.5.3 EU Directive 2002/24/EC

A new proposition concerning pedelecs is submitted in 1999 into the Council of Europe and the European Parliament[21]: The European Commission makes an agreement to exclude pedelecs up to 250 W and 25 km/h from type approval. The European Parliament and the Council have released the EU-Directive 2002/24/EC [22] concerning this type approval for two and three wheeled vehicles on March 18, 2002. This EU-Directive replaces the former 92/61/EEC Directive. In article 1 (h) one can read that 'cycles with pedal assistance which are equipped with an auxiliary electric

[2] The EC/Euratom directive, expressed by the EU council, is in the EU the most important legislative instrument alongside the regulation. The idea is to remove contradictions and conflicts between national laws and regulations or gradually iron out inconsistencies so that, as far as possible, the same material conditions obtain in all the Member States.

Country	Legal status	Type approval	Speed limit	Motor limit	In-surance	Helmet	Age Limit
Austria	bicycle	no	25 km/h	n.a.	no	no	no
Belgium	bicycle	no	no	300 W	no	no	no
Denmark	bicycle	no	25 km/h	250 W	no	no	no
Finland	bicycle	no	25 km/h	250 W	no	no	no
France	bicycle	no	25 km/h	500 W	no	no	no
Germany	bicycle	no	24 km/h	250 W	no	no	no
Holland	bicycle	no	25 km/h	250 W	yes	no	no
Ireland	moped	yes	n.a.	n.a.	n.a.	n.a.	n.a.
Italy	bicycle	no	no	no	no	no	no
Luxembourg	bicycle	no	no	no	no	no	no
Spain	bicycle	no	25 km/h	500 W	no	no	no
Sweden	moped	yes	30 km/h	no	yes	yes	15
UK	bicycle	bicycle	15 mph	200 W	no	no	14

Table 1.1: Legislation of EU member states regarding pedelecs before November 2003[23]

motor having a maximum continuous rated power of 0,25 kW, of which the output is progressively reduced and finally cut off as the vehicle reaches a speed of 25 km/h, or sooner, if the cyclist stops pedalling' are excluded from type approval.
One should note however that the directive text specifies this power as a 'continuous rated power' and not as a 'peak power'[21]. It could thus be acceptable to have a higher peak power level during limited time (e.g. during acceleration). A reference has to be made to standards describing how this rating of an electric motor is to be defined and measured (see table 1.2).
Pedelecs that exceed the technical specifications must have a type approval and are classified as 'mopeds' and must consequently meet all additional laws, i.e. motorcycle helmet, adequate brakes, mirrors, insurance, they will not be allowed in reverse one way directions in cities etc. These additional features might be seen as a barrier for a real breakthrough because it might weaken the advantages of pedelecs on conventional bicycles. Although the market study (chapter 3) shows that so far neither users nor dealers are really concerned about speed.
Moreover some pedelec manufacturers (BionX, Swizzbee,...) made a simple compromise by introducing the 'fast pedelec' as a 'low-performance moped'[24]. These are mopeds with pedals, with an auxiliary motor power not exceeding 1 kW and a maximum design speed not exceeding 25 km/h. Low-Performance Mopeds are subordinate to the European category 'Mopeds' (maximum speed 45 km/h), but type approval requirements are simplified or do not apply for certain components (9 exceptions out of 35 characteristics[23])
This has some interesting advantages as compensation for the extra requirements:

- the possibility of motor power without pedalling until a certain speed

- higher motor power limit: 1kW instead of 250W

The directive does not suggest any relationship between the motor and the cyclist's power, except that motor power has to disappear when the cyclist stops pedalling. This possibility is handely used by manufacturers (e.g. the Estelle pedelecs by Heinzmann) to introduce a pedelec with twist-grip. The motor power is determined by the user on condition that the pedals are turning. In some cases, motor power without pedalling may be tolerated beneath 6 km/h.

1.5.4 Preliminary European Standard prEN15194

The European Committee for Electrotechnical Standardisation CENELEC proposes in 2005 a draft for a pedelec standard.
'The prEN15194 European Standard gives requirements for electric power assisted cycles, and has been developed in response to demand throughout Europe. Its aim is to provide a standard for the assessment of electrically powered cycles of a type which are excluded from type approval by Directive 2002/24/EC' [25].

Aspect	Standard(s) and Directive(s)
The electrical circuit	ISO 2575, IEC 60227-1, IEC 60245-1
The batteries	EN 50272-3, EN 61429
The charger	EN 55011, EN 61000-3-2, EN 61000-4-2, EN 61000-4-3, ENV 50204, EN 61000-4-4, EN 61000-4-5, EN 61000-4-6, EN 61000-4-11
The brakes	pr EN 14764
EMC	emission directive 89/336/EC, Annex C (see 1.5.4), immunity directive 89/336/EC
Measuring Continuous Rated Power	EN 60034-1, clause 3.2.1 Duty type S1

Table 1.2: Related standards for different pedelec aspects[25]

For many aspects the draft standard refers to existing standards. Table 1.2 gives an overview of these related standards.

A lot of requirements that are mentioned in the preliminary European standard are only meaningful for electrically assisted bicycles. They are listed below per pedelec aspect.

- *Motor power*
  - Assistance is provided only when the cyclist pedals forward

  - Assistance is cut off when the cyclist stops pedalling forward such that the cut off distance does not exceed 5 m with brake lever cut off switch or 2m without brake lever cut off switch.
  - The output or assistance is progressively reduced and finally cut off as the vehicle reaches the maximum assistance speed as designed.

- *EMC*
  In Annex C of the prEN 15194 radiation limits and field strengths limits are defined to assure electromagnetic compatibility of two pedelecs and electrical/electronic sub-assemblies. In the scope of the lending service of section 2, a complaint is received about EMC problems with police communication infrastructure. In appendix A the result of an EMC measurement to examine the susceptibility of this complaint is included.

- *Electrical hazard*
  Due to the limitation of the voltage to 48V, there are no special requirements applicable to the pedelec about protection against electrical hazards. When the battery charger is a part of the bicycle, the pedelec may be connected to the higher grid voltage

- *Maximum speed*
  The maximum speed for which the electric motor gives assistance may differ by $\pm$ 5% from the values specified by the manufacturer. During a production conformity check, the maximum speed may differ by $\pm$ 10% from the above-mentioned determined value.

- *Labelling*
  Each pedelec has to be visibly and durably marked with the requirements of PrEN14764 and a special label with 'EPAC, according to EN15194, cut off speed, and continuous rated power'.

- *Instruction for use*
  In addition to the instruction required by the bicycles standard EN 15194, each pedelec shall be provided with a set of instructions containing

  - the concept and a description of the electric assistance
  - a recommendation for washing
  - the maximum range as determined according to the EN15194
  - the control and indicators
  - specific pedelec recommendations for use
  - specific pedelec warnings
  - recommendations about battery charging and charger use

Standard measuring methods to determine continuous motor power and maximum speed are also included in the prEN15194 preliminary standard.

Part I

A Subjective Approach of the Pedelec's Performance

Over 130 million bicycles are worldwide sold every year and over 10 million electric bicycles were sold in 2005[15]. This means that less and less people are surprised if one uses the words ‘electric’ and ‘bicycle’ in one sentence. Also while cycling along the side of a Flemish river, one can be surprised by the performance of some older cyclists, until it gets clear that they cycle with electrical assistance. Anyway, the pedelec starts to take its place in mobility. However, there are neither data about the exact number of pedelecs on Flemish roads, nor about the acceptation/appreciation of the cycling community (dealers and users) of these vehicles in Flanders.

In part II of this book, a scientific and objective method is developed to quantify the performance of a pedelec. Before the start of this objective performance analysis, it is interesting to get an idea of the market potential of the pedelec and the aspects that make people distinguish between good and bad pedelecs. These topics are discussed in this part I.

The intended subjective performance analysis is done by a market research that focusses on the appreciation and the acceptation of the pedelec by the cycling community. Therefore two independent inquiries are organised: one for the daily users of pedelecs and one for the bicycle dealers.

As a first step, an extended lending service with opinion poll was organised to investigate the market potential and daily use appreciation of the pedelec. In the heart of Brussels Capital-Region people could borrow a pedelec and test it during several weeks. They were asked to keep a log with trip information and pedelec experiences. Each test period was concluded with the answering of a standard questionnaire. The data and conclusions from the logs as well as the standard questionnaires are gathered in chapter 2:‘The Pedelec and its Daily User’.

A second way to get data was to send an electronic questionnaire to the dealers of bicycles. They were interrogated about their sales figures, their (good as well as bad) experiences with pedelecs, the support of the manufacturers and their opinion about the pedelec. Especially the last item may influence the market because more than 80% of the Flemish bicycles are bought in a specialized dealershop. The data and conclusions from this electronic questionnaire are given in chapter 3:‘The Pedelec Market in Flanders’.

2

The Pedelec and its Daily User

Within the framework of the European E-tour project (see section 2.1) a lending service of pedelecs was started at the *Vrije Universiteit Brussel* to get an idea of the appreciation of pedelecs by their daily users. From november 2000 until april 2003 more than 250 persons could intensively test one of five different pedelec models for an average period of 7 weeks. Together they drove over 44600 km. A standard questionnaire sounded out their experiences about the strengths and weaknesses of the tested electric two-wheeler and their view on the market potential of pedelecs. The results of this questionnaire are discussed in section 2.3. The test persons also had to fill in a log with their daily trips. In those books a lot of interesting free remarks were given. They are seperately discussed in section 2.4.

2.1 The E-Tour project

The European E-Tour (Electric Two wheelers On Urban Roads) project has been set up to demonstrate, evaluate and promote the advantages of electric two-wheelers as a substantial contribution to sustainable mobility in urban areas [21]. It was approved for funding under the Energy Program of the European Commission. The E-tour project ran from January 2000 until January 2003 and involved 7 European cities, 2 Mediterranean islands, 3 universities, the network organisations CITELEC and ISLENET and several private companies. The project was coordinated by the Public Works Department of the city of Rotterdam in the Netherlands. The major aims of E-tour were [21]:

- To demonstrate the suitability of electric two-wheelers as a practical mobility means in urban and/or other restricted areas.

- To promote these vehicles as an environmentally friendly alternative for (private) cars and scooters with an internal combustion engine.
- To evaluate the practical and technical experiences from the users
- To set up a valid evaluation methodology for the comparative assessment at local level (cities/islands) on a European scale.
- To link alternatively generated (renewable) energy sources to mobility means.
- To analyse the attainable reduction in energy use and polluting emissions.
- To gain insight in the physiological and bio-mechanical aspects of the physical impact of using an electric power assisted bike.

The contribution of this PhD to the project laid in the evaluation of pedelecs by polling their users and the development of an objective performance test for pedelecs. The first item is discussed in the next sections, the last item is discussed in part II of this book.

2.2 The objectives of the lending service

A lending service for pedelecs is organised to get insight in the pleasures and annoyances pedelec users are dealing with, if they use the pedelec for a longer period. There were already different demonstration projects for pedelecs, but the participants could only make a single test ride. The experience learned that some problems only showed up when the pedelec was used on a more frequent base.
The lending service also wants to evaluate the suitability of pedelecs as a practical mobility means in city environment.
The results of these duration tests are useful for manufacturers because they uncover a lot of sensitivities of the pedelec's daily user. The results also delivers input for the objective performance analysis of part II.
However, because of practical reasons, the sample size of the test population was limited to 244. According to the formula of Cochran [35], for a 95% confidence level, the level of precision for this sample size is 6.4%. The results in this chapter should be interpreted according to this sampling error.
Remark that the statistical sample of the test population is somehow biased because only volunteers that were interested in electric bicycles took effort to participate. So, the test results could not be used to to sketch the market potential. The market is sketched by means of the investigation of chapter 3.

2.3 The standard questionnaire

When a person decided to test one of the pedelecs of the lending service, he was asked after the test period to fill in a standard questionnaire including questions on 10 pedelec topics. The complete questionnaire is given in appendix B. The answers are collected and discussed in the following subsections.

2.3.1 The pedelecs of the lending service

Type/ Brand	bicycles [#]	Tests [#]	Weight [kg]	Motor Type	Battery Type
Yamaha Pas MBK Axion	8 2	76	28	pedal axis DC 24V 235W	NiCd/NiMh 24V 5/7Ah
Yamaha Easy MBK Fizz	2 9	72	27	pedal axis DC 24V 235W	NiMh 24V 7Ah
Sachs Elo-bike	10	50	31	Hub DC 24V 300W	NiCd 24V 7Ah
Merida Prescoot	10	29	29	Pedal axis	Lead acid $2 \times 12V$ 9Ah
Merida Stepscoot	1	4	25	DC 24V 230W	NiMh 25.2V 9Ah
Flyer F6	5	12	33	Pedal axis BDC 36V 170W	NiCd/NiMh 36V 5/9Ah

Table 2.1: The pedelecs of the lending service

To start up the lending service, the ETEC research group of the *Vrije Universiteit Brussel* acquired 47 power assisted bicycles. The test persons could choose between five different power assist systems. They are all mentioned in table 2.1 with their most important characteristics: the available number of each brand, the number of tests that were performed per pedelec type, the weight, the mounting place of the motor, the motor power and voltage, and the battery type, voltage and capacity.

2.3.2 The test persons

The participants were mainly interested volunteers who heard about the lending project. They were equally distributed between male (#133) and female (#111). The questionnaire started with some personal data. All ages between 22 and 80 years old were represented. Their physical condition differed a lot: their body mass index (BMI) varied between 17 and 44 kg/m^2. The age and BMI distributions of all participants are given in figure 2.1. A difference is made between male and female participants. Most of the test persons used the pedelec for about one month, but the test duration was varying between 3 days and 10 months. The average test period was about 50 days.

2.3.3 The covered distance

The total distance covered by all users was 44.600 km. The histograms of figure 2.2 show the percentage of male and female test persons that cycled a certain total number of kilometers and a certain daily average. The averages mentioned in figure 2.2 show that the female test persons cycled on the average 25 km more than their

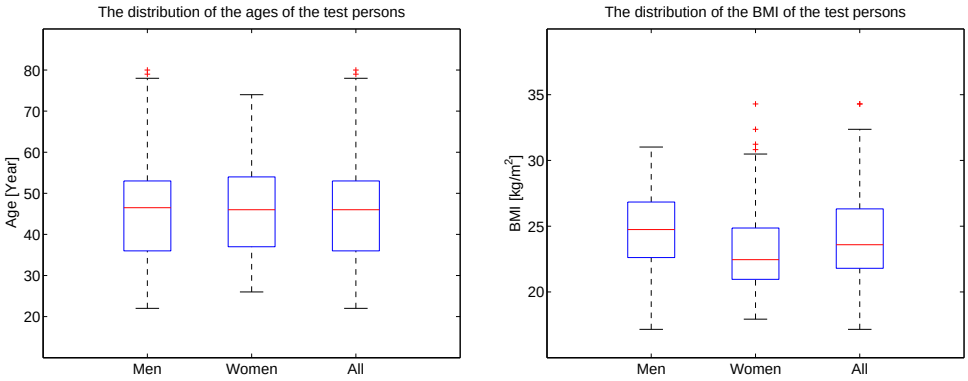

(a) Age distribution (b) BMI distribution

Figure 2.1: Boxplots of the age and BMI of the test persons

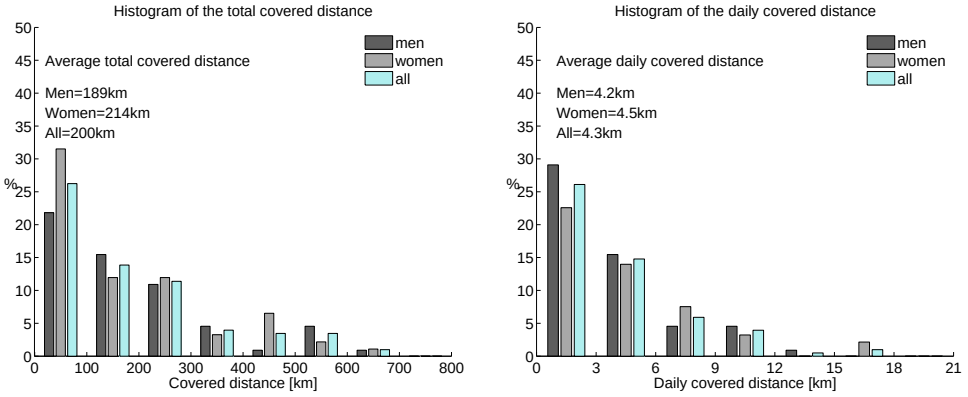

(a) Total covered distance during the test (b) Average daily covered distance during the test

Figure 2.2: Histograms of the total covered distances and the average daily covered distances

male colleagues. A possible reason can be found in figure 2.3. In this figure the percentage of test persons that were dissatisfied about the ease of use, the weight, the charging, the motor assistance level, the battery range and the overall quality of the pedelec are given seperately for men and women.

Men were more sceptical about all aspects of the pedelec. Maybe the image of an assisted bicycle is difficult to reconcile with the healthy and sporty image where men like to be identified with.

By far the most disappointing aspect is the autonomy or battery range. The dissatis-

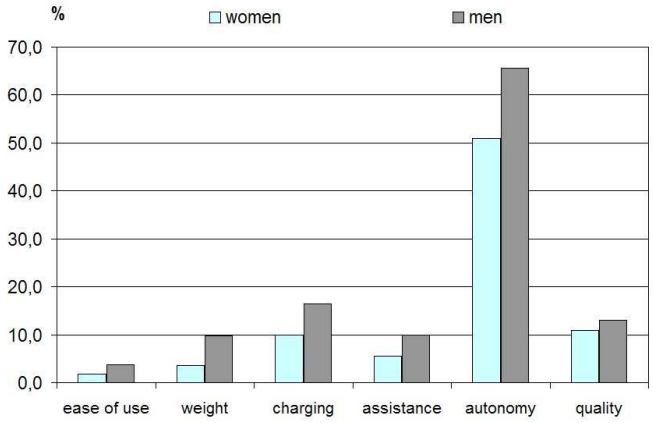

Figure 2.3: Percentage of 244 persons that are dissatisfied with different pedelec aspects

faction about the autonomy of the pedelecs is rather remarkable when looking at the short daily covered distances in table 2.2. The energy in the batteries (about 150 Wh) should be enough to drive about 20 km on a hilly circuit with 3 m/s head wind at an average speed of 13 km/h [1], while the average covered distance is only 4.3 km. However, the capacity of the batteries decreases quickly with lifetime, so the fear of ending up with an empty battery is not totally groundless.
Figure 2.4 shows how many kilometers were ridden per pedelec model. The wider boxes and the left vertical axis represent the totally covered distance by all users of one pedelec model and the smaller boxes (right vertical axis) represent the average covered distance of these users during their test period.
The first place for the Swiss Flyer in average covered distance is not really a surprise. They were seen as the upper class pedelecs of the lending service and were mainly placed at the disposal of people who were used to cycle. The low average covered distance for the Yamaha Easy may be due to the higher percentage of technical problems with this model (see figure 2.9).

2.3.4 Changes in the behaviour patterns of pedelec users

The addition of an electric auxiliary motor to a conventional bicycle has lead to a new means of transportation. These electric bicycles will take their own share of the existing trips and/or may introduce new trips. This may lead to changes in the mobility patterns of the people. Therefore the test persons were asked which means of transportation they replaced by their pedelec. Also the main reason for their pedelec trips were asked. Three reasons were suggested: commuting (trips home-work), shopping and leisure. Most of the respondents mentioned several categories. Figure

[1] simulation with the graphical user interface of chapter 12 based on the ID drive cycle from chapter 11 and a Sparta Ion pedelec

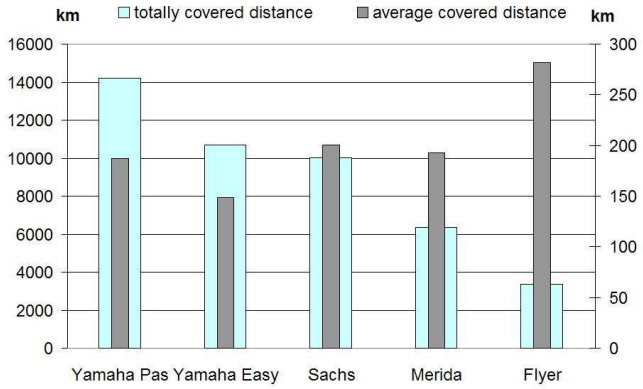

Figure 2.4: Covered distance versus pedelec model

2.5 summarizes the answers. The height of the bars represent the number of people that replaced the respective means of transportation by their pedelec. The different fillings represent different reasons for the trip. The high score of the conventional

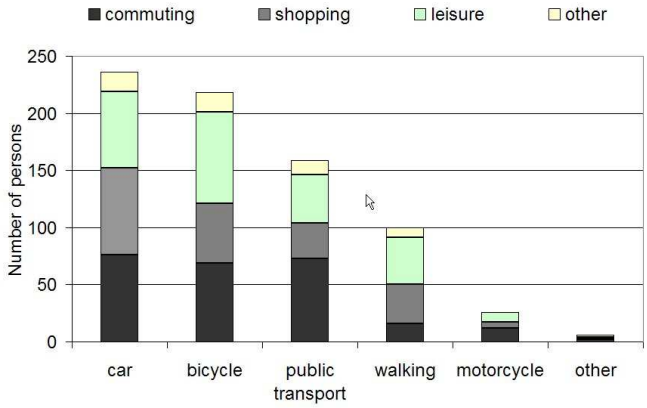

Figure 2.5: Which means of transportation are replaced by the pedelec and what are pedelecs used for?

bicycle replacement is not surprising, considering the resemblance with the pedelec. It is encouraging to see that almost everybody mentioned that at least for some trips the pedelec could replace King Car [28]. The pedelec was also appreciated as a good alternative for the public transport, especially in city environment. Except for the (typically male) motorbike, there was no difference between the sexes. The reasons for the trips where equally distributed between commuting, shopping and leisure:

- 66% used the pedelec at least once for commuting.
- Probably due to the first contact of most of the test persons with the phenomenon of the pedelec, 60% of the respondents made trips for pure leisure.
- In spite of some complaints of the bad facilities for shopping, 57% succeed doing his/her shopping with the pedelec.
- 43% of the respondents also made mention of new trips due to the availability of the pedelec.

So at first sight people seem to become more mobile with the possession of the pedelec.

2.3.5 Time gain

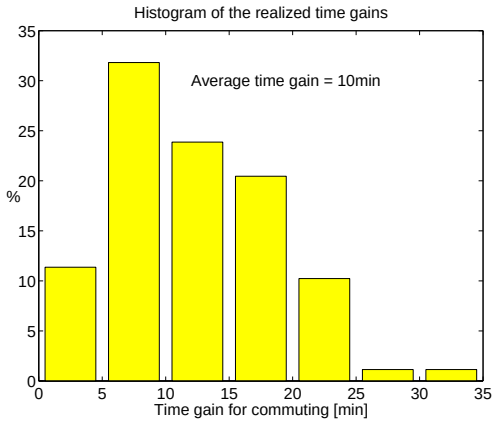

Figure 2.6: Histogram of the realized time gains by using the pedelec for commuting

A time gain was realized by 37% of the test persons when using the electric two-wheeler for commuting instead of their normal commuting vehicle. The histogram of the time gains realized by those test persons is given in figure 2.6. The average time gain is 10 minutes for a single trip. This means that a pedelec commuter may gain about 76 hours on a yearly base. This is time that otherwise would be passed getting stuck in traffic, or waiting for a bus/tram. Although the pedelec is intrinsic slower than cars or public transport, the waiting time may be much shorter.

2.3.6 Appreciation of the pedelec

The test persons were asked about the performance of the tested pedelec on 6 domains: the global ease of use, the weight, the ease of charging, the level of the motor assistance, the autonomy and the global quality and reliability.

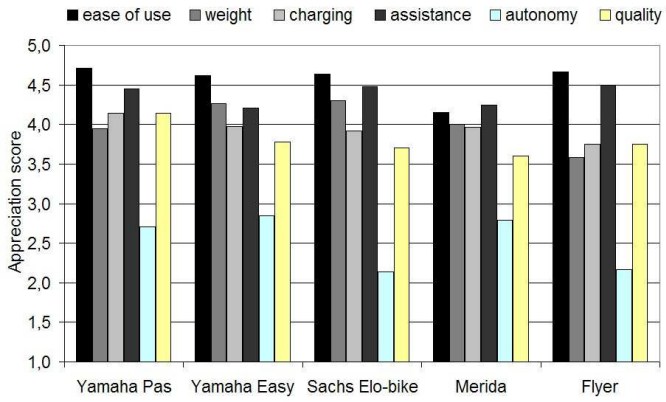

Figure 2.7: Appreciation of some pedelec aspects: excellent=5, very poor=1

In figure 2.7 the appreciation scores are given per pedelec model. A score of 5 means an excellent performance on the topic, a score of 1 means a very poor performance. A two-sided rank sum test was performed to quantify the differences in appreciation between the different models. Because the rather small number of test persons per pedelec, the following assertions only have a limited probability (p).

- The Merida scores worst for ease of use (p=90%)
- The users of the Flyer seem to suffer the most of the weight (p=75%)
- The limited autonomy is more experienced by Sachs and Flyer riders (p=90%)

The last two remarks can be partly explained by the fact that the Flyer users were mostly trained cyclists with other expectations from a pedelec. Except for the autonomy the pedelec seems to pass for all mentioned categories, although the results (see also figure 2.3 betray that there are still a lot of things to improve:

- 8% of the respondents found the level of assistance inefficient
- 12% had doubts about the quality/reliability of the tested pedelec
- 13% disagreed with the quote ‘the charging is easy’
- 58% wanted the pedelec to have a greater autonomy

2.3.7 After the test

One of the positive effects of the test period is the changed cycling behaviour of the participants. At least 36% said that they ride more kilometres with their conventional bicycle since they finished the test.
About purchasing pedelecs there was more doubt: Mentioning a (rather low) catalogue price of €1000, 56% of the male respondents called themselves prepared to buy an electric bicycle, although only less than 3% really bought one. From the

female participants only 43% was prepared to buy one despite their more positive remarks.

2.3.8 Infrastructure

Everybody that cycled once in a city like Brussels knows that the cycle infrastructure is often inadequate. So also in this test 79% of the respondents complained about the lack of cycle tracks. 65% was dissatisfied about the number of parking places for bicycles.

2.3.9 The most typical user

Another question asked to all participants was: 'Who is, according to you, the most typical pedelec user?' The answers were very different and are categorized in table 2.2. Only 197 test persons gave a valid answer on this question.

	Most typical user	**%**
1	Commuters	61.4
2	(Middle)aged people	32.5
3	Less sporty people looking for physical training	24.9
4	People in hilly regions	12.7
5	Everybody	11.7
6	Disabled persons	10.7
7	Sporty people	6.6
8	Shopping people	5.6
9	Recreational users	4.6
10	Workers in suit	3.6
11	People living in rather flat areas	3.6
12	Long distance cyclists	1.5
13	Students and daredevils	1.5

Table 2.2: The most typical user according to 197 respondents

Commuters are supposed to be the main target group. Of course the distance between work and place of residence cannot be too long. If the distance is out of the autonomy range, a combination of public transport and pedelec may be a solution. Considering the fear for theft (table 2.3) there should be at least a guarded parking place at work or at the station. Because of the time people spend at their job, charging at work is no problem. In that case a portable battery is certainly an advantage.
There were some remarkable things about the answers on this question: The young and sporty participants mentioned the elder and less sporty people as target group. They mainly mentioned the categories 2, 3, 4 and 6 of table 2.2. The elder and less sporty participants on the other hand mainly answered that a pedelec is something for young and dynamic people (categories 7, 9, 10 and 13).

Should we conclude that these bicycles are still too much human powered for the people who already gave up cycling long time ago and give too few surplus value for the real cyclists?
According to 11% of the respondents the pedelec is a typical product for slightly disabled people (people with heart or breathing problems, with limited force,...) while the test persons with heart problems still doubted about the product.
Also the contrast in opinion about the adequacy for hilly regions (table 2.2) is remarkable. This is not merely a subjective feeling, because the performance analysis of part II also shows that different pedelecs can have very different climbing-abilities.
Other rather unexpected target groups were 'people with a lot of time' and 'environmental conscious people'. Some participants explicitly told us that the pedelec is neither suitable for the busy city traffic nor for leisure cycling.

2.4 Analysis of the logs

2.4.1 General remarks

	Remarks	**%**
1	Technical problems	51.6
2	Too heavy	46.7
3	Small autonomy	42.9
4	Lack of cycling infrastructure in the city	25.8
5	Dangerous in busy traffic	22.0
6	I used the eco-assistance	22.0
7	It is a real pleasure to cycle	21.4
8	Too expensive	19.8
9	Fear of theft	19.8
10	The weather conditions influenced my cycling behaviour	19.8
11	Parking place on ground floor without treshold is needed	18.7
12	Insufficient assistance power	15.9
13	Inadequate gearbox	15.4
14	Electric cycling needs a learning process	13.7
15	Luggage problems	9.9
16	Bad seat comfort	9.3
17	Needs extra suspension	6.0
18	Assistance should last above 25 km/h	6.0
19	Poor design	4.9
20	I enjoyed the curiosity of the people in the street	4.9
21	Assisted cycling results in laziness	3.8
22	I was really dissatisfied	3.8

Table 2.3: General remarks of 182 respondents

Next to the standard questionnaire of appendix B, people were asked to keep a log with daily trip information. A textbox for remarks was available per trip. In the logs people gave a lot of comment about their experiences with the electrical bicycle. An attempt is made to categorize this spontaneous information. The reference group became smaller because not everyone took the time to write down his experience. So only people giving at least 2 remarks were seen as valuable. This resulted in a group of 182 test persons. The most quoted remarks with the percentage of respondents by whom they were mentioned are given in table 2.3.

2.4.2 Technical problems

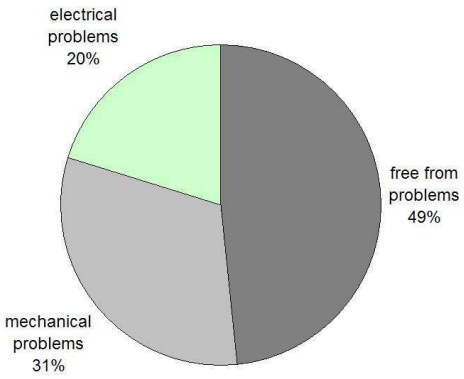

Figure 2.8: Percentage of technical problems

Technical problems were the number one cause for annoyance among respondents: more than 50% of the participants had to cope with one or another technical problem during the test period. A distinction has been made between mechanical problems that could have happened with a conventional bike too and problems due to the electrical character of the bicycle. As shown in figure 2.8 most of the problems (31%) were mechanical. A selection of the most occurring mechanical problems is given below:

- flat tyre
- malfunctioning of the mileometer
- defective light
- problems with gears
- chain problems
- bad seat attachment
- problems with pedal brake
- ...

A problem was considered electric if it was due to the presence of the battery and/or motor. The following problems were mentioned:

- sudden break down of the motor
- annoying noise while charging
- difficulties with charging during cold weather
- unreliable assistance
- inadequate brakes for the heavy motor and battery weight
- battery charging problems
- bad mounting of the battery
- instability due to the heavy motor and battery weight
- ...

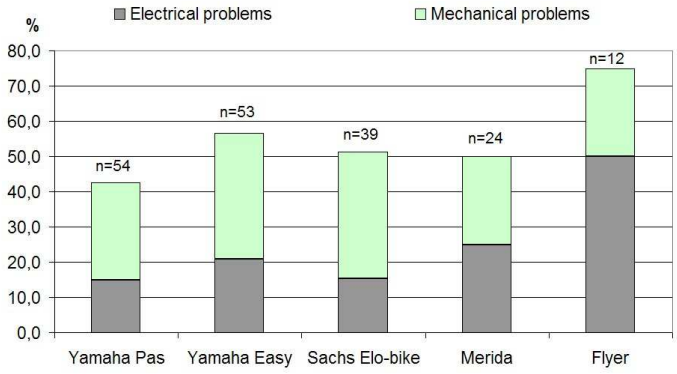

Figure 2.9: Percentage of technical problems per pedelec. The size n of the samples are given for every pedelec.

The share of technical problems seems to be high. The percentages of mechanical and electrical problems per pedelec are shown in figure 2.9. Concluding that all those pedelecs are worthless, would be unfair. The pedelecs were lent to a lot of people who were not always taking enough care of them. Of course the opinion about pedelecs will be hardly influenced by the number of technical problems people had to cope with. Moreover the users were asked not to repair the bikes themselves, but to bring the defective pedelecs back to the university to repair. This extra effort also may have caused annoyance.

2.4.3 The weight and suspension

The second most occurring remark concerned the weight of the pedelecs. While the respondents were rather mild in the condemnation of the weight in the standard

form (see figure 2.7), 47% complained about weight and ease of use in their spontaneous comment. These remarks were often given by people ending up without battery power during a cycling tour. It is a fact that although a pedelec can be used without assistance, the efficiency is often lower than that of a common city bike. The remarks learnt that the users of the Yamaha Easy suffered statistically more from the extra weight (64% against 40% for the users of other pedelecs) although it is one of the lighter pedelecs. The demand for extra suspension is most mentioned by the users of the Sachs.

2.4.4 Other remarks

Table 2.3 with general remarks also shows the importance of a parking place on the ground floor. 19% of the test persons mentioned that they had parking problems because of one or more steps. The extra effort to lift the pedelec out of its parking place, combined with the multiple anti-theft systems make the pedelec less attractive for very short distances. Knowing that their autonomy is also rather small, we can conclude that the electrically assisted bicycle is most interesting for distances between 5 and 15 km: a distance within conventional bicycle range, but often covered by car...

2.4.5 The correlation of the remarks with the covered distance

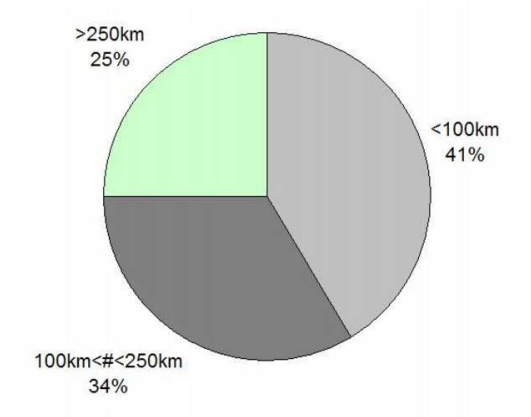

Figure 2.10: Subcategories of respondents according to the covered distance during the test period

In order to investigate the correlation of the remarks with the covered distance, the respondents were divided into three subcategories: respondents who rode less than 100 km, respondents who rode more than 100 km but less than 250 km and respondents who rode over 250 km during the test period. There relative numbers are given

in figure 2.10.
The remarks mentioned on the abscis of figure 2.11 seemed to correlate with the covered distance. If one uses the common statistical significance level of 95% to reject the null hypothesis, only the number of complaints about the weight correlate with covered distance.

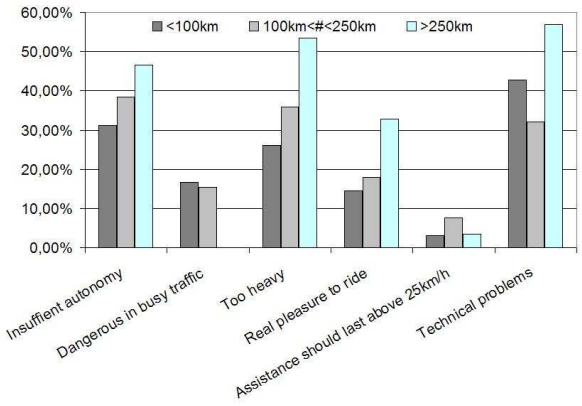

Figure 2.11: Correlation of the remarks with the covered distance

- The problems of the weight and the autonomy become bigger by covered distance. Knowing that people of the third category ($> 250km$) were used to cycle, they had different expectations from their pedelec. Some of them suggested that they were faster with their light conventional bicycle. However speed seems to be of secondary importance for most of the manufacturers: the reduction of the effort has the priority. Also the restriction by law cannot be denied (see section 1.5).
- It may sound contradictory, but those who cycled least kilometres were complaining the most about the busy traffic.
- It is mainly the middle category that enjoyed riding. That can be partly explained by the smaller number of technical problems that this category experienced.

2.5 Conclusions of the lending service

Three years of organized test rides with pedelecs yielded a lot of feedback from the users. The standard questionnaire and the logs of the test persons gave a good idea of the appreciation by the daily users. Unfortunately, the number of tests was too small to make statistically significant differences between the different pedelec and battery types concerning the free remarks, the typical user, the time gain,...
The results of the lending service are summarized as follows:

- The pedelecs are well appreciated according to the results of the standard questionnaire. Only the small battery range is seen as a real problem.
- The log books somehow shade the positive feedback of the standard questionnaire: A lot of test persons find them too heavy, not attractive enough and are frightened by the many technical problems. Although the last generation of pedelecs countered a lot of the complaints, still prices and weights stay above the client's wish.
- The electric bicycle is certainly not a simple alternative for normal bikes, but a new mobility means, especially suited for distances between 5 and 15 km.
- Pedelecs are suitable for commuting as well as shopping and leisure.
- A substantial time gain can be realized when using the pedelec for commuting.
- Appreciation of the tested pedelecs is highly dependent on the cycling history of its user.
- Cycling infrastructure still has to be optimized for a real breakthrough.

A repetition of the lending service could already be interesting to see how things changed since the finishing of the last tests. The city of Brussels, for instance, made quite some effort to improve the poor cycling infrastructure [27]. Also the pedelec technology has evolved a lot (better batteries, lighter weights,...) since the introduction of Yamaha's PAS system in 1995. And as is proved in the next chapter, a lot of new bicycle manufacturers joined the pedelec market.
Based on the knowledge from these lending service, a better experimental design is possible and would lead to more distinctive results with the same research efforts.

3

The Pedelec Market in Flanders

As a first part of the subjective performance analysis of pedelecs, chapter 2 polled for the user's needs. This chapter will focus on the Flemish pedelec market as it is seen through the bicycles dealer's eyes.

The worldwide pedelec market has been growing fast during the last ten years. Many bicycle producers introduced a motor assisted bicycle model and launched it under a promising 'e-name'. According to the National Institute of Statistics of Belgium, there are about 4 million bicycles in Flanders. Compared to a total number of 6 million inhabitants, Flanders might be called a bicycle region. Estimated 400.000 bicycles are bought each year. 30% of the commuters in cities use the bicycle and 53% of the displacements to school are done by bicycle [26]. Looking at the resemblence of the pedelec with the bicycle, these figures prove that Flanders is a potential market for pedelecs.

Research by a Flemish consumer organization for bicycles showed that 82% of the Flemish cyclists bought their (conventional) bicycle in a specialized bicycle dealer shop [29]. This means that Flemish people trust the advice and service of these dealers for making their bicycle choice.

In december 2005, 450 of these dealers were asked to fill in an electronic questionnaire about their pedelec experiences. More than hundred of them were prepared to answer and helped sketching the market situation. The answers also clearly show how dealers appreciate today's pedelec generation. Next to this questionnaire 110 websites of bicycle shops were checked for data about pedelecs. The data of the dealer inquiry and the websites are discussed in this chapter.

3.1 The questionnaire

Searching the Flemish 'Gouden Gids' and the internet yielded 866 addresses of dealer shops. The option of sending them a letter with a questionnaire was left when appeared that 468 of them could be reach by e-mail. The electronic questionnaire was kept simple to increase the reply rate. Table 3.1 shows the queries. The answers are discussed in the next sections.

Do you offer pedelecs or power kits to your clients?
☐ Yes
1. Which brands/types do you offer?
2. What is the shop price of these products?
3. How many pedelecs did you approximately sell in the past year?
4. How many conventional bicycles did you sell in the same period?
5. Do you get enough information from the manufacturer to be able to repair/test the electric parts (motor, controller, battery,...) in your own workshop?
6. Are you satisfied yourself about the performance of these products?
7. What could be improved to the technology?
☐ No
1. What is the main reason for not offering pedelecs?

Table 3.1: The electronic questionnaire sent to the bicycle shops

3.2 Brands on the Flemish market

In table 3.2 all occurring brands are alphabetically listed in the first column. The second column mentions whether this brand represents a full mounted pedelec, a power kit or both. Also two folding bicycles are mentioned. The third column is a link to the website of the manufacturer, or a link to a website where the discussed pedelec can be found.

The total number of reached dealers was 212: 102 via e-mail, 110 via their website. According to the formula of Cochran adapted for small populations [35], for a 95% confidence level, the level of precision for the sample size of 212 is 6.0% and for a sample size of 102, 9.3%. The results in this chapter should be interpreted according to these sampling errors.

In figure 3.1 the absolute number of contacted dealers selling a certain brand is given. Brands that only occurred once were excluded. Also some brands were put together because of the similarity in their electric drive system.

The most occurring brand in the inquiry was Electronic Bike Developments, a Flemish firm offering the pedelecs called E-move and E-manuel. EBD is followed by two

brand	type	website
Antec	pedelec/kit	www.antec.nl
Batavus (Ion)	pedelec	www.onzichtbaremotor.nl
Bertin/Sparc	pedelec	www.fietsenvanneste.be
Binbike	pedelec/kit	www.euromoto.be
Bionx	kit/pedelec	www.bionx.be
Eazy mouv	pedelec	www.eazymouv.com
Electronic Bike Development	pedelec	www.ebd.be
Enik/bionx	pedelec	www.elektrischefiets.be/elekfietsenbionx.html
Enik/sparc	pedelec	www.elektrischefiets.be/elekfietsenenik.html
E-zee bike	pedelec	www.ezeebike.com/home.htm
Flyer	pedelec	www.flyer.ch
Gazelle	pedelec	www.gazelle.nl/www2/easyglider
Giant	pedelec	www.lafree.com
Heinzmann	kit/pedelec	www.heinzmann.de www.estelle.de/e/fahrradmodelle.asp
Joris E-bike	pedelec	www.joris-e-bike.com
Koga Miyata (Ion)	pedelec	www.koga.com/nl
Kynast	pedelec	www.extraenergy.org
l'Avenir	pedelec	www.lavenir.be
MBK	pedelec	www.mbk-cycles.com
Panasonic	folding bicycle	www.pocketnsoul.com/evstart
Piaggio	pedelec	www.piaggio.com
Powabyke	pedelec	www.powabyke.com
Renault zapping	folding bicycle	www.pocketnsoul.com/evstart
Sachs	pedelec	www.sachs.be
Schachner	pedelec/kit	www.elektrobikes.com
Sparta Ion	pedelec	www.sparta.nl
SRAM sparc	kit	www.sram.com
Swizzbee	pedelec	www.swizzbee.ch
Thompson/bionx	pedelec	
Venturelli	pedelec	www.venturelli.be
Yamaha	pedelec	www.yamaha-motor.co.jp

Table 3.2: Alphabetic list of pedelec brands found in flemish bicycle shops

dutch firms, Sparta and Batavus, who both use the same electric drive technology. In the top ten also two other dutch firms, Gazelle and Antec, are present. Remarkable is also the presence of 2 North American products: Bionx from Canada, and Sram from the USA. The only other Belgian manufacturer in the top ten is l'Avenir. Giant and the Yamaha PAS system are representing Asia in the top ten.
Figure 3.2 learns that 71% of the brands have their origin in Europe. Although the pedelec is far more popular in many Asian countries, (e.g. China sold 1 million pedelecs in 2002 [30]) only 13% is from Asian origin.

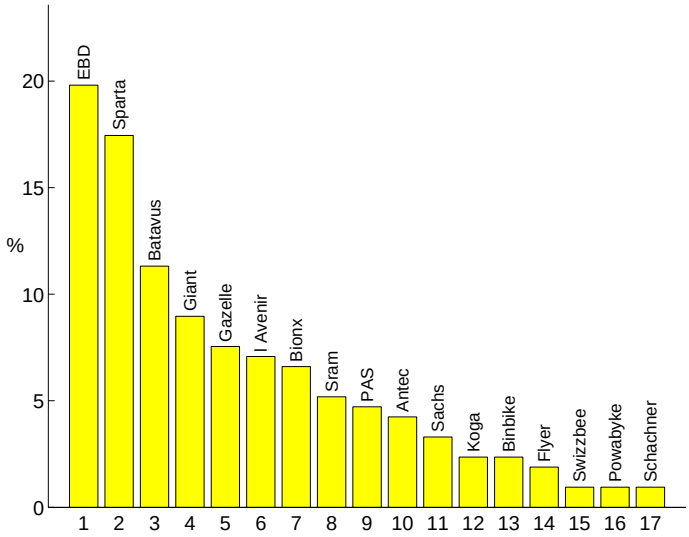

Figure 3.1: Percent of offering dealers per brand (the sample size is 212 dealers).

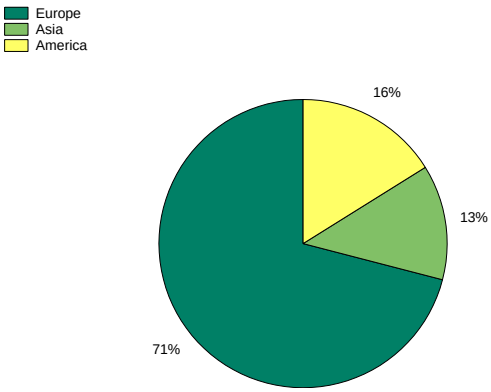

Figure 3.2: Origin regions of the brands

3.3 Dealers and pedelecs

About 85% of the responding dealers were offering pedelecs or power kits. One third of the dealers offer one single brand. More than 50% offer at least 2 different brands of pedelecs. The maximum number of brands for one dealer was 8! Most of them were selling full mounted pedelecs. The main reason may be that most of the occurring brands were only offering full mounted pedelecs. But even the power kits of

Average number of pedelecs per dealer	13.4
Average number of conventional bicycles	402
Maximum number of pedelecs for 1 dealer	200
Average number of brands per dealer	2

Table 3.3: Sales figures of the year 2005 for dealers offering pedelecs

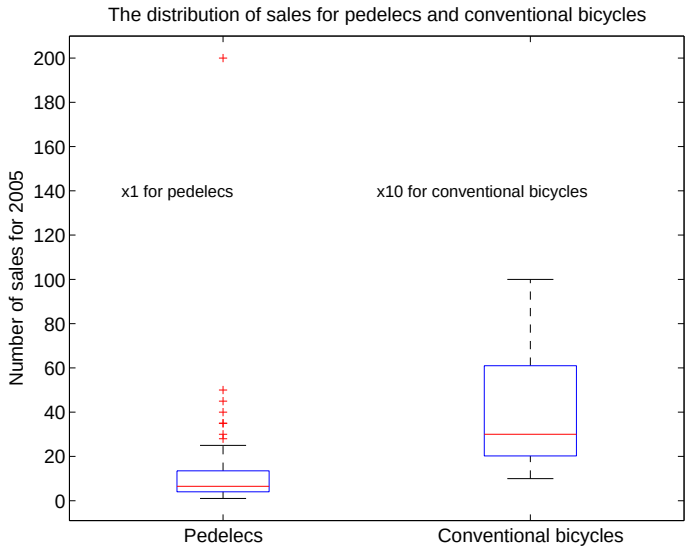

Figure 3.3: Boxplots of the sales figures for pedelecs and conventional bicycles for the year 2005

the manufacturers were sold already mounted by the dealer in a conventional bicycle. Only two dealers mentioned the sale of power kits without a bicycle.
Hardly 38% of the visited websites were mentioning pedelecs. This is much less than what would be expected from the results of the responding dealers. Whether the result may be skewed either because dealers who do not offer pedelecs did not take trouble to answer the inquiry, or because the dealers find it unnecessary to make publicity for these products on their websites. This means that a lot of dealers are not actively promoting the pedelec. Their main concern is the conventional human powered bicycle.
The last reason is understandable if one looks at the average sales number of pedelecs and conventional bicycles in table 3.3 and figure 3.3. For dealers offering pedelecs, only 3.3% of the sold bicycles are pedelecs. And as 3 dealers did not want to offer pedelecs because of the small profit margin, the profit part coming from pedelecs sales will be even less than 3.3% of the total dealer profit.
Of course there were some proverbial exceptions: one respondent stated to be special-

ized in electric bicycles and two visited websites were only offering electric bicycles. However, the conclusion may be that one cannot expect a market boost by the marketing efforts of the dealers. They seem not to be waiting for a breakthrough. The marketing has to be done by the manufacturers or by the government.
The pedelec offering dealers in Flanders were divided in 4 categories:

1. dealers who sold less than 5 pedelecs in 2005
2. dealers who sold less than 10, but at least 5 pedelecs in 2005
3. dealers who sold less than 20, but at least 10 pedelecs in 2005
4. dealers who sold more than 20 pedelecs in 2005

Table 3.4 shows the percentage of dealers belonging to each of these categories, and the relative number of pedelecs that they represent.

Category	Dealers percentage	Pedelecs percentage
$0 < \# < 5$	29	6
$5 \leq \# < 10$	29	13
$10 \leq \# < 20$	24	21
$\# > 20$	18	60

Table 3.4: The division of dealers in 4 categories

So 15% (18% of the 85% offering dealers) of all responding dealers account for more than 60% of the pedelec sales.

3.4 The number of pedelecs in Flanders

An idea of the total number of pedelecs (TNP) sold in Flanders in 2005 is obtained by a combination of the following data:

- 82% (p_1) of flemish cyclists buy their bicycle in the specialized dealer shop [29]
- There are about 950 (dn) bicycle dealer shops in Flanders [31]
- 13.4 (pn) is the average sales number of pedelecs per dealer in 2005
- 402 (cn) is the average sales number of conventional bicycles
- 61% (p_2) of the dealers offer pedelecs (combined data of visited websites and inquiries)

$$TNP = \frac{dn \cdot p_2 \cdot pn}{p_1} = \frac{950 \cdot 0.61 \cdot 13.4}{0.82} = 9470 \tag{3.1}$$

Verification of this total pedelec sales number of 9470 in Flanders in 2005 can be done by calculating the number of conventional bicycle sales (TNC) in the same way:

$$TNC = \frac{dn \cdot cn}{p_1} = \frac{950 \cdot 402}{0.82} \approx 466000 \tag{3.2}$$

This number is close to the number given by the national institute of statistics [26].

In the Netherlands, the year 2005 was good for 1,2 million conventional bicycle sales and 30000 electric bicycles. For the latter category, this was an increase of 50% compared to 2004 [32]. So, the Netherlands as well as Flanders have about 1 pedelec for 600 people, but the Netherlands have a small lead to Flanders.

3.5 Pedelec prices in Flanders

Many dealers gave detailed customer prices for their products. Other dealers only gave minimum and maximum prices. For the latter category, all prices between the minimum and maximum were also included in order to get a distribution of prices between the all dealer minimum (see table ref 3.5) and the all dealer maximum. This distribution is presented in figure 3.4.

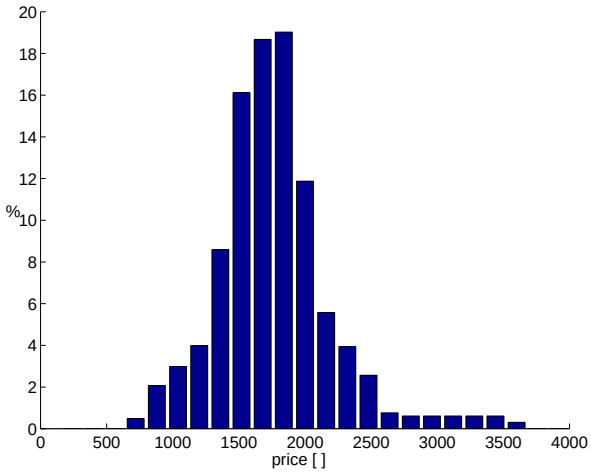

Figure 3.4: The distribution of pedelec prices in Flanders

Compared to the international prices given in table 3.6 these prices seem to be at the high end. One may conclude from this price discrepancy that pedelec prices are increased the last years, or that the prices for Europe in reference [30] are a bit underestimated.

Minimum price	€695
Maximum price	€3600
Average price	€1691

Table 3.5: The 2005 market price of pedelecs in Flanders

Region	Average price	Sales number 2003 [x1000 units]
China	€260	1000
Japan	€650	180
EU	€900	65
USA	€1300	35

Table 3.6: The market price of pedelecs in the world in the year 2003 [30]

3.6 Main reasons for not distributing pedelecs

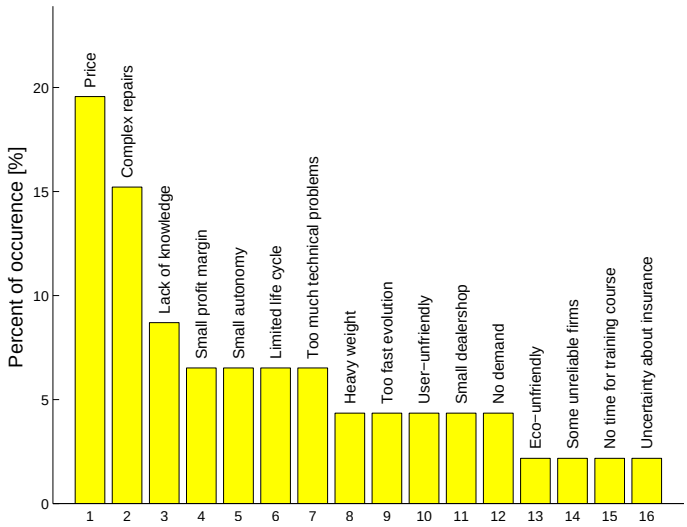

Figure 3.5: Reasons for not distributing pedelecs

The 15% respondents who told not to offer pedelecs gave many different reasons for this absence. These reasons are collected in figure 3.5 in order of importance.
These reasons are subdivided in 4 categories shown in table 3.7. More than one half of the reasons deals with a distrust in the pedelec technology. A lot of work is left to be done by manufacturers to convince the dealers of their product quality. At the same time we have to admit that sellers of the best selling pedelecs were quite

Reason	Occurrences [% of n=46]
Distrust in pedelec technology	52
Price	26
Practical reasons	11
Lack of pedelec knowledge	11

Table 3.7: Main Reasons for not distributing pedelecs and their relative occurrence

satisfied with the two-wheelers and the support of the manufacturers (see 3.7).

3.7 Satisfaction with the technology and the manufacturer support

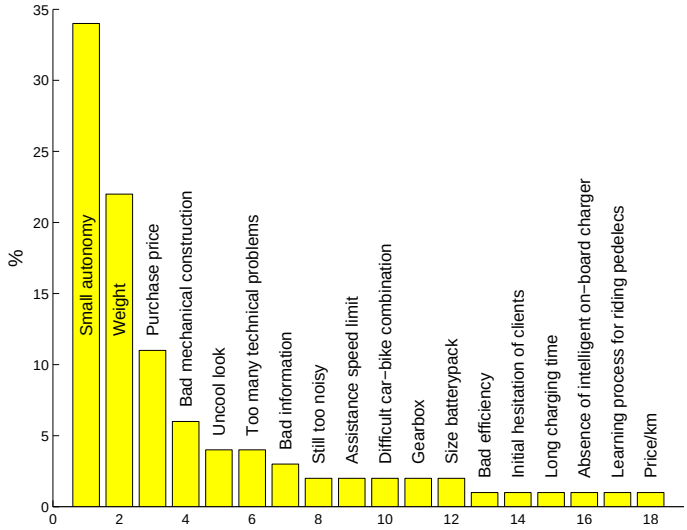

Figure 3.6: The shortcomings of the pedelec through the dealer's eyes

Generally, the dealers offering pedelecs are satisfied with the performance of their pedelecs. Although only 11% was really disappointed about the technology, a lot of possible improvements were given as an answer to question 7 of the questionnaire (table 3.1).
The shortcomings that were mentioned are ordered by importance in figure 3.6. For the matter of the shortcomings, the dealer response paralleled user response 2.3.6: also dealers would like to see a higher autonomy and a lower weight and price. Table 3.8 split up the mentioned shortcomings in 4 categories that were also mentioned by

the users. The total number of shortcomings mentioned by all users was 743, the total number of shortcomings mentioned by all dealers was 100.

Shortcomings	Dealers n=100	Users n=743
Technical shortcomings	81%	55%
The high market price	12%	7%
The lack of information	5%	4%
The external barriers	2%	34%

Table 3.8: Comparison between mentioned shortcomings from dealers and users

The second column is the percentage of dealers that mentioned the shortcoming specified in the first column. The third column of table 3.8 is the percentage of test persons (derived from section 2.3) that mentioned the same shortcoming.
More than 80% of the mentioned remarks by dealers are complaints about the imperfect technology. Although only 7% of the given remarks by the test persons is a complaint about the price, still 20% of these persons would like to see a lower price (table 2.3). Only 11% of the dealers think a lower price is required to convince the client.
Concerning the external barriers, only the legislative speed limit was mentioned by the dealers. Users had many more remarks about external barriers such as infrastructure problems, fear of theft,weather dependency,... This could be an indication of the lack of real world riding experience of the dealers with the pedelecs.
According to figure 3.7 79% of the dealers was satisfied with the support of the

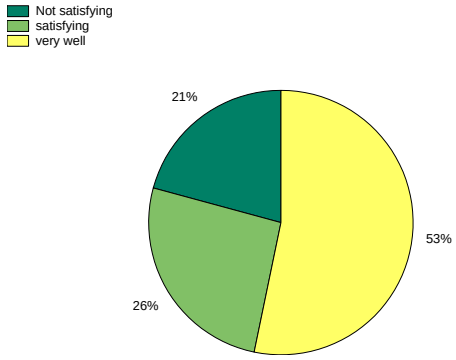

Figure 3.7: The appreciation of the support from the manufacturers

manufacturer. Most manufacturers are aware of the need for support, looking at the positive feedback that many dealers gave about service points, education and the ease of getting spare parts. 21% was dissappointed about the service of the manufacturer. Part of them decided on this base to stop the cooperation.

3.8 Misunderstandings

Another conclusion withdrawn from the answers of the dealers is that there are still a lot of misunderstandings about the technical working principle of the pedelec. Some dealers persistently ignore the first law of thermodynamics and wonder why one has to reload the battery from the grid, while a simple dynamo could do the same during cycling.
Other dealers suggest a financial intervention of the National Health service, to help disabled people to purchase their pedelec.

3.9 Conclusions of the market research

The electronic questionnaire to the dealer shops learned a lot about the pedelec penetration into the Flemish market and the dealer's experiences with pedelecs.

- A lot of brands are found on the Flemish market and most of them are European products.
- About 10.000 pedelecs are sold in Flanders in 2005.
- A minority of the dealers account for a majority of the pedelecs sales.
- For the matter of the shortcomings, the dealer response paralleled the user response.
- Quite some effort is left to be done by the manufacturers to convince the dealers of their product quality.
- Although most dealers are satisfied with the electrical assistance, they are not actively promoting the pedelec.
- However, promotion of pedelecs is justified and necessary, because
  - they might be a possible solution for the traffic congestions (see figure 2.5) within cities, as far as they move people from car-driving to cycling.
  - frequent cycling on a pedelec can also improve physical condition [33].
  - they move people with light physical constraints to (re)discover the benefits of cycling.
  - and they could free us from road unsafety, noise pollution, CO_2-emissions, alienation amongst people, corpulence, lack of space, oil problems,...[3]
  - Recent research stated that there are also psychological benefits of cycling to work [34].
- The condemnation as 'bicycle for disabled people' is never far away nor by users neither by dealers (see chapter 2).
- Some persistent misunderstandings about the working principle of pedelecs (by users as well as dealers) still have to be removed.

Part II

An Objective Approach of the Pedelec’s Performance

User feedback is far from sufficient to get an objective idea of the performances of a pedelec. The smoother the motor power assists, the less people noticed that they really got motor help. Reversely, some users praised the electrical assistance to the sky while it was not even turned on. So the perception did not always parrallel the amount of assisted power. There is need for a standard testing method to quantify the net motor contribution and the battery range.
The standard test results could be used

- to enable the consumers to compare different pedelecs independent from manufacturer data
- to help manufacturers in the design process of their pedelecs
- to check whether the pedelecs are conform the legislation (see section 1.5).

Part II of this work describes the development of a test installation and a test method to measure the performance of a pedelec in an objective way.

4

The Performance Analysis of a Pedelec

4.1 Objectives of the performance analysis

There were two major goals for the intended performance analysis:

- *The development of a test method for measuring the performances of the complete drive train of a pedelec under realistic driving conditions*.
  Therefore a new test application is designed. This testbench design is explained in chapter 5. The applied measuring method is described in chapter 6.

- *The defining of unambiguous performance parameters*.
  This will be the main topic of this part II. Before the performance parameters can be calculated, the pedelecs were modelled to estimate their behaviour in every possible operation point. The regression modelling that is used for this purpose is discussed in chapter 7. Chapter 8 discusses the application of this regression technique on the pedelecs. The visualisation of the models is a first tool to interprete the performance of a pedelec. This is shown in chapter 9. The definition of the performance parameters is given in chapter 10. In chapter 11 the introduction of a standard drive cycle is discussed. The objective performance analysis is concluded by the presentation of a graphical user interface that enables a faster and easier processing from the measurements to the performance parameters chapter 12).

Of course there are standard methods to measure separately battery efficiency, motor efficiency and bicycle drive train efficiency under laboratory conditions. Test installations for complete bicycles do exist (e.g. figure 4.1), although the working conditions often differ a lot from the road conditions. In contrast to these installations, fixing the

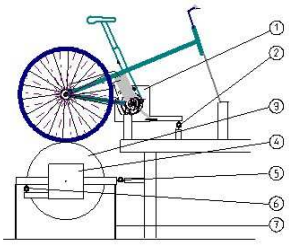

Figure 4.1: Existing test bench [36]

frame or removing a wheel is considered as no option for this performance analysis. The performance of the pedelec has to be considered in normal position, both wheels rolling freely on a flat surface. Because of their poor reproducibility, simple road tests are also rejected.

4.2 Basic idea

Figure 4.2: Comparing input and output power of a pedelec

The basic idea for the performance analysis of pedal electric cycles is to consider the pedelec as a black box. The cyclist is supplying a certain human input power (P_c) to this box. Based on one or more measurements, the pedelec controller reacts by adding a certain amount of auxiliary power resulting in a total 'useful' traction power (P_t). This control strategy will differ by manufacturer and by pedelec. Analyzing the relation between both power flows in the normal operation area (6.2) will be sufficient to model the pedelec behaviour.
This analysis is enabled by the construction of a pedelec test installation. Figure 4.3 shows the schematic line-up of the pedelec test installation. The implementation of the basic idea is realized by controlling two input parameters:

- The *bicycle speed* v
- The *torque on the pedals* or the *cyclist torque* T_c

The combination of both inputs should result in an acceleration of the bicycle on a conveyor belt, but a chain fastening the back of the bicycle to a fixed point keeps the bicycle from moving forward. The *traction force* F_t on this chain is a measure for the withdrawn acceleration, and thus for the developed traction power (see figure 4.3 and section 6).

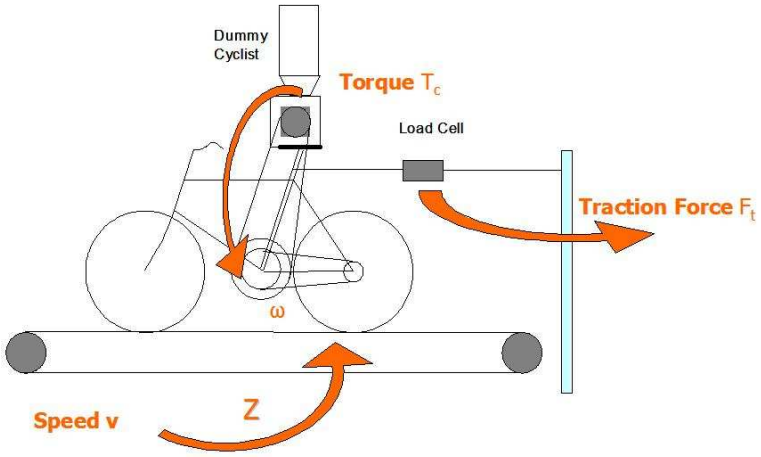

Figure 4.3: The line-up for the pedelec performance tests

5
The Design of a Pedelec Testbench

This chapter will discuss the practical realization of a testbench enabling the performance analysis of a pedelec.

5.1 The treadmill

Figure 5.1: The treadmill

An old runner's treadmill is extended to a $3m$ long bicycle treadmill and equipped with a new conveyor belt. The result is shown in figure 5.1. The belt has a width of $0.5m$ and is composed of four layers (total thickness = $2.8mm$) of which the uppermost is a smooth adhesive PVC layer, imitating the road surface. The belt is

driven by a speed controlled induction machine (frequency controller = ABB Sami GS, rated power = $4.0kW$). So, any linear speed of the conveyor belt between 0 and $30km/h$ can be forced to the pedelec.

5.2 The dummy cyclist

Figure 5.2: The 'dummy cyclist'

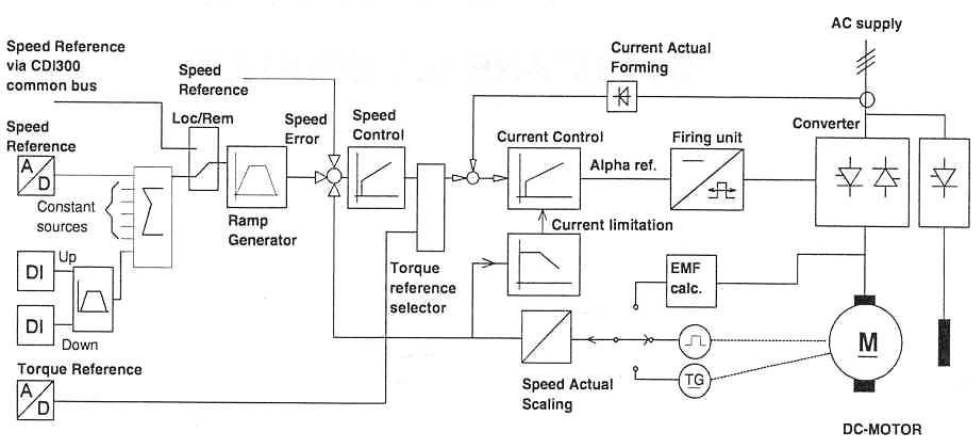

Figure 5.3: The automate torque control of the dummy cyclist

In order to quantify the human power input on the pedals, a controllable 'dummy cyclist' is required. Therefore a DC-motor with an angular gearbox is mounted on

the saddle rod. A pulley replaces the pedals and their cranks. The transmission is performed by a V-belt. The DC motor (rated power = $2.3kW$) is current-controlled (figure 5.3) by means of a power converter (ABB DCS500).
The weight of the motor, the gearbox, the pulley and the torque sensor is approximately that of a human being and also the position of the center of gravity corresponds more or less with the real cycling situation.

5.3 The sensors

5.3.1 The traction force

Figure 5.4: The load cell

A load cell is attached to the chain (see figures 4.3 and 5.4) to measure the traction force resulting from a certain forced conveyor belt speed and pedal torque. Because of the mass of this load cell, gravity may influence the measurement of the force when the chain is not completely stressed. This influence is negligible when the load cell is mounted in the middle of the chain.
The load cell is a Sensy model 2712 of $50daN$ calibrated to reach its full-scale range for $15daN$ (accuracy class 0.1). This showed to be useful for measuring at relative low traction forces while protecting against peak forces at the same time. The output signal is a $4-20mA$ current signal.

5.3.2 The cyclist torque

The torque exercised on the crankshaft is measured by a torque sensor (Lorenz MR-12, $500Nm$), which is mounted onto the pulley and has an accuracy class of 0.15. The output is a voltage signal between $0-10V$.

5.3.3 The bicycle speed

An optical encoder in the torque sensor delivers a TTL-signal from which the angular speed of the pulley can be derived. There is no slip established between the pulley and the bicycle chain, neither between the bicycle chain and the back wheel nor between the rear wheel and the conveyor belt. So the TTL-signal is a good measure for

Figure 5.5: The torque sensor

the linear speed of the conveyor belt and thus the bicycle wheels, supposing that the transmission ratio Z (see 6.1) is known.

5.4 The data acquisition system

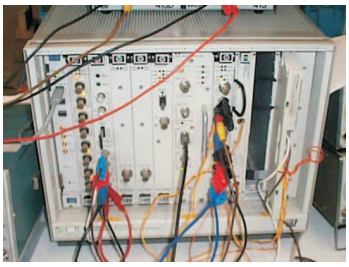

Figure 5.6: The VXI system for the data acquisition [37]

The data acquisition applied for the tests is a VXI system of HP combined with a Labview user interface (see figure 5.6) . The data acquisition system is slightly oversized, so certainly not the cheapest solution for this purpose, but is used because of its availability at the ETEC laboratory. The system was developed in the framework of a master thesis [37] and will be discussed in more detail in the next subsections.

5.4.1 The controller

The HP 8491A controller enables ($400Mb/sec$) communication between the mainframe with all measurement equipment and the PC by an IEEE 1394 interface.

5.4.2 The digital multimeter

The HP E1411B $5\frac{1}{2}$ digit multimeter is made for DC and AC voltage measurements, or 2- or 4-wire resistance measurements at a maximum frequency of $13kHz$. This multimeter performs in the latest line-up only the offset measurements of the force and the torque, which are taken once every time the test bench is restarted. The load cell current signal is converted by a 100Ω resistance to obtain a voltage signal.

5.4.3 The multiplexer

The measurement of multiple signals (torque and force) with the multimeter was first realised with the multiplexer HP E1343. The switching relais time is about 50ms, which was considered to be too slow for the simultaneous measurement of torque and force. Only for the offset measurements, the multiplexer is still used.

5.4.4 The time interval analyser

The TTL signal coming from the torque sensor is used to measure the angular speed of the pedal axis (=ω). The TIA HP1740A enables us to measure frequencies up to 80Mhz. The biggest time interval that can be measured is only $26.2ms$. The torque sensor gives 360 pulses per rotation, which means that the minimal measurable pedalling frequency f_{min} could be derived as

$$f_{min} = \frac{1}{26.2 \cdot 10^{-3} \cdot 360} = 0.106Hz \tag{5.1}$$

This shows that the TIA was not really adapted for the slow frequencies of the pedal turns. However this is still considered to be good enough because a pedalling frequency of 0.106 is rather unrealistic in steady-state driving conditions ($\approx$ driving less than 3 km/h in the highest gear). The TTL signal had to pass through a low-pass filter and a differential amplifier to filter out higher frequencies and common mode noise before giving good results.

5.4.5 The 2-channels digitizer

If one wants to measure the power balance in case of pulsating forces and torques, simultaneous measuring of both signals is necessary. This is realised with the HP E1429B 2 channels digitizer. Using a 12 bit conversion and a $\pm 5,1175V$ range, the accuracy is about $2,5mV$, which is considered to be more than enough.

5.4.6 The labview measuring program

The Labview 6.0 graphical programming was used for controlling the VXI system through a personal computer. One measurement is a $10s$ record of the angular speed of the pedal axis, the torque of the dummy cyclist and the developed traction force

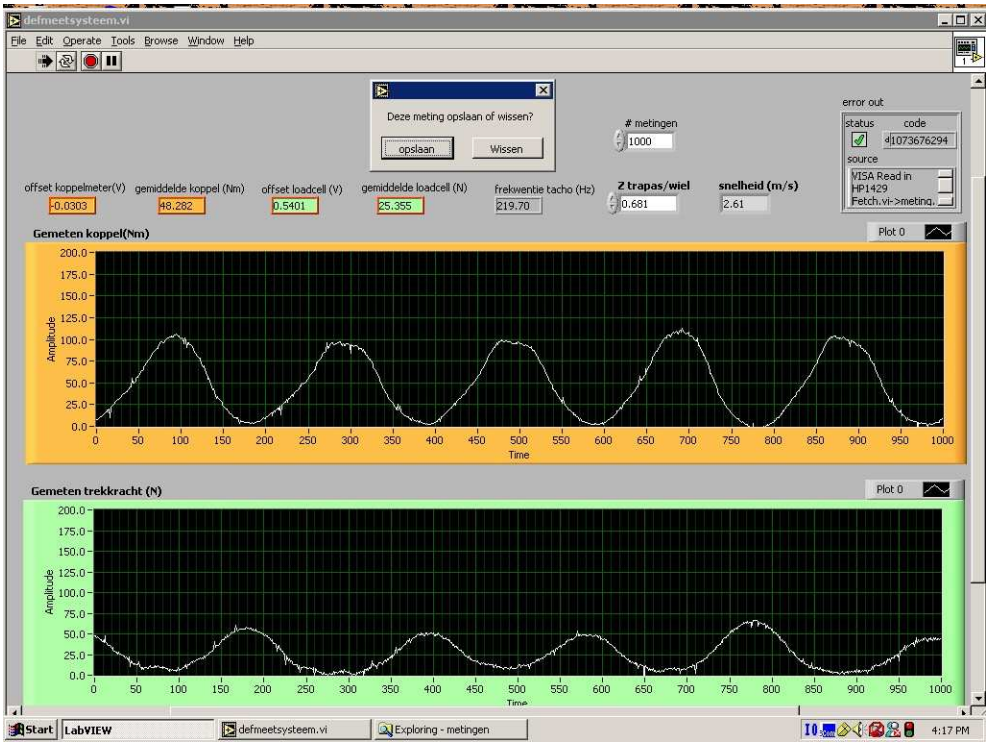

Figure 5.7: The front panel of the Labview 6.0 interface

(a) (b) (c) (d) (e)

Figure 5.8: Developed subVIs for the use by the Laview program

of the bicycle on the testbench. The goal of the program is to write average values for the torque, the force and the speed of this record to a data file. For this task, the labview program needs 2 extra inputs next to the measuring signals: The transmission ratio Z (see 6.1) and the sampling rate for the input channels.
Visualisation of the 10 second record enables the operator to judge the quality of the measurements and there is always the possibility to reject the given record. The user interface for measurement controls is given in figure 5.7. For every subtask of the measuring program, a subVI was developed. SubVIs are Labview subroutines that maybe called from the main program. They are shown in figure 5.8.

(a) offset.vi initialises and configures the multimeter and multiplexer to get the off-

set values of torque and force.

(b) **metingen.vi** initialises and configures the digitizer and executes the given number of measurements of the two voltage signals.

(c) **vanvoltnaarnewton.vi** converts the value in volts to values in Nm and N.

(d) **snelheidsmeting.vi** filters out the frequency of the TTL-signal coming from the torque sensor, and calculates the speed of the bicycle by using the transmission ratio Z.

(e) **write2file.vi** averages out the values of speed, force and torque and writes them (if not rejected) to one of two separate Excel-files depending whether the measurement was executed with or without assisting motor power.

The complete block diagram of the main Labview program is shown in figure 5.9.

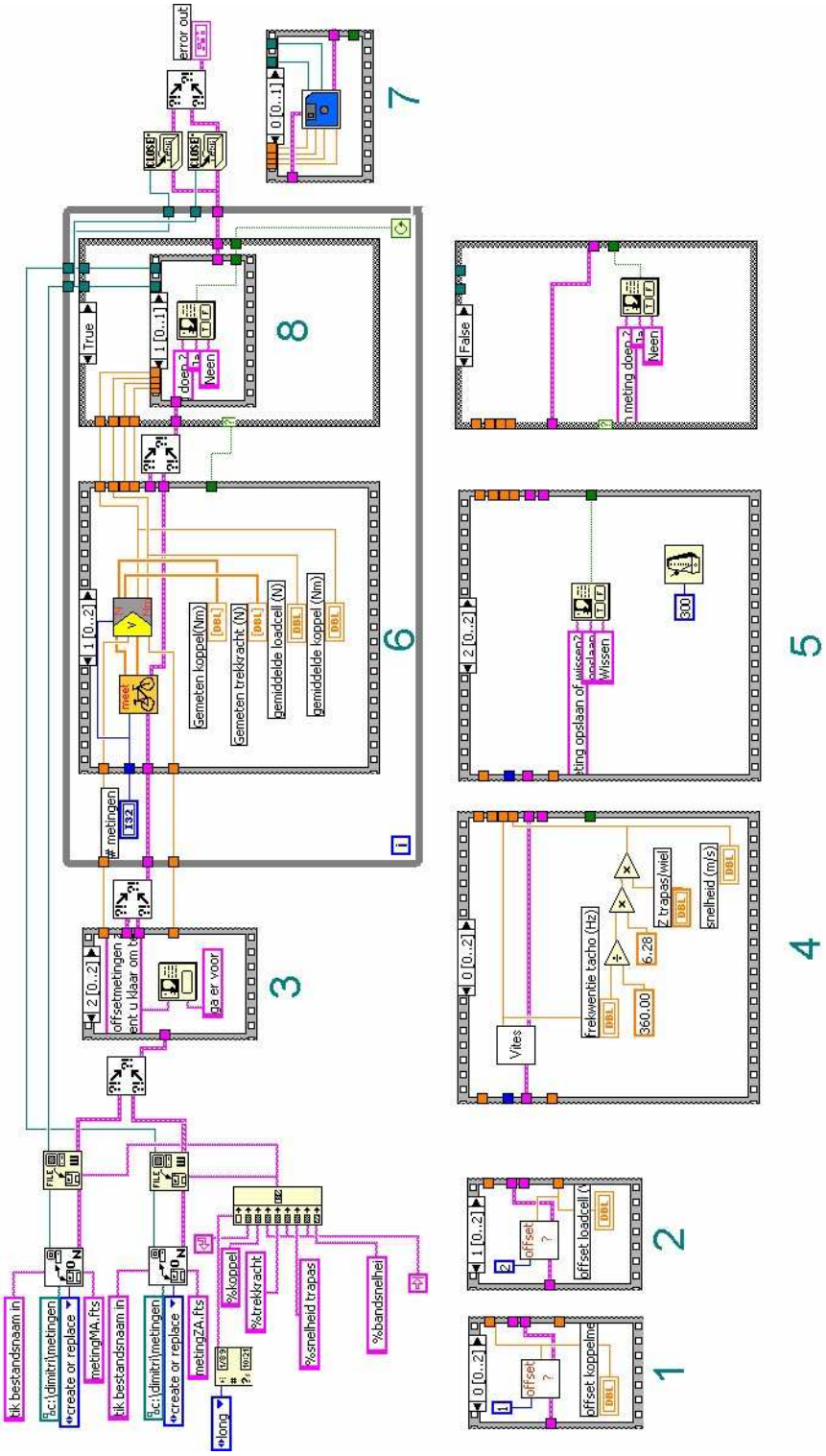

Figure 5.9: The block diagram of the Labview measurement program

5.5 The control of the test bench

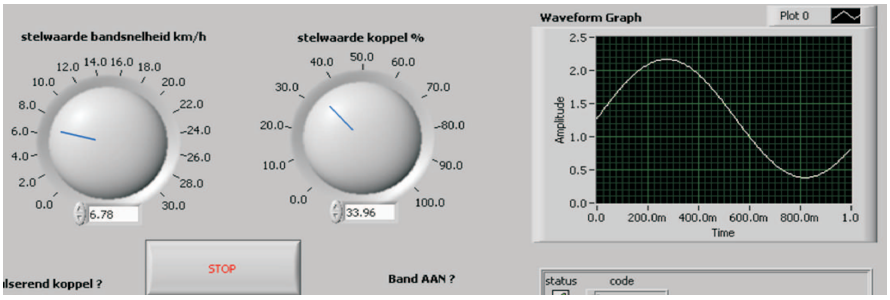

Figure 5.10: The Labview interface for the setting of the speed and torque references

The characterisation of a pedelec's performance is done by the measurement of the traction forces at different speeds and torques. The reference values for the speed and the torque are adjustable via another labview interface presented in figure 5.10. There is the possibility to choose between a pulsating or a constant torque. An open loop control system is considered to be sufficient, because only roughly scattered measurement samples are necessary for the intended performance analysis.
In accordance with the data acquisition system, a VXI D/A converter (HP E1328) is used for the setting of these reference values. The Labview block diagram is designed to convert the two chosen 16 bits values to analog voltage signals that have to be sent to the DC motor drive and the induction motor drive respectively. In a short time, the speed and torque of the bicycle can be adjusted to perform a new measurement.

5.6 The electrical design

After the first provisional line-up it became clear that it would be impossible to transport the test bench because of the many connections to external devices. Therefore all electric equipment (power supply, drives, control switches, electrical protection, emergency stops,...) is put together in one enclosure with one connection for a power supply of $3 \times 380V$ [38]. The electric diagram of figure 5.11 shows:

- the power supply for the drives
- the connection of some supplementary sockets
- the transformers
- the extra DC power supply
- the electrical protection equipment

Because the total loss power inside the enclosure is estimated at 1100W also a fan and air intake grid had to be installed to keep the temperature under control.
For demonstration reasons a remote control is also installed (figure 5.12). The remote

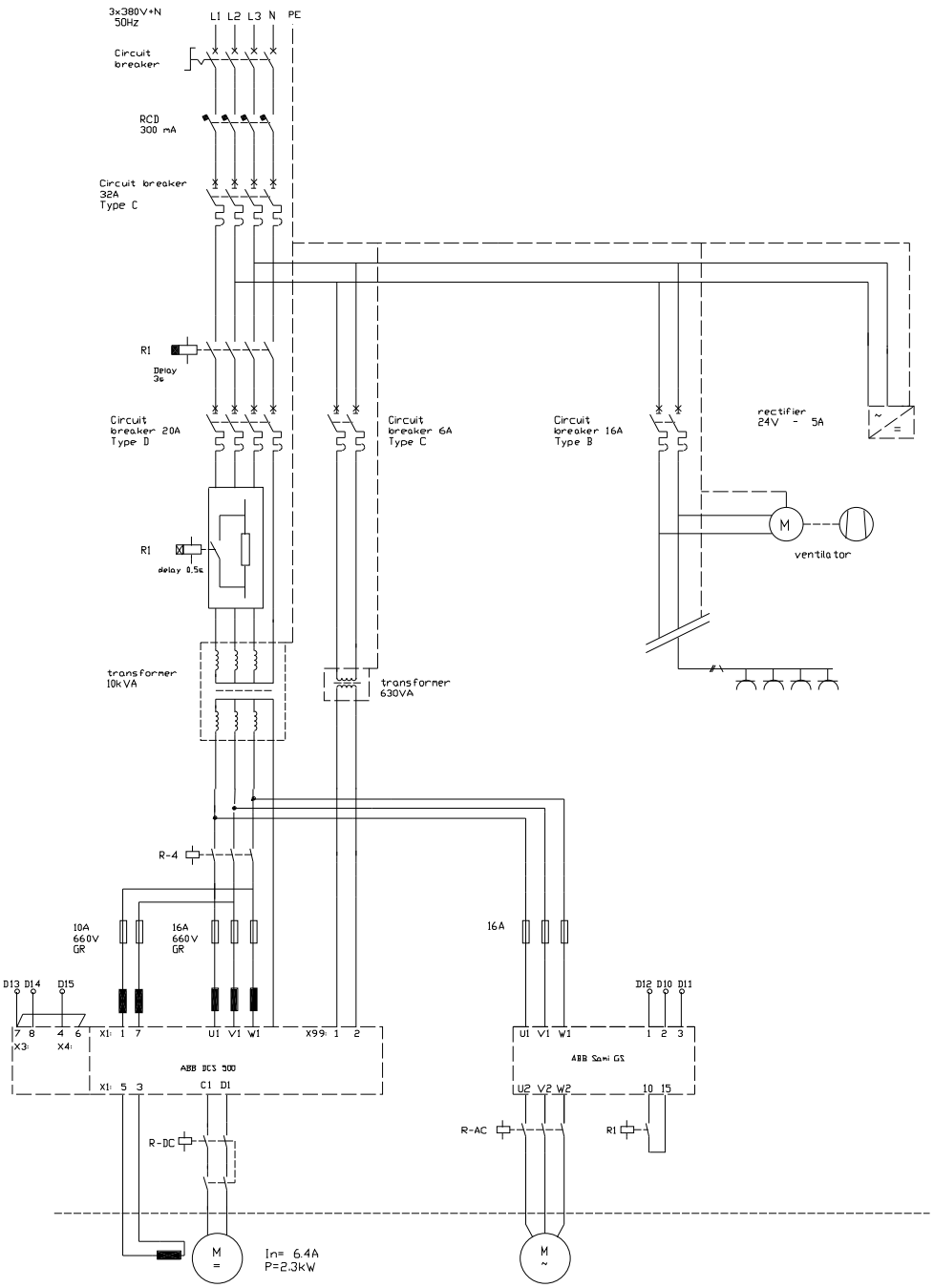

Figure 5.11: Power supply

control has a power button, an emergency stop, 2 signal lights (‘green’ when main power is on, ‘red’ when motor drives are operating). Potentiometers allow to set the references for the torque and speed when the standard data acquisition is not available.

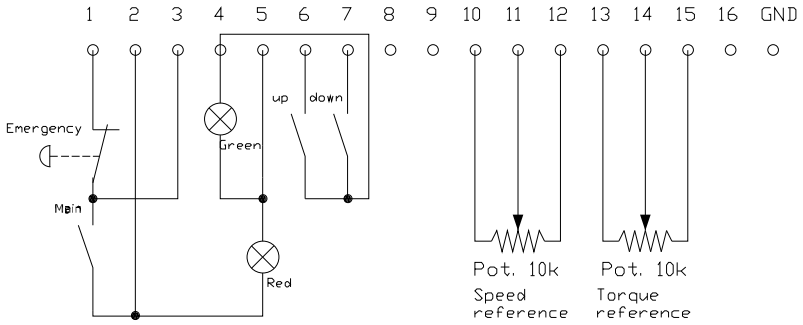

Figure 5.12: The remote control

5.7 Safety measures

Figure 5.13: The pull safety device

Next to the electrical safety measures, the test bench has to meet the specifications of the European machinery directive. Dangerous situations can originate from the movement of the conveyor belt ($\geq 25km/h$), the wheels, the V-belt or the torques developed at the pedalling axis (peak values of $125Nm$ can be reached). The person holding the bicycle has to stay on a safe distance of the moving parts. This is realised by the construction of a cage enclosing the test bench (figure 5.1). At this cage an emergency stop is fixed within reach of the operator.
When the load cell connection at the back would break loose for one or another reason, all drives will be stopped. The used pull safety device is shown in figure 5.13.

For the torque and speed drivers, it is important to bring the reference values to zero before cutting the power.
Other emergency stops are found at the electrical switchboard: one fixed at the switchboard and one at the remote control. The practical implementation of the emergency electrical circuit of the relays is given in figure 5.14 [38].

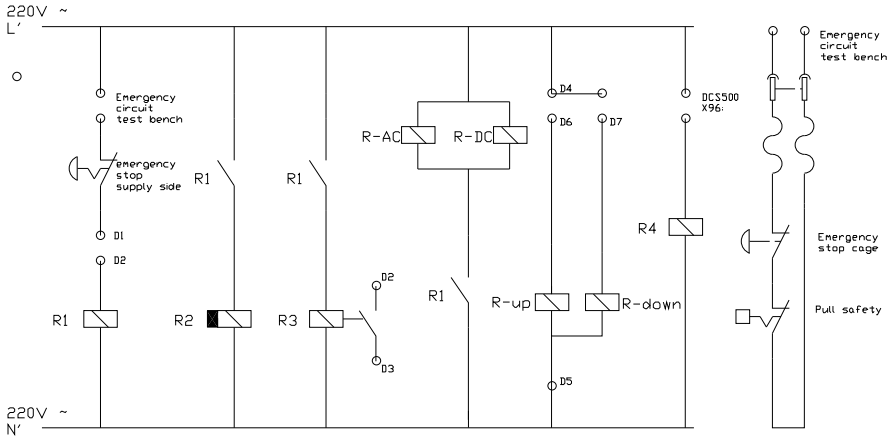

Figure 5.14: The emergency circuit

5.8 Remarks before Testing

A number of things are worth mentioning before one decides to start the measurements.

- The preparation of the pedelec for the performance analysis may take more time than could be expected at first sight:
  - One pedal crank has to be removed to install the pulley for the dummy cyclist (figure 5.2)
  - There seems to be no standard size for the saddle rod of a pedelec. Most of the time, a new coupling part had to be manufactured to fix the DC-motor (which is part of the 'dummy cyclist' of figure 5.2) on the bicycle.
- Two persons are required to perform the test bench measurements: One has to prevent the bicycle from falling by steering, the other one has to control the speed and the torque and has to execute the effective measurement.
- It is recommended to wear ear protection because of the high noise level which is increasing with the belt speed.

- It turned out to be very important to correctly stretch the V-belt, to prevent slip between the V-belt and its pulleys.
- It is not necessarily required to measure the pedelec in all its different gears to characterize its performance. Depending on the place where the input signals for the controller (torque and/or speed) are taken, the influence of gear on the pedelec behaviour may be negligible or not.

5.9 Conclusions

A complete testbench is designed to enable the performance analysis of a pedelec. An effort is made to get as close as possible to the road situation.
A speed can be imposed to a conveyor belt of an old runner's treadmill on which the pedelec is rolling. A torque can be independently imposed to the pedal axis. The resulting traction force is measurable via a loadcell mounted at the back of the bicycle.
A data acquisition is developed to control the speed and torque and to read the sensor signals. Also different safety measures are taken to protect the pedelec as well as the steering person.

6
The Measuring Method

6.1 Determination of the transmission ratio

Figure 6.1: The input and output parameters of the test bench

For the determination of the input and output power described in section 4.2, normally 4 measurements are required:

- T_c = the cyclist torque applied to the pedal axis
- ω = the angular speed of the pedal axis
- F_t = the traction force measured at the load cell
- v = the linear speed of the bicycle

The transmission ratio Z between the linear speed (v) of the wheels and the angular speed of the pedals (ω) is used to eliminate one speed measurement for the bicycles tested on the bench. Because there was no noticeable slip between the bicycle wheels and the belt, nor between the pedal axis and the rear wheel, the transmission ratio is a constant depending on the chosen gear, and the wheel radius. The angular speed of the pedal axis (= ω) multiplied by the transmission ratio (=Z) is a good measure for the average linear speed.

$$Z = \frac{2\pi n_r r_r}{2\pi n_p} = \frac{v}{\omega} \tag{6.1}$$

These transmission ratios are determined for every measured gear by counting the number of turns of the pedal axis (n_p measured by the TTL sensor) while the rear wheel was making a whole number of turns (n_r). Also the radius of the rear wheel (r_r) had to be measured. For the tested pedelecs, Z is varying between 0.37 and 1.44. The exact Z-values per pedelec are represented in table 13.1.

6.2 The area of operation

The bicycles are measured in the on-road operation area:

- The pedalling frequency is changed from 0 to 120 rpm
- The average torque is controlled between 0 and 75 Nm
- The average power is limited at 400 W

In this way we get the marking out of the operation area as illustrated in figure 6.2.

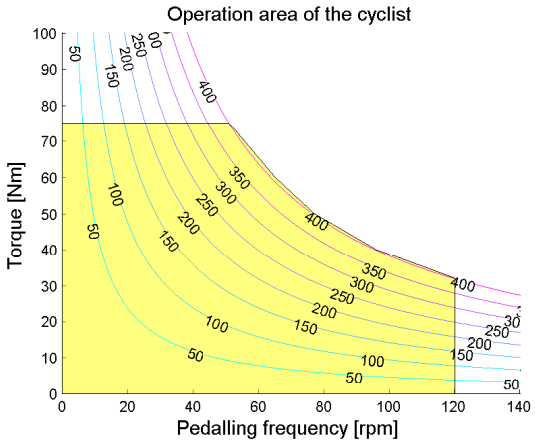

Figure 6.2: The applied limits for power [W], torque [Nm] and pedalling frequency [rpm]

6.2.1 The pedalling frequency limit

The top value of $120rpm$ is experimentally determined as hardly ever reached in city cycling situations. This roughly agrees with riding $20km/h$ in the first gear.

6.2.2 The torque limit

The torque limit is justified by the following reasoning: when a person of $75kg$ pushes the pedals with his full mass, the peak torque on a crank of $17cm$ will reach

$$T_{max} = F_g \cdot l = m \cdot g \cdot l = 75 \cdot 9.81 \cdot 0.17 = 125Nm \tag{6.2}$$

A single recording of the torque during cycling is shown in figure 6.3. The torque can be approximated by a sine wave of twice the pedalling frequency, and an offset of 135% of the amplitude.

$$T_c(t) = \bar{T_c}\left(1 + 0,74sin\left(2\bar{\omega}t\right)\right) \tag{6.3}$$

For a peak torque of $125Nm$, an average torque of

$$T_a = 1.35 \cdot \frac{T_{max}}{1 + 1.35} = 72Nm \tag{6.4}$$

is reached.
The transport services of the French postal operator specifies a maximum human force of $40daN$ exercised by a postman on the pedals. With a crank of $17cm$ this corresponds with a peak torque of $68Nm$.

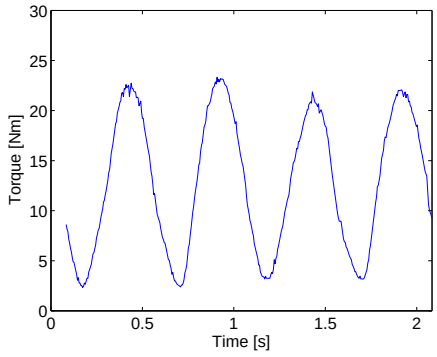

Figure 6.3: A record of the cyclist's torque as a function of time during cycling

6.2.3 The power limit

As experienced during tests on a home trainer, the production of $400W$ can be taken as upper limit for a person of excellent fitness. By comparison, Eddy Merckx needed an average power of $485W$ for his world hour record in 1972 [39]. In figure 6.4 the power of a touring cyclist of $85kg$ (frontal area=0.511m^2, tyre pressure=345kPa) and a racer of $75kg$ (frontal area=0.340m^2, tyre pressure=$689kPa$) is given as a function of speed [40]. This reference also takes $400W$ as a power limit.

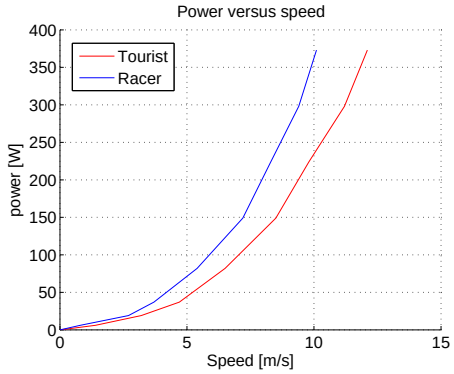

Figure 6.4: The power of a cyclist as a function of speed

6.3 Measurements

According to section 6.1, three parameters left to be recorded: the dummy cyclist torque imposed by the DC-motor, the bicycle speed imposed by the treadmill, and the resulting traction force.
The data acquisition system averages out these parameters over a time interval of $10s$:

$$\bar{T_c} = \frac{1}{T}\int_0^T T_c(t)dt \tag{6.5}$$

$$\bar{\omega} = \frac{1}{T}\int_0^T \omega(t)dt \tag{6.6}$$

$$\bar{F_t} = \frac{1}{T}\int_0^T F_t(t)dt \tag{6.7}$$

where

- ω = the angular speed of the pedal axis
- T_c = the torque applied to the pedal axis
- F_t = the traction force measured at the load cell
- T = the 10 s time of recording.

The measurements are taken in a limited number of operation points: Randomly chosen speed and torque combinations are applied and the resulting traction force of the bicycle is measured. Interpolation of these discrete measurements helps to get an idea of the traction force in every point of the whole operation area. The interpolation and averaging techniques are described in chapter 7.

6.4 Power definitions

The characterisation of the performance of a pedelec is based on a power flow reasoning. Therefore the cyclist's power and the traction power will be defined first.

6.4.1 The cyclist's power

When applying a torque, the calculation of the average power delivered by the (dummy) cyclist can be written as:

$$P_c = \frac{1}{T}\int_0^T T_c(t)\omega(t)dt \tag{6.8}$$

For steady-state measurements (constant speed and torque) the integral can be reduced to

$$P_c = \bar{T}_c \cdot \bar{\omega} \tag{6.9}$$

In the case of a pulsating torque (expression 6.3) combined with a constant speed, the average cyclist's power would be theoretically:

$$P_c = \frac{1}{T}\int_0^T \bar{T}_c\left(1 + 0.74sin\left(2\bar{\omega}t\right)\right)\bar{\omega}dt \tag{6.10}$$

$$= \bar{T}_c\bar{\omega} + \bar{T}_c\bar{\omega}\cdot\frac{1}{T}\int_0^T 0.74sin(2\bar{\omega}t)dt \tag{6.11}$$

The integral of the second term in this expression is zero if T encloses a whole number of evolutions. Because T is fixed for our data acquisition, an error will be introduced depending on the pedalling frequency. The error will be maximum 5.3% for a pedalling frequency of $20rpm$. For a pedalling frequency of $120rpm$ the maximum error is reduced to 0.9%.
No further effort is made to make the interval T variable, because the dynamics of the test bench make it impossible to keep the speed constant for a pulsating torque. The elasticity of the load cell connection at the back of the bicycle causes oscillations in the bicycle movement. So the traction force and speed are also pulsating. There are also phase shifts between those oscillations, what makes a separate averaging of the signals useless.
The correct way of determining the cyclist's power in the oscillatory case is to simultaneously sample the torque and speed, and average the product of both signals.
Experiments with an extra spring at the load cell are performed to improve the dynamic response. However, these experiments were ended because the existing data acquisition could not perform the required simultaneous measurements without extra investment (read also chapter 15).
The steady-state case is seen as sufficiently accurate for the intended performance analysis.

6.4.2 The traction power

On the road, the cyclist's power is required to maintain a certain speed because there are several forces resisting forward motion:

- the mechanical losses in the transmissions of the bicycle
- the rolling resistance
- the air-resistance
- the slope resistance

Using Newton's law, one can state that a propulsive force $\vec{F}_p$ is needed to overcome the above mentioned resistances and to be able to accelerate.

$$\vec{F}_p = m_{tot}\frac{d\,\vec{v}}{dt} + \vec{F}_{air} + \vec{F}_{slope} + \vec{F}_{roll} + \vec{F}_{loss} \tag{6.12}$$

On the test bench, the rolling resistance and the mechanical losses are comparable to the road situation and are not included in the measured traction force.
The air and slope resistances are absent.[1] However, the bicycle exercises a traction force $\vec{F}_t$ (equation 6.13) on the loadcell that is a measure for the net propulsive power or the traction power P_t. This is the power that in normal road condition can be used to

- accelerate
- defeat the air resistance
- defeat the slope resistance

$$\vec{F}_t = \vec{F}_p - \left(\vec{F}_{roll} + \vec{F}_{loss}\right) = m_{tot}\frac{d\,\vec{v}}{dt} + \vec{F}_{air} + \vec{F}_{slope} \tag{6.13}$$

In steady-state conditions the traction power can be written as:

$$P_t = \frac{1}{T}\int_0^T F_t(t)v(t)dt = \bar{F}_t\bar{v} \tag{6.14}$$

where

- $\bar{F}_t$=average traction force
- $\bar{v}$=average linear speed

The traction power can be derived from the measured quantities (F_t and ω), by eliminating the linear speed.

$$P_t = \bar{F}_t\bar{v} = \bar{F}_t Z\bar{\omega} \tag{6.15}$$

In the next chapters only steady state measurements will be discussed.

[1] In the first design of the test bench also a slope resistance could be introduced by lifting the bench with a hydraulic pump, unfortunately the dynamics of the existing pump were to slow to react on the cyclist's power variation (read also chapter 15).

6.5 Conclusions

The intended performance analysis will model the pedelec's behaviour by means of the relationship between the cyclist's input power and the traction output power. The definitions of these powers are given in this chapter.
The measurement method is based on 4 quantities: the pedal torque, the traction force, the angular speed of the pedal axis and the linear speed of the wheels. One of the speeds can be eliminated by introducing the transmission rate.
The measuring of three remaining quantities is limited to the real area of operation of a pedelec on the road. This area is marked out based on measurements and scientific references. The next chapters will show how these quantities are translated into performance plots and performance parameters of a pedelec.

7
Regression Modelling

The intended objective analysis of the pedelec's perfomance will be based on two presentation techniques

- The performance plots (chapter 9)
- The performance parameters (chapter 10)

Both techniques will rely on the same test bench measurements. A measurement data set is a $n \times 3$ matrix, where n represents the number of *steady state* measurements. The three columns represent respectively the speed, the cyclist torque and the traction force.
The behaviour of a pedelec on the test bench is a relative complex phenomenon. There are several energy sources, motor drives and internal and external measurements involved during testing. All these apparatus have a limited accuracy. So the recorded measurement data are subject to measurement errors. The relationship between the torque, the speed and the traction force during the tests is not deterministic, but has to be interpreted in a probabilistic way. Moreover measurements can only be taken in a limited number of operation points, a regression technique will be necessary to predict the behaviour in the whole operation area.
Because of these difficulties, different *regression models* will be derived from the measurement data set. These models will be used to highlight different aspects of the pedelec's behaviour. The description of these models will be treated in detail in chapter 8.
Many ways of solving multiple regression analysis problems are available in the literature (for example [41],[42],[43]). This chapter will look for a suitable one for the test bench measurements.

7.1 Regression analysis for the test bench measurements

Figure 7.1: The test bench measurement as a datagenerator for the regression analysis

In the case of the modelling of a pedelec's behaviour, the measurement of the pedelec on the test bench is the experiment that serves as a data generator for the regression analysis. This regression analysis should result in a measurable function (the model) that predicts the output $\hat{Y}$ given any new input data $X^* = (x_1^*, x_2^*)$. This is represented in figure 7.2.

Figure 7.2: The regression model as output prediction for new inputs

Which variables or combination of variables that will be considered as input and which ones as output will depend on the intended performance plot or parameter. All combinations of interest are given in chapter 8.
In all cases, the input exists of two of the three measured quantities (e.g. the pedelec speed and cyclist torque) and will be referred to as $X = (x_1, x_2)$. The third measurement (e.g. the traction force) or a combination of measurements will be considered as the output Y. This is schematically represented in figure 7.1.
In the next sections, the following notation will be used:

- $X = (x_1, x_2) \in \mathcal{X} \subseteq \mathbb{R}^2$, where $\mathcal{X}$ are all possible pairs of the input
- $Y \in \mathcal{Y} \subseteq \mathbb{R}$, where $\mathcal{Y}$ are all possible values of the output

The regression problem can be stated as follows:
Find a measurable function $m : \mathcal{X} \rightarrow \mathcal{Y}$, such that $m(X)$ is an 'optimal approximation' of Y.
Distinction between different 'well approximating functions f' are made by a penalization of the errors. Therefore the mean squared error criterium is typically used. In this case, the theoretical risk functional $\mathcal{R}_{theor}(f)$ of expression 7.1 is to be minimized .

$$\mathcal{R}_{theor}(f) = E\left[(f(X) - Y)^2\right] \tag{7.1}$$

So the 'optimal' approximation m will be the one where [43]

$$E\left[(m(X) - Y)^2\right] = \min_{f:\mathbb{R}^2 \rightarrow \mathbb{R}} E\left[(f(X) - Y)^2\right] \tag{7.2}$$

The function $m(X)$ is called the regression function. This function can be obtained explicitly as follows:

$$m(x_1, x_2) = E[Y|X = (x_1, x_2)] \tag{7.3}$$

Since the output Y is only given for a limited number of measurement data, finding the exact mininum of expression 7.1 is impossible. So, one is obliged to *estimate* the regression function $m(X)$ from these measurement data.

7.2 The regression estimation problem

For the modelling of the behaviour of the pedelec on the test bench, one wants to use a dataset of n measurements $\mathcal{D}_n = \{(X_1, Y_1), ..., (X_n, Y_n)\}$ in order to construct an optimal estimate $\hat{m}_n : \mathcal{X} \to \mathcal{Y}$ of the regression function m. The hat on the function name $\hat{m}_n$ indicates that it concerns an estimate for the regression function, the index n indicates how many measurement data there are considered.

In general, estimates will not equal the regression function. Several error criteria, which measure the difference between the regression function and an arbitrary estimate f are used [43]. In this case the L_2 risk functional $\mathcal{R}_{emp}$ of expression 7.4 will be used to measure the quality of an estimate f.

$$\mathcal{R}_{emp}(f) = \frac{1}{n}\sum_{k=1}^{n}(f(X_k) - Y_k)^2, \tag{7.4}$$

The smaller $\mathcal{R}_{emp}(f)$, the better the estimator f. Unfortunately minimizing the empirical L_2 risk functional leads to infinitely many solutions: any function passing through the measurement points $\mathcal{D}_n$ is a solution.
In order to obtain useful results for finite n, one must *restrict* the possible solutions by choosing a suitable function class $\mathcal{F}$ for the functions f.
The restricted regression estimation problem can be stated as follows: Find $\hat{m}_n \in \mathcal{F}$ such that

$$\frac{1}{n}\sum_{k=1}^{n}(\hat{m}_n(x_k) - Y_k)^2 = \min_{f\in\mathcal{F}}\frac{1}{n}\sum_{k=1}^{n}(f(X_k) - Y_k)^2. \tag{7.5}$$

In the test bench measurement system, the input-output pairs (X, Y) do not have a deterministic relationship $Y_k = m(X_k)$. There are unmeasurable variables that also contribute to Y, including measurement errors.
The additive error model of expression 7.6 *assumes* that one can capture all these deviations via an error *e*.
In this way, an arbitrary output Y_k may be written as

$$Y_k = m(X_k) + e_k. \tag{7.6}$$

Here the Gauss-Markov conditions are assumed:

- the error term in the model is supposed to have mean zero ($E[e_k] = 0$)
- the error term in the model is supposed to have a constant variance ($E[e_k^2] = \sigma^2 < \infty$)
- the $\{e_k\}$ are uncorrelated random variables ($E[e_k, e_l] = 0; \forall k \neq l$)

The choice of the function class $\mathcal{F}$ and the above mentioned assumptions lead to different classes of restricted regression estimators.
For the applied performance analysis of pedelecs, two different regression estimate methods are tried out: a parametric and a non-parametric one. They are described and illustrated with an example in the next sections.

7.3 Parametric modelling

The classical approach for estimating a regression function is the parametric regression estimation. One assumes that the structure of the regression function is known and depends only on a finite number of parameters.

7.3.1 Polynomial regression

The parametric modelling used for the test bench is a *polynomial regression*. Because of the presence of the assistance motor, and internal losses, linear regression will not suffice. In all probability there will be higher order and interaction effects. In the case of the test bench, a typical dataset of n measurements may be written as $\mathcal{D}_n = \{(X_1, Y_1), ..., (X_n, Y_n)\}$, where X_i represents the input existing of a pair of two measurements (x_{1i}, x_{2i}).
The polynomial regression estimate function should be a polynomial of 2 variables x_1 and x_2. The highest degree of variable x_1 is called p, the highest degree of variable x_2 is called q. The regression estimate function should be an element of the function class $\mathcal{F}$ of expression 7.7.

$$\mathcal{F} = \left\{ f : f(x_1, x_2) = \sum_{i=0}^{p} \sum_{j=0}^{q} \beta_{ij} x_1^i x_2^j,\ \beta_{ij} \in \mathbb{R} \right\} \tag{7.7}$$

The coefficients $\hat{\beta}_{00}, \ldots, \hat{\beta}_{kl} \in \mathbb{R}$ of the optimal regression estimator

$$\hat{m}_n(x_1, x_2) = \sum_{i=0}^{p} \sum_{j=0}^{q} \hat{\beta}_{ij} x_1^i x_2^j \tag{7.8}$$

may be calculated by minimalizing the empirical risk functional.

$$\left(\hat{\beta}_{00}, ..., \hat{\beta}_{kl}\right) = \min_{\beta_{00},...,\beta_{kl} \in \mathbb{R}} \left[\frac{1}{n} \sum_{k=1}^{n} \left(Y_k - \sum_{i=0}^{p} \sum_{j=0}^{q} \beta_{ij} x_1^i x_2^j) \right)^2 \right] \tag{7.9}$$

This minimization may be executed by a numerical computing program. In this work the Matlab toolbox 'Polybase' was used, which offers tools for multidimensional polynomial interpolation and approximation. This toolbox is developed by Giampiero Campa [44].

7.3.2 Example

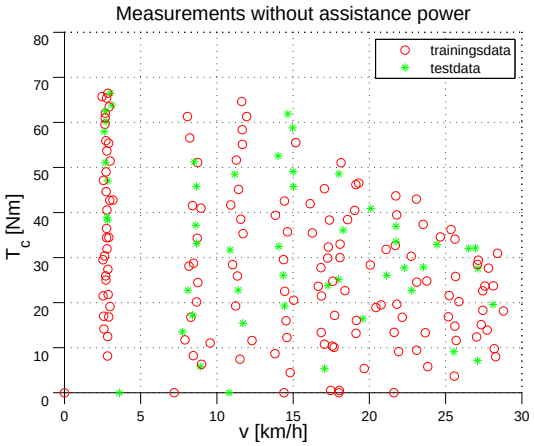

Figure 7.3: Random split of measurement data in a training (*) and test (o) data set

As an example the polynomial regression will be applied on the measurement data of the Sparta Ion without motor assistance and with normal motor assistance. The speed and the cyclist torque will be considered as the input X, the resulting traction force as the output Y. Or more specifically,

- x_{1i} represents the recorded speed during the i-th measurement
- x_{2i} represents the recorded torque during the i-th measurement
- Y_i represents the recorded traction force during the i-th measurement

If all the measurement data would be used to determine the coefficients, there would be no data left to evaluate how 'good' the polynomial predicts the output for new inputs. Therefore, it is common sense to split the measurement data randomly in a training data set and a test data set as shown in figure 7.3. In this case, there is chosen to withhold 75% of the measurements as training data to estimate the regression function. The other 25% are used as test data to verify the model using the RMSE. The choice for the 75-25% split is based on the fact that this RMSE should be statistically relevant even with the rather small number of measurement data available. The splitting of data in training and test data is extensively discussed in reference [45].

$$RMSE = \sqrt{\frac{1}{n_t}\sum_{k=1}^{n_t}\left(Y_k - \hat{m}(x_{1k}, x_{2k})\right)^2} \tag{7.10}$$

where n_t is the number of test data. Note that the RMSE on the training data is not a good indicator for the 'goodness' of the estimation since it does not tell anything about the output for new data and because the algoritms for minimization of expression 7.9 try to bring this RMSE to zero. So only the RMSE on the test data will be used to compare the estimations.

One can imagine that the traction force will be proportional to the cyclist's torque in the case without assistance power. There might be only a small influence of the speed due to internal losses of the transmission. So the highest degree for both input variables $x_1 = v$ and $x_2 = T$ is chosen to be 1.
A Matlabscript is written to calculate the coefficients of the polynomial according to the least square criterium of expression 7.9. The resulting regression estimation function $\hat{m}_t(v, T)$ for the traction F_t force looks like

$$\hat{F}_t = \hat{m}(v, T) = -2.67 + 0.053v + 1.20T + 0.0007vT \tag{7.11}$$

Comparing the coefficients is difficult in this absolute form because they all have different dimensions. It is better to rescale the polynomial by dividing it by a reference value, so that all coefficients become dimensionless. Based on a single set of values that are measured without assistance, the references will be:

- $v_{ref} = 25km/h$
- $T_{ref} = 75Nm$
- $F_{ref} = 90N$

The notation of the dimensionless or per unit variables will be the originally variable names with the subscript pu. The rescaled polynomial becomes in per unit

$$\hat{F}_{t_{pu}} = -0.0295 + 0.0147v_{pu} + 1.00T_{pu} + 0.0145v_{pu}T_{pu} \tag{7.12}$$

The function 7.11 is visualised in the left plot of figure 7.4. The independency of speed is visuable as well in the coefficients as in the figure 7.4. The RMSE of this estimation is $2.1N$ or $0.023\ per\ unit$.
Including higher order terms seems not to be interesting, but was done to see if the suggestion of linearity was a good starting point. The result of a third order approximation is shown on the right plot of figure 7.4. Except of some borderphenomena, both plots are very simular. The RMSE in the latter case is $1.8N$ or $0.020\ per\ unit$.

Performing the same regression analysis on the measurements of the Sparta Ion with normal assistance, the assumption of linearity has to be quit. The behaviour of the controller is not known in advance, and higher order terms will have to be included. An estimate of the highest degree has to be made for the input $x_1 = v$ (degree p) and the input $x_2 = T$ (degree q) as written in expression 7.9.
The resulting per unit regression estimation function $\hat{F}_{t_{pu}}(v_{pu}, T_{pu})$ with

- the highest order for v_{pu} : $p = 2$

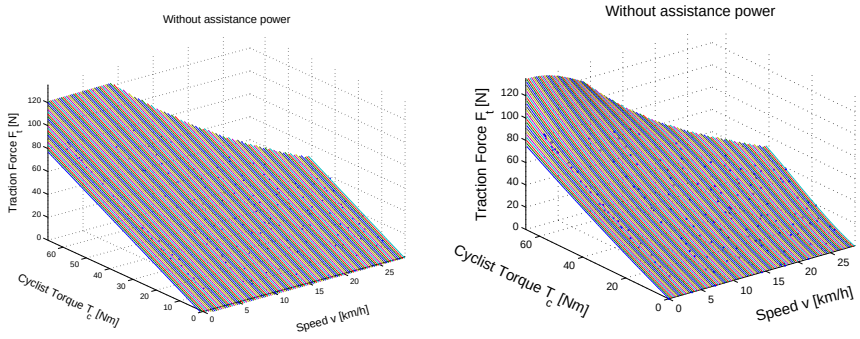

Figure 7.4: Polynomial regression estimation for the Sparta Ion without assistance with first order approximation (left) and with third order approximation (right)

- the highest order for T_{pu} : $q = 4$

looks like

$$\begin{aligned}\hat{F}_{t_{pu}} \quad = \quad & -0.0053 + 0.111v_{pu} - 0.0849v_{pu}^2 + 0.397T_{pu} - 0.609v_{pu}T_{pu} + \\ & 0.692v_{pu}^2T_{pu} + 4.94T_{pu}^2 + 17.2v_{pu}T_{pu}^2 - 20.4v_{pu}^2T_{pu}^2 - 6.21T_{pu}^3 \\ & -42.5v_{pu}T_{pu}^3 + 47.1v_{pu}^2T_{pu}^3 + 2.67T_{pu}^4 + 26.0v_{pu}T_{pu}^4 \\ & -27.0v_{pu}^2T_{pu}^4 \end{aligned} \tag{7.13}$$

This function (in absolute values) is visualised in the left plot of figure 7.5.

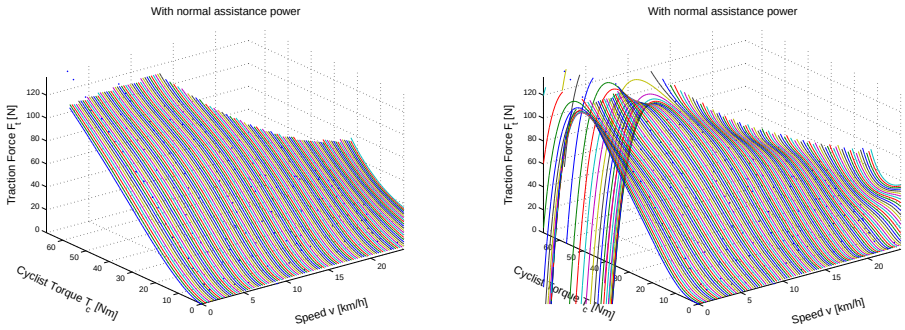

Figure 7.5: Polynomial regression estimation for the Sparta Ion with normal assistance lower order approximation (left) and higher order approximation (right)

The lower degree terms in expression 7.13 may be neglected in comparison to the higher degree terms. The RMSE of the estimation for the described case with assistance is $2.6N$ or $0.029\ per\ unit$.

Chosing higher numbers for p and q results in higher root mean squared errors and unreliable side effects as shown in the right plot of figure 7.5. For this plot $p = 4$ and $q = 6$ is chosen. The RMSE on the test data is $5.1N$ or $0.056\ per\ unit$. Chosing a 'good' highest order term seems to be an important issue: with $p = 6$ and $q = 8$ the RMSE becomes already $22.5N$ or $0.25\ per\ unit$.

As shown in the example, parametric estimates have a drawback. Choosing the order of the polynomial stays a bit arbitrary and has to be done over for every new set of measurement data. Regardless of the data, a parametric estimate cannot approximate the regression function better than the best function with the assumed parametric structure. This inflexibility concerning the structure of the regression function is avoided by non-parametric regression estimates [43].

7.4 Non-parametric modelling

Different classes of non-parametric modelling methods can be found in literature:

- local averaging and local modelling
- global modelling
- penalized modelling

7.4.1 LS-SVM

For the performance analysis of pedelecs, a combination of local and penalized modelling will be used: Least Squares Support Vector Machines or LS-SVM regression modelling. The key ingredient of the support vector machine is the following[43]:
It maps the random input vector $X \in \mathcal{X} \subseteq \mathbb{R}^2$ into a high-dimensional feature space $\Psi \subseteq \mathbb{R}^{n_f}$ through some nonlinear mapping $\varphi : \mathcal{X} \rightarrow \Psi$. In this space, one consider the class of linear functions

$$\mathcal{F}_\Psi = \left\{ f : f(x_1, x_2) = w^T \varphi(x_1, x_2) + b, \varphi : \mathcal{X} \rightarrow \Psi,\ w \in \mathbb{R}^{n_f},\ b \in \mathbb{R} \right\} \quad (7.14)$$

The goal is to find the parameters w and b (primal space) that minimize the empirical risk functional

$$\mathcal{R}_{emp}(w, b) = \frac{1}{n} \sum_{k=1}^{n} \left(\left(w^T \varphi(x_{1k}, x_{2k}) + b \right) - Y_k \right)^2 \quad (7.15)$$

under constraint $\|w\|_2 \leq a$, $a \in \mathbb{R}_+$.
The optimization problem can be reduced by finding the vector w and $b \in \mathbb{R}$ by solving the following optimization problem [43]

$$\min_{w,b,e} \mathcal{J}(w, e) = \frac{1}{2} w^T w + \frac{1}{2} \gamma \sum_{k=1}^{n} e_k^2, \quad (7.16)$$

such that

$$Y_k = w^T \varphi(x_{1k}, x_{2k}) + b + e_k,\ k = 1, ..., n \tag{7.17}$$

Note that the cost function $\mathcal{J}$ consists of a fitting error and a regularization term. The relative importance of these terms is determined by the positive real constant γ. In the case of noisy data one avoids overfitting by taking a smaller γ value.
Constructring the linear function 7.17 in the feature space can be done without considering this feature space in explicit form. One may replace the inner product $\varphi(x_{1k}, x_{2k})^T \varphi(x_{1l}, x_{2l})$ with the corresponding Kernel $K((x_{1k}, x_{2k}), (x_{1l}, x_{2l}))$ satisfying Mercer's condition. The resulting LS-SVM model for function estimation becomes [43]

$$\hat{m}_n(x_1, x_2) = \sum_{k=1}^{n} \hat{\alpha}_k K((x_1, x_2), (x_{1k}, x_{2k})) + \hat{b}, \tag{7.18}$$

where $\hat{\alpha}$ and $\hat{b}$ can be derived using Lagrangian functionals and Mercer's theorem [47]. This complete optimization process is automatically performed by the LS-SVM toolbox developed for Matlab [46].

7.4.2 Example

As an example the LS-SVM regression method will be applied on the same measurement data of the Sparta Ion as in section 7.3.2. The LS-SVM toolbox [46] is adapted to give the estimated regression function of the traction force.

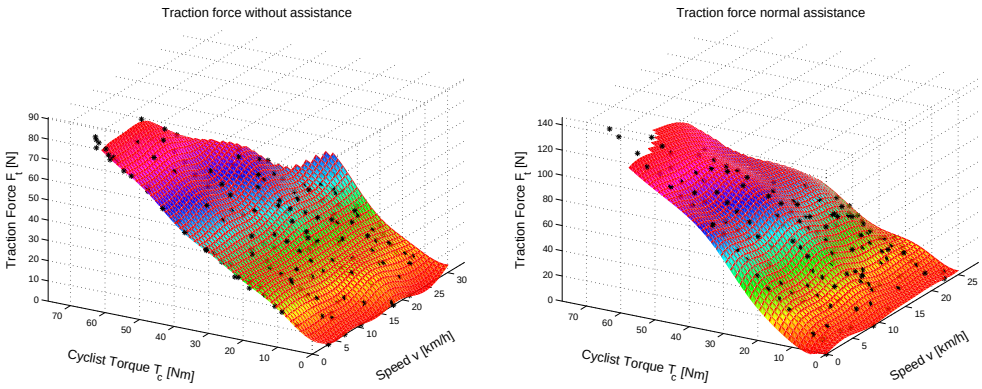

Figure 7.6: LS-SVM regression estimation for the Sparta Ion without motor assistance (left) and with normal motor assistance (right)

The same training and test data set of figure 7.3 are used. The training data set helps to construct the regression estimator and the data set will help to evaluate the

predictabitity for new data. The RMSE on these test data will be used to compare the LS-SVM estimations with the polynomial ones.
In the case without assistance, the regression estimate plot looks like the left surface of figure 7.6.
The RMSE on the test data is $2.2N$.
In the case of normal motor assistance, the regression estimate plot looks like the right surface of figure 7.6. The RMSE is $2.3N$, which is smaller than in the polynomial case.
The more non-linear the assistance power, the more interesting it will be to use the LS-SVM. Because the behaviour of an assisted pedelec is rather unpredictable, the LS-SVM was chosen to create the pedelec models.
For the analysis of the pedelec's performance more than one regression function will be used. They are all discussed in chapter 8.

7.5 Conclusions

Regression analysis is necessary to estimate the output for an input that was lying in between different testbench measurements. After all, the calculation of the performance parameters and the presentation of the performance plots require all intermediate values. In this chapter different regression techniques were tried out to make a regression model of the behaviour of the pedelec on the testbench. In order to choose the best regression method, the measurements were split into a training and test data set. Each regression estimate was derived by means of the same training set and was evaluated by calculating the root mean squared error (RMSE) on the same test data set. The non-parametric LS-SVM method turned out to give the smallest RMSE and will be used in the next chapters.

8

The Regression Models for a Pedelec

The data acquisition system described in chapter 5.4 automatically generates lists of measurement data sets. They are saved as tables where every row represents a measuring point with 3 columns: the speed, the cyclist torque and the traction force. The place where these quantities are measured are found in figure 4.3.
These data sets are transformed by regression analysis in different models describing the pedelec's behaviour. These models are obtained by different choices for the (independent changing) input variables X and the (dependent changing) output variables Y. The preferred regression technique is the LS-SVM method according to the qualities described in chapter 7.
Normally a set of three LS-SVM models will be worked out for one measurement data set:

- The traction force model
- The required cyclist torque model
- The efficiency model

A fourth type of regression model, *the assistance factor model*, is derived by comparing two traction force models (see section 8.4) of the same pedelec.
All investigated pedelecs have the possibility to ride with or without the motor power switched on. And although most manufacturers have a pre-programmed control strategy, the user can often choose between different assistance modes.
The measurement of one pedelec may so exist of different data sets corresponding with

- different motor assistance levels or power modes
- different gears

- different battery charging levels
- different peripheral conditions: tyre conditions, lubricating conditions,motor temperature...

This would lead to a multitude of regression models, which will not always be useful. The standard method choosen is to record one data set without motor power and one data set per motor assistance level with a fully charged battery. Only one representative gear has been recorded.

8.1 The traction force model

The basic LS-SVM models are the traction force models. They estimate the regression function $m_1(\bar{v}, \bar{T_c})$ for the traction force. The combination of a bicycle speed ($\bar{v}$ in km/h) and a cyclist torque ($\bar{T_c}$ in Nm) will be considered as the input variables X. The traction force ($\bar{F_t}$ expressed in N) is the output Y of the regression problem. All variables are average values taken over $10s$ of steady-state operation. The LS-SVM model gives an estimate $\hat{F_t}$ of the traction force in an arbitrary point of the operation area.

$$\hat{F_t} = \hat{m_1}(\bar{v}, \bar{T_c}) \tag{8.1}$$

Instead of the notation 8.1, the shorter notation $\hat{F_t}(\bar{v}, \bar{T_c})$ for this traction force model will be used in the remaining of the text.
The LS-SVM model $\hat{F_t}(\bar{v}, \bar{T_c})$ is derived for all measured assistance levels. The data set is randomly splitted in 75% training data and 25% test data. The model is derived by only using the training data as explained in chapter 7.
The graphical user interface (developed to handle the test bench measurements and discussed in chapter 12) foresees a standard of 4 traction force models for a single pedelec:

- $F_t\_ModelZA$: the traction force model of the pedelec without motor assistance (Zero Assistance)
- $F_t\_ModelMAe$: the traction force model of the pedelec with a low motor assistance (Motor Assists Economically)
- $F_t\_ModelMAn$: the traction force model of the pedelec with normal motor assistance (Motor Assists Normally)
- $F_t\_ModelMAp$: the traction force model of the pedelec with extra motor power (Motor Assists Powerfully)

Two graphical representations of traction force models are already shown in the figure 7.6.
The predictive capacity of the models is evaluated by looking at the RMSE on the test data. These RMSE values are available for all models via the graphical user interface.

8.2 The required torque model

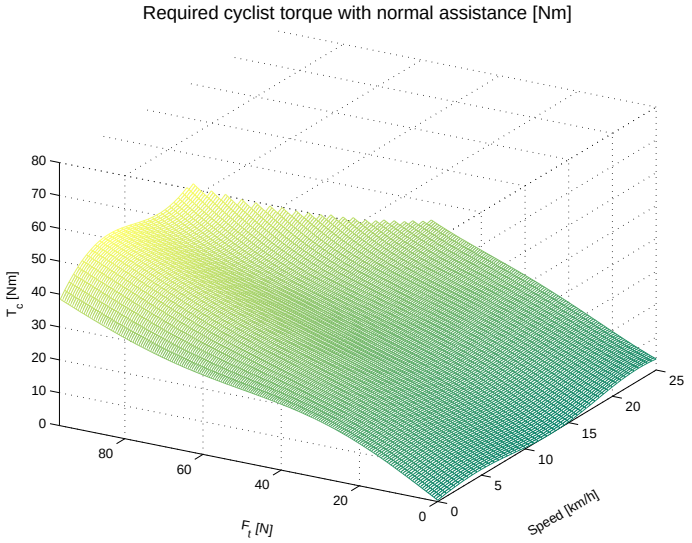

Figure 8.1: Graphical representation of a required torque model

The traction force model gives an idea of the traction power resulting from the cyclist's efforts and the assistance motor contribution. Another idea is to model the cyclist's efforts required to reach a certain traction power. Rather than merely inverting the traction force model, a new model is calculated. Therefore the speed and the traction force of the measurement data are considered as the input X and the torque will be the output Y for the estimate of the regression function $m_2(\bar{v}, \bar{F}_t)$ for the torque.
So, the required torque LS-SVM model will give an estimate $\hat{T}_c = \hat{m}_2(\bar{v}, \bar{F}_t)$ for the steady state torque that is necessary to realize a certain (steady-state) traction force at a certain speed. Similar to the shorter traction force model notation, the notation $\hat{T}_c(\bar{v}, \bar{F}_t)$ will be used to indicate this regression model.
The model will be derived by using the training data set. The estimation will be checked by calculating the RMSE on the testdata as defined in equation 7.10.
The graphical user interface of chapter 12 foresees a standard of 4 required torque models for a single pedelec:

- $T_c\_ModelZA$: the required cyclist torque model of the pedelec without motor assistance
- $T_c\_ModelMAe$: the required cyclist torque model of the pedelec with a low motor assistance
- $T_c\_ModelMAn$: the required cyclist torque model of the pedelec with normal motor assistance

- $T_c\_ModelMAp$: the required cyclist torque model of the pedelec with extra motor power

The graphical representation of a $T_c\_ModelMAn$ model is shown in the figure 8.1.

8.3 The efficiency model

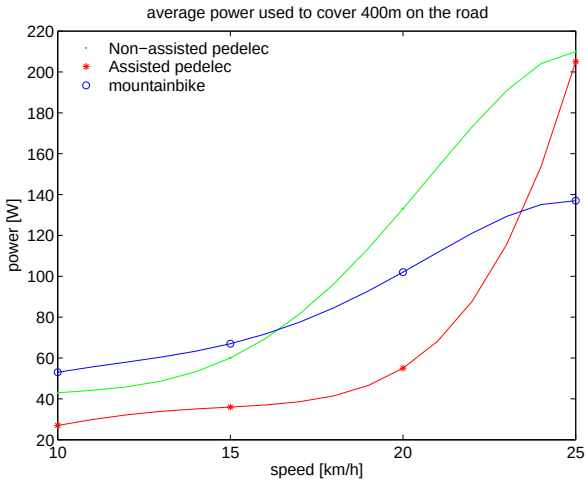

Figure 8.2: Results of an exploring road test

Pedelecs are heavier and have a more complex drivetrain than a common bicycle. This might result in a worse mechanical efficiency. One of the first pedelec tests performed at the *Vrije Universiteit Brussel* is a road test with a heart rate measurement to get an idea of the power that is required to cover a distance on a pedelec with and without motor assistance. The same distance is also covered with a common mountainbike [37] to compare the required efforts. The result of this small road test is given in figure 8.2. It looks like the pedelec without assistance has a worse efficiency than the (old and heavy) mountainbike. That is the reason why also the mechanical efficiency of the pedelecs is investigated over the whole operation area.
The *mechanical efficiency of the non-assisted pedelec on the test bench* will be defined as the ratio of the output traction power without motor power ($P_{t_{ZA}}$) and the cyclist's input power (P_c).

$$\eta = \frac{P_{t_{ZA}}}{P_c} \tag{8.2}$$

Because there are no power flows measured, only a steady-state efficiency $\bar{\eta}$ can be derived from the test bench measurements without assistance using the equations 6.9

and 6.14.

$$\bar{\eta} = \frac{P_{t_{ZA}}}{P_c} = \frac{\bar{F}_{t_{ZA}}\bar{v}}{\bar{T}_c\bar{\omega}} = \frac{\bar{F}_{t_{ZA}}}{\bar{T}_c}Z \tag{8.3}$$

The constant Z is the transmission ratio of the measured gear as defined in 6.1.
Two possibilities for the calculation of the efficiency of the pedelecs in the whole operation area starting from the discrete measurement data are considered.

1. The calculation of the efficiencies by applying equation 8.3 for the whole operation area using the LS-SVM regression model $\hat{F}_{t_{ZA}}(\bar{v}, \bar{T}_c)$ (section 8.1).
2. The creation of a new LS-SVM regression model starting from the calculated efficiencies of the measurement data only.

The second possibility is preferred because it gave a smaller RMSE error when applied on a new test data set.

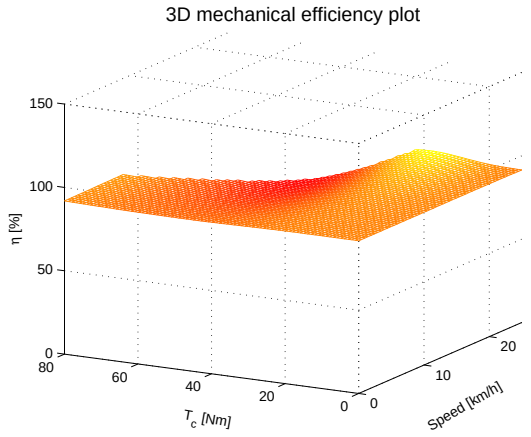

Figure 8.3: Graphical representation of an efficiency model

So, the efficiency $\bar{\eta}$ is first evaluated in all the measurement points of the pedelec without motor assistance. As a result, the data set without assistance is extended with an extra column of efficiency data. Considering the speed and the torque as the input variables X and the efficiency as the output variable Y, a LS-SVM regression model for the efficiency $m_3(\bar{v}, \bar{T}_c)$ over the whole operation area may be calculated [1]. Again only 75% of this data set is used to derive the LS-SVM model that estimates the steady-state efficiency $\hat{\eta}$.

$$\hat{\eta} = \hat{m_3}(\bar{v}, \bar{T}_c) \tag{8.4}$$

[1]The efficiency could also be modelled as a function of the speed and the traction force $\hat{\eta_2} = \hat{m}_{3b}(\bar{v}, \bar{F}_t)$ but this was seen as unuseful for the rest of the performance analysis (see section 10).

The efficiency model will also be noted shorter as $\hat{\eta}(\bar{v}, \bar{T_c})$. It may be clear from expression 8.3 that the accuracy of this LS-SVM model will be rather poor for smaller torques and speeds. The ability of the model to predict the efficiency for new data points is again evaluated by calculating the RMSE on the remaining 25% of the data set.

The graphical user interface of chapter 12 foresees the calculation of one efficiency model per pedelec. It is called the ETA_model.
The graphical representation of an example efficiency model is given in figure 8.3.

8.4 The assistance factor model

In the case of a pedelec, the resulting traction power (P_t) is partly coming from the cyclist's effort (P_{tc}) and partly from the electric assistance motor (P_{tm}).

$$P_t = P_{tc} + P_{tm} \tag{8.5}$$

An important parameter for the pedelecs will be the relationship between those two power sources. This is expressed in the so-called assistance factor (ξ), the net contribution of the motor divided by the total traction power.

$$\xi = \frac{P_{tm}}{P_t} \tag{8.6}$$

The assistance factor is a number between 0 and 1.

- $\xi = 0$: all traction power is coming from the cyclist's efforts
- $\xi = 1$: all traction power is coming from the motor

The motor power is not directly measured. This could have been done by measuring the voltage and current at the motor connection, but this was not always within easy reach (see section 15). Moreover our main interest is not the electrical power of the motor, but the net contribution of the battery-motor system to the traction power. This net contribution P_{tm} can be derived from the comparison of the traction power with electrical assistance $P_{t_{MA}}$ and without electrical assistance $P_{t_{ZA}}$ for the same input speed and torque.

$$P_{tm} = P_{t_{MA}} - P_{t_{ZA}} \tag{8.7}$$

Expression 8.6 is in this way changed in expression 8.8.

$$\xi = \frac{P_{t_{MA}} - P_{t_{ZA}}}{P_{t_{MA}}} = 1 - \frac{P_{t_{ZA}}}{P_{t_{MA}}} \tag{8.8}$$

Using equation 6.14 for the cases with (MA) and without (ZA) assistance power results in a practical formula 8.9 for the calculation of the steady-state assistance factor $\bar{\xi}$ starting from the measurement data:

$$\bar{\xi} = 1 - \frac{\bar{F}_{t_{ZA}}}{\bar{F}_{t_{MA}}} \tag{8.9}$$

$\bar{F}_{t_{ZA}}$ is the measured traction force at a given speed v resulting from the cyclist torque T_c without motor power.
$\bar{F}_{t_{MA}}$ is the traction force at the same speed v and for the same cyclist torque T_c while the motor assists.

Two possibilities for the modelling of the assistance factor of the pedelecs in their operation area starting from the discrete measurement data are considered:

- The calculation of the assistance factors by applying equation 8.9 for the whole operation area using the LS-SVM regression models $\hat{F}_{t_{ZA}}(\bar{v}, \bar{T}_c)$ and $\hat{F}_{t_{MA}}(\bar{v}, \bar{T}_c)$ (section 8.1).
- The creation of a new LS-SVM regression model starting from the calculated assistance factors in the measurement points only.

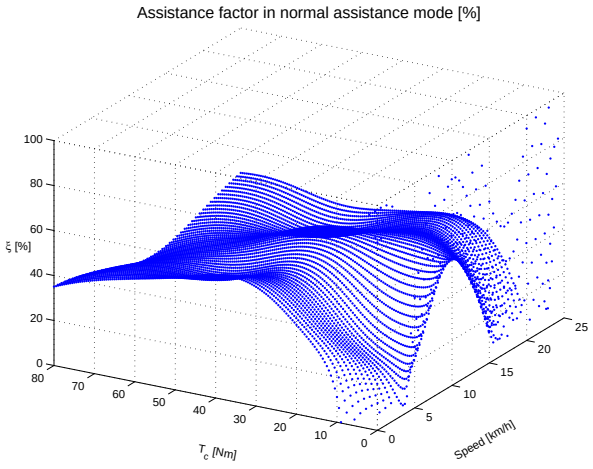

Figure 8.4: Graphical representation of an assistance factor model

The second possibility is difficult with the applied open loop control of the test bench. The calculation of equation 8.9 requires the traction forces $F_{t_{ZA}}$ and $F_{t_{MA}}$ at exactly the same speed and cyclist torque.
So for the estimation of the assistance factor $\hat{\xi}$ over the whole operation area, there is decided in favour of the first method. The determination of the assistance factor

model $\hat{\xi}(\bar{v}, \bar{T}_c)$ requires no extra LS-SVM modelling but is derived from two other LS-SVM models as is shown in equation 8.10.

$$\hat{\xi}(\bar{v}, \bar{T}_c) = 1 - \frac{\hat{F}_{t_{ZA}}(\bar{v}, \bar{T}_c)}{\hat{F}_{t_{MA}}(\bar{v}, \bar{T}_c)} \tag{8.10}$$

An estimation of the RMSE is given by applying the fault analysis on the formula of equation 8.10. The percent error on the estimation of the assistance factor $\delta\hat{\xi}$ is estimated to be the sum of the percent errors on the traction force measurements. This is expressed in equation 8.11 where $\Delta\hat{\xi}$, $\Delta\hat{F}_{t_{ZA}}$ and $\Delta\hat{F}_{t_{MA}}$ represents respectively the absolute errors on the assistance factor, the traction force without and the traction force with assistance.

$$\delta\xi = \frac{\Delta\hat{\xi}}{\hat{\xi}} = \frac{\Delta\hat{F}_{t_{ZA}}}{\hat{F}t_{ZA}} + \frac{\Delta\hat{F}_{t_{MA}}}{\hat{F}_{t_{MA}}} \tag{8.11}$$

Using the RMSEs of the LS-SVM models for the traction forces as absolute error estimators, the RMSE of the assistance factor is estimated by using equation 8.11.
The graphical user interface of chapter 12 foresees a standard of 3 assistance factor models for a single pedelec:

- $XI\_ModelMAe$: the assistance factor with low motor assistance (Motor Assists Economically)
- $XI\_ModelMAn$: the assistance factor with normal motor assistance (Motor Assists Normally)
- $XI\_ModelMAp$: the assistance factor with extra motor power (Motor Assists Powerfully)

A graphical representation of an assistance factor model $XI\_ModelMAn$ is given in figure 8.4.

8.5 Conclusions

In this chapter four regression models are introduced, starting from one measurement set of speeds, cyclist torques and traction forces. The *traction force model* estimates the traction force that should be measured on the testbench for a given cyclist torque and pedelec speed. The *required cyclist torque model* estimates the torque that should be exercised at the pedal axis to realize a certain traction force at a given speed. The *efficiency model* gives the relationship between the cyclist's input power and the resulting output power when the motor is switched off. The *assistance factor model* splits the traction power in the part coming from the motor and the part coming from the cyclist's efforts and expresses this in a dimensionless way. These models are used in the following chapters to derive performance plots and performance parameters of the measured pedelec.

9 The Performance Plots of a Pedelec

In chapter 10 a number of performance parameters are defined. Although these parameters give valuable information about the performance of a pedelec, they only focus on a single aspect of the behaviour of a pedelec. A better idea of the complete control strategy may be obtained by the analysis of a number of plots derived from the different pedelec models of chapter 8.
This chapter discusses which aspects of the pedelec models that are the most interesting to plot, and which plottypes that fits the best to analyse the pedelecs performance.

9.1 The plots and plottypes

There are different aspects of the measured pedelec that are interesting to plot. From the models of chapter 8, the next aspects are derived:

- The traction force
- The climbing-ability
- The required cyclist torque
- The mechanical efficiency
- The motor assistance factor

These aspects may be represented by using different plottypes:

- $3D$ plots
- Contourplots
- Slice plots

Different interesting combinations of plot and plottypes are given in the next sections. These plots may all be evoked via the graphical user interface of chapter 12.

9.2 The traction force plots

Based on the traction force models $\hat{F}_t(\bar{v}, \bar{T}_c)$ of section 8.1 a number of traction force plots can be created.

9.2.1 The 3D traction force plot

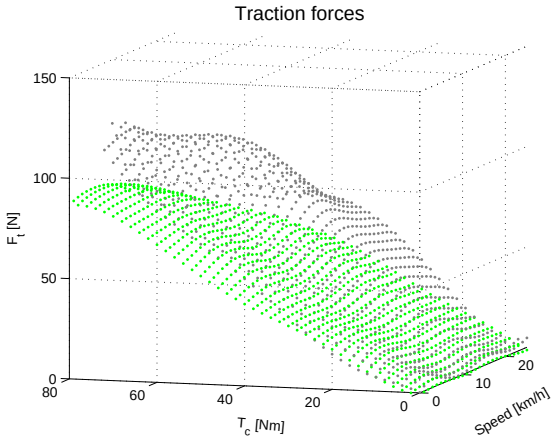

Figure 9.1: Example of a $3D$ plot of the traction force of the Sparta Ion without motor power (green lower surface) and with economic motor power (grey upper surface)

The $3D$ traction force plot is a direct plot of the traction force regression estimation $\hat{F}_t(\bar{v}, \bar{T}_c)$ in an orthogonal x, y, z axes system. The traction force plot for a single assistance mode and a fixed gear already gives a first idea of the implemented control strategy of a pedelec. Examples of traction force surfaces are already given in the figure 7.6. It may be interesting to put the surfaces of different assistance modes together in one graph. The more motor power, the higher the traction force surface will be situated. The vertical distance between the two surfaces is a measure for the difference in motor power. An example of a $3D$ traction force plot for two assistances modes of one pedelec is shown in figure 9.1.
Because $3D$ plots are not always easy to interprete, also two types of $2D$ plots (derived from these traction force plots) are used for the performance analysis of the pedelecs.

9.2.2 The contourplot of the traction force

The contourplot of the traction force displays isolines (= lines with the same traction force) in the operation area of the pedelec. Given the speed of the pedelec and the torque of the cyclist, the upper and lower limits of the traction force value in that

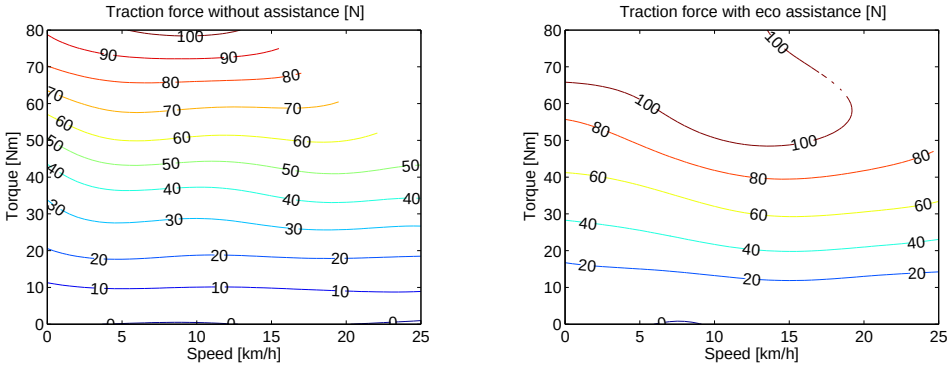

Figure 9.2: Contourplot of the Sparta Ion traction force [N] without assistance and with economic assistance

operation point can be easily read. An example of a traction force contourplot can be found in figure 9.2. The traction forces are expressed in newton.

9.2.3 Slice plots of the traction force

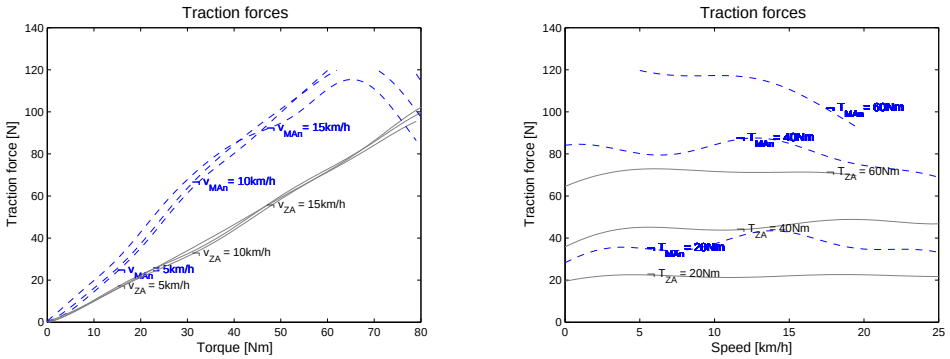

Figure 9.3: Slices of the traction force with (blue dashed) and without (grey solid) assistance for the Sparta Ion for constant speed (left) and for constant torque (right)

By making slices of the $3D$ plot a good idea of the applied assistance motor control strategy can be obtained. One possibility is making slices of constant speed. The traction force is plotted versus the cyclist's torque for a certain speed. The vertical distance between slices of the traction force with and without motor assistance is a measure for the added motor power. An example of constant speed slices are given in the left plot of figure 9.3 for speeds of 5, 10 and 15 km/h. The traction force hardly

changes with speed but is almost proportional to the torque input.
Another possibility are the slices of constant torques. The traction force is plotted versus the speed for a certain cyclist's torque. These plots may be interesting to see at which speed the controller stops adding motor power. An example of constant torque slices is given in the right plot of figure 9.3 for 20, 40 and 60 Nm.

9.3 The cyclist torque plots

Based on the required cyclist torque models $\hat{T}_c(\bar{v}, \bar{F}_t)$ of section 8.2 a number of torque plots may be created.

9.3.1 The 3D cyclist torque plot

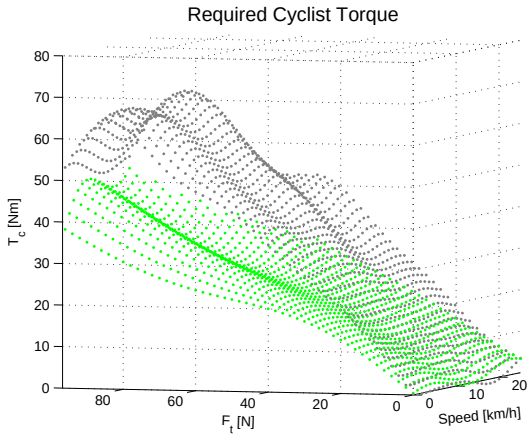

Figure 9.4: Example of a $3D$ plot of the required cyclist torque for the Sparta Ion without motor power (grey upper surface) and with normal motor power (green lower surface)

The $3D$ cyclist torque plot is a direct plot of the cyclist torque regression estimation $\hat{T}_c(\bar{v}, \bar{F}_t)$ in an orthogonal x, y, z axes system. This results in a surface as is already shown in figure 8.1. This surface will be used to calculate the required energy to cover a certain drive cycle as is explained in section 10.2. The more motor power is added, the lower the required cyclist torque surface will be situated. So when plotting different assistance modes in one figure, the highest surface will be the one without assistance. Again the vertical distance between the surfaces is a measure for the difference in motor power. An example of a $3D$ cyclist torque plot for different assistance levels is given in figure 9.4.

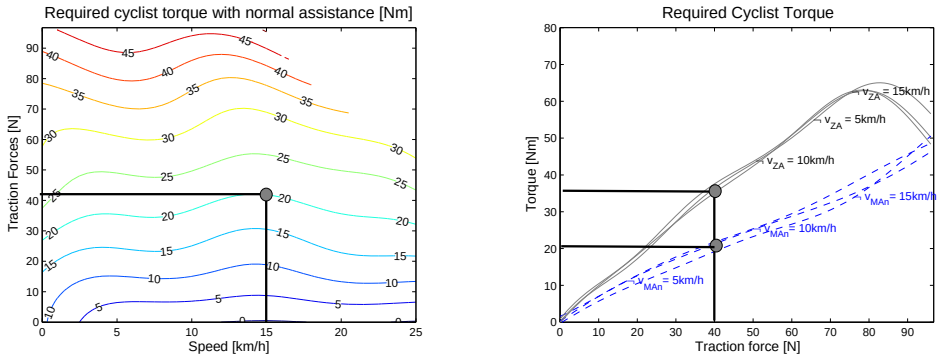

Figure 9.5: $2D$ plots of the required cyclist torque for the Sparta Ion:
Left: the contourplot in normal assistance mode
Right: slices of constant speed without (grey solid) and with (blue dashed) normal assistance

9.3.2 2D plots of the cyclist torque

Two derived $2D$ plots for the cyclist torque are shown in figure 9.5: the contourplot and the slices of constant speed. The contourplot is an interesting tool to find the upper and lower limit of the required cyclist torque to reach a certain speed and traction force. For instance, to reach a traction force of 40N at a speed of 15km/h with the pedelec of figure 9.5, the cyclist need to deliver a pedal torque of about 20Nm.
On the slice plot one can for instance read that at a speed of 15km/h and for a desired traction force of 40N, the assistance motor reduces the required cyclist torque from 36 to 20Nm.

9.4 The climbing-ability plots

Using the traction force to characterize the performance of a pedelec may be interesting and unambiguous, the practical interpretation is not directly clear for the daily user. Therefore the traction force may be transformed into the ability to overcome a certain percentage of slope in steady state.
The *climbing-abilitity* or *slope-ability* in a point of the operation area is defined as the maximum slope that can be overcome with the pedelec at a constant speed and with a constant cyclist torque input accepting a zero air-resistance.
The climbing-ability is calculated from the measured traction force by means of equation 6.13, by accepting a constant speed ($\frac{dv}{dt} = 0$) and a zero air-resistance. Equation 9.1 states that the traction force F_t needed to climb a slope of α degrees should equal the slope force F_{slope} as illustrated in figure 9.6.

$$F_t = m_{tot} \cdot g \cdot sin\alpha \tag{9.1}$$

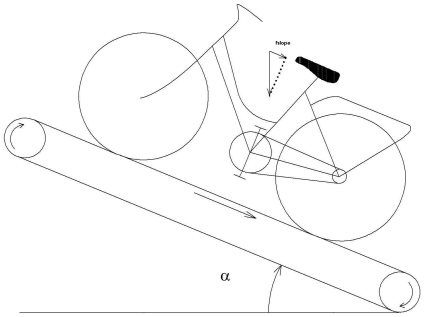

Figure 9.6: Calculation of the climbing-ability

The slope that can be overcome is finally calculated using equation 9.2.

$$Slope[\%] = 100 \cdot tan\left(arcsin\left(\frac{F_t}{m_{tot} \cdot g}\right)\right) \tag{9.2}$$

As an extra input parameter, the total mass m_{tot} appears. This mass should include the weight of the pedelec, the cyclist and, if any, the luggage. the letter g represents the gravitational constant.

9.4.1 The 3D climbing-ability plot

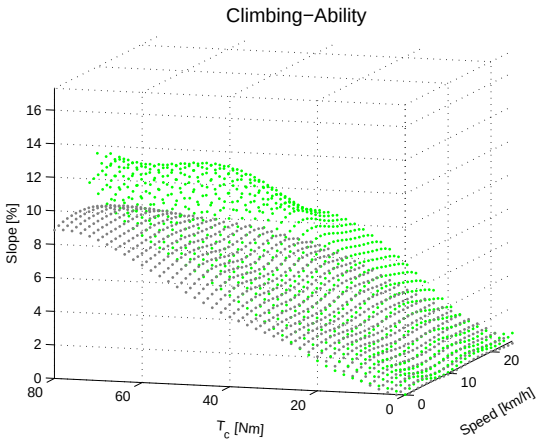

Figure 9.7: Example of a $3D$ plot of the climbing-ability of the Sparta Ion without motor power (grey lower surface) and with economic motor power (green upper surface) for a total mass of 100kg

Rescaling the $3D$ traction force model $\hat{F}_t(\bar{v}, \bar{T}_c)$ of section 8.1 with equation 9.2 results in the $3D$ climbing-ability plots. These plots give the maximum slope percentage that can be overcome as a function of the given pedelec speed and the cyclist's effort. Again different assistance modes can be put together to evaluate the extra power coming from the motor-battery system. An example is given in figure 9.7.
The climbing-ability can be further investigated by deriving several two-dimensional plots.

9.4.2 The contourplot of the climbing-ability

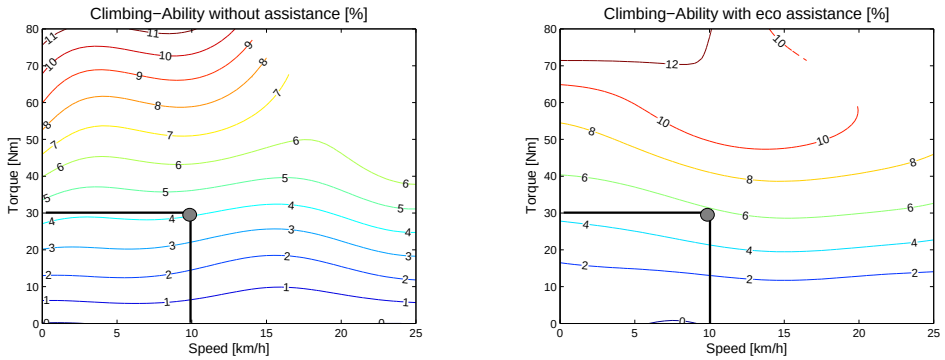

Figure 9.8: Contourplot of the Sparta Ion climbing-ability (m_{tot}=100kg) without assistance and with eco-assistance

Similar to the traction force contourplot, the contourplot of the climbing-abilitiy displays lines with the same climbing-ability in the operation area of the pedelec. The contourplots of figure 9.8 are rescaled versions of figure 9.2. The applied total mass is $100kg$. With a cyclist torque of $30Nm$ at a speed of $10km/h$ for instance, this pedelec can climb almost 4% slope without assistance and already a 5.5% slope with the lowest assistance level.

9.4.3 Slice plots of the climbing-ability

Also slices of the climbing-ability can contribute to interprete the behaviour of the controller of the pedelec. The plots are the same as for the traction force slices, but the vertical axis shows the more comprehensible slope percentage.

9.5 The efficiency plots

Based on the efficiency regression model $\hat{\eta}(\bar{v}, \bar{T}_c)$ of section 8.3 also a number of efficiency plots can be created via the graphical user interface of chapter 12.

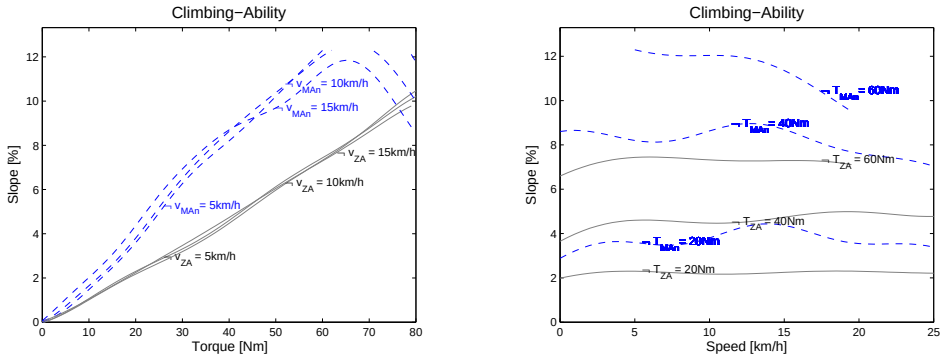

Figure 9.9: Slices of climbing-ability (m_{tot}=100kg) with (blue dashed) and without (grey solid) assistance for the Sparta Ion for constant speed (left) and constant torque (right)

9.5.1 The 3D efficiency plot

Plotting the efficiency $\hat{\eta}$ versus the cyclist's torque $\bar{T}_c$ and the pedelec speed $\bar{v}$ for a certain gear, results in an efficiency surface above the operation area. An example of a three dimensional efficiency surface is already given in figure 8.3.

9.5.2 The efficiency contourplot

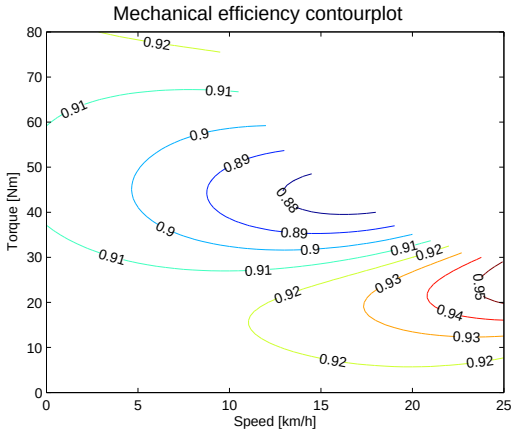

Figure 9.10: Example of the efficiency contourplot for the Sachs Elo Bike in the 1° gear

The interpretation of the efficiency along the area of operation is much easier using a contourplot. An example of such a contourplot is given in figure 9.10.

$2D$ slice plots of the efficiency are seen as less interesting and are not included in the graphical user interface.

9.6 The assistance factor plots

Based on the assistance factor regression model $\hat{\xi}(\bar{v}, \bar{T}_c)$ of section 8.4 a number of assistance factor plots are made available via the graphical user interface of chapter 12.

9.6.1 The 3D assistance factor plot

The plotting of the assistance factor $\hat{\xi}$ versus the cyclist's torque $\bar{T}_c$ and the pedelec speed $\bar{v}$ for a certain gear, results in an assistance factor surface lying above the operation area. An example of such a $3D$ assistance factor surface is already given in figure 8.4.

9.6.2 The contourplot of the assistance factor

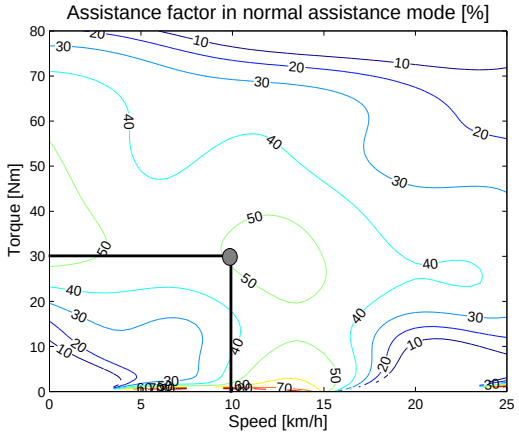

Figure 9.11: Contourplot of the assistance factor for the Sparta Ion in normal assistance mode

The contourplot of the assistance factor may be one of the more interesting instruments to interpret the behaviour of the pedelec. It shows lines of constant relative motor contribution to the traction power. An example is given in figure 9.11. The assistance factor for a cyclist torque of $30Nm$ at a speed of $10km/h$ is 50%. This means that both the motor as well as the cyclist deliver half of the traction power.

9.6.3 Slice plots of the assistance factor

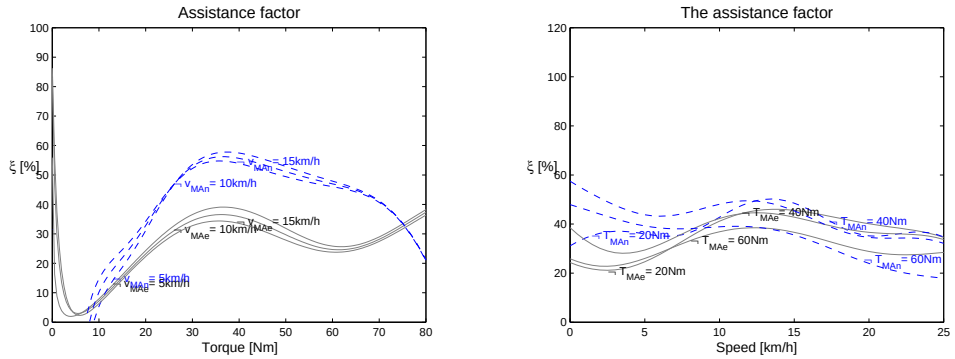

Figure 9.12: Slice plots of the assistance factor for the Sparta Ion in economic (grey solid) and normal (blue dashed) assistance mode

The slices may be interesting to evaluate the evolution of the assistance factor with speed changes for a constant cyclist torque or with torque changes for a constant speed. Both type of slices are given in figure 9.12 for 2 different assistance modes. For this particular case there is little difference between the two assistance modes for small torques. A maximum assistance factor of almost 60% is reached near a cyclist torque of $40Nm$.

9.7 Conclusion

In this chapter a first tool to analyse the performance of the pedelec by means of the derived models is shown. $3D$-plots, contourplots and slice plots of the traction force, the climbing-ability, the required cyclist torque, the mechanical efficiency and the assistance factor are introduced. These plots help to get an idea how the pedelec system with its different assistance levels behave in its operation area. Next to this visual analysis tool, performance parameters will be introduced in the next chapter.

10

The Performance Parameters of a Pedelec

In chapter 7 different regression pedelec models are derived by using the LS-SVM regression technique. These models are worked out in order to visualise different aspects of the pedelec in chapter 9. In this chapter an objective measure for the comparison of the performance of different pedelecs will be introduced. For that reason a number of performance parameters will be defined. These parameters are well defined combinations of different measurements that can be expressed as a single number.
Two groups of performance parameters will be distinguished.

- *The user-independent performance parameters* that are totally determined by the pedelec itself:
  - The $100W$ efficiency
  - The $75W$ assistance factor
  - The $100W$ slope-ability
- *The user-dependent performance parameters* that may change by the way the cyclist is using the pedelec:
  - The drive cycle efficiency
  - The drive cycle assistance factor
  - The human energy need during a drive cycle
  - The motor energy need during a drive cycle
  - The drive cycle battery range

For the calculation of these performance parameters, the pedelec models described in chapter 8 are supposed to be known. More specifically the regression functions for

- the traction force $\hat{F}_t(\bar{v}, \bar{T}_c)$ without and with (different) motor assistance(s)
- the required cyclist's torque $\hat{T}_c(\bar{v}, \bar{F}_t)$ without and with (different) motor assistance(s)
- the efficiency $\hat{\eta}(\bar{v}, \bar{T}_c)$
- the assistance factor $\hat{\xi}(\bar{v}, \bar{T}_c)$ with (different) motor assistance(s)

should be known along the area of operation.

10.1 The user-indepent performance parameters

10.1.1 The 100W efficiency

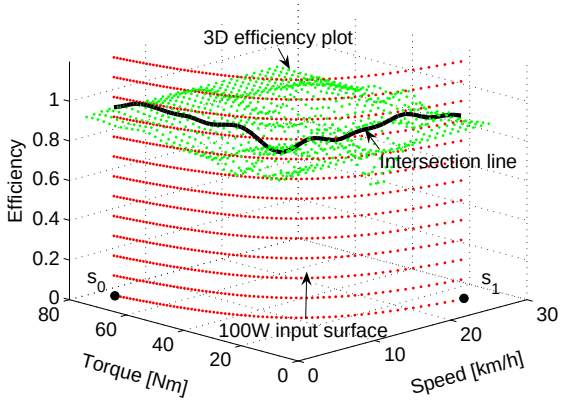

Figure 10.1: The determination of the 100W-efficiency for the Sparta Ion

As stated by James B. Spicer [48] it is tough to beat a bicycle when it comes to efficient use of energy. The energy losses in a well designed chain drive are less than 2%. The worse efficiency of a series of conventional bicycle chain tests was still 81% [48].
The introduction of the motor and transmission system might lower this high mechanical efficiency. At first sight, some pedelec motor systems seem hardly able to compensate their own introduction of extra friction.
The energy losses in the chain are not measured seperately. The test bench measures the global efficiency as defined in section 8.3. This means that next to the chain losses also the friction losses of the rolling wheels are included. The *100W-efficiency* quantifies this global efficiency loss.
If one wants to catch the efficiency as a single number, averaging out the estimated efficiency $\hat{\eta}(\bar{v}, \bar{T}_c)$ over the whole operation area would be a possible performance parameter. However, to reduce the influence of the boundary effects introduced by

interpolation, another strategy is chosen, based on what is found in reference [48].
The efficiency will be considered in all the operating points with 100 watt human input power and the average of these efficiencies will be called the $100W$ efficiency η_{100}. The value of $100W$ is used because it approaches the limit of what a person of common fitness is able to deliver on a continuous base [49].
The $100W$ efficiency is derived from the calculation of the intersection (the black line in figure 10.1) of two surfaces:

- The surface of the $3D$ efficiency plot as defined in section 9.5 (The horizontal surface in figure 10.1)
- The $100W$ human input surface (The vertical surface in figure 10.1)

In other words, the $100W$ effiency is the average of the locus of points that are a solution of the system of equations 10.1.

$$\begin{cases} \hat{\eta} = \hat{m}_3(\bar{v}, \bar{T_c}) \\ \bar{T_c} \cdot \bar{v} = c \end{cases} \tag{10.1}$$

If the speed is given in km/h, the constant c is determined by equation 10.2

$$c = 100 \cdot 3,6 \cdot Z \tag{10.2}$$

This locus can also be written in its parametric form in the parameter s: where $\hat{m}_3$

$$\begin{cases} \bar{v} = s \\ \bar{T_c} = \frac{c}{s} \\ \hat{\eta} = \hat{m}_3(s, \frac{c}{s}) \end{cases} \qquad g(s) = \left[s, \tfrac{c}{s}, \hat{m}_3\left(s, \tfrac{c}{s}\right)\right]$$

represents the regression function for the mechanical efficiency from section 8.3. The average of these locus points can be analytically expressed with equation 10.3[50].

$$\eta_{100} = \frac{\int_{s_0}^{s_1} \left|\frac{d}{ds} g\left(s\right)\right| ds}{\int_{s_0}^{s_1} \sqrt{1 + \frac{c^2}{s^4}} ds} \tag{10.3}$$

The integrals of η_{100} are numerically solved. This results in a finite number of locus points for the efficiencies. This number depends on the chosen integration step Δs. The default value for Δs was chosen to be 1. The borders s_0 and s_1 are determined by the borders of the operation area and are shown in figure 10.1. The $100W$ efficiency for a number of tested pedelecs is given in table 13.2.

Instead of only comparing a single number η_{100} of equation 10.3 for different pedelecs, it is more suitable to compare the *distributions* of the efficiencies along the $100W$ path. Therefore the graphical user interface of chapter 12 allows the representation of the distribution of the $100W$ efficiencies as a boxplot. Such a boxplot is a graphical representation showing five important numbers of a distribution:

- the smallest value
- the lower quartile
- the median
- the upper quartile
- the largest value

An example of these boxplot distribution is given in figure 10.2.

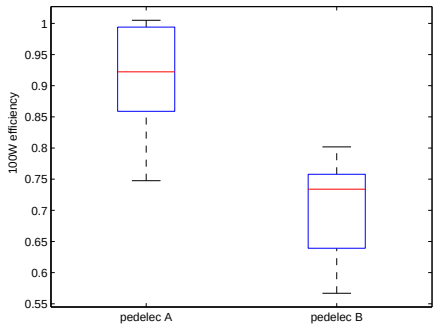

Figure 10.2: Boxplots of the $100W$ efficiencies of two different pedelecs

A *wilcoxon test* is used to compare the distributions of two different pedelec efficiencies. In casu the *ranksum* preprogrammed function of Matlab is used. The smaller the result of this test, the more unprobable the hypothesis that the two independent samples come from distributions with equal medians, or the more unprobable that the efficiencies of both pedelecs are equal. In this way, the comparison of two pedelec efficiencies is reduced to a merely objective mathematical procedure.

10.1.2 The 75W assistance factor

Next to the qualitative approach with the assistance factor plots of section 9.6, there is need for a more quantitative approach to compare assistance strategies. How can one quantify the difference between

- the assistance strategy of two pedelecs?
- the assistance levels of two assistance modes of the same pedelec?

A global averaging of the assistance factor over the whole operation area is rejected because the pedelec's behaviour is described by means of estimations of regression models. A solution is found in the 75W assistance factor ξ_{75}.
The value of $75W$ is justified with the following reasoning. Most pedelecs have the possibility to ride with an assistance factor of almost 50%. Theoretically, the cyclists who decide to replace their conventional bicycle by such a pedelec may choose between two ways of using their pedelec.

- whether they decide to deliver only half of the power they would use with a conventional bicycle, having the same traction performances with the pedelec as with their conventional bicycle ($\approx 100W$ output requires only $50W$ input)
- or they decide not to lower the effort, roughly resulting in doubling their former traction performances ($\approx 100W$ input results in $200W$ output).

The truth will lie in between these two extrema. That's why there is decided to take $75W$ of human input power as a reference line to average out the assistance factor of a pedelec.
The $75W$ assistance factor ξ_{75} will be defined as the average of all assistance factors of the operating points with 75 watt human input power.
Therefore, similar to the $100W$ efficiency, the intersection of two surfaces has to be calculated:

- The assistance factor surface as defined in 9.6
- The $75W$ human input surface (analog with the $100W$ surface of section) 10.1.1

A number of measured ξ_{75} values are given in table 13.2.

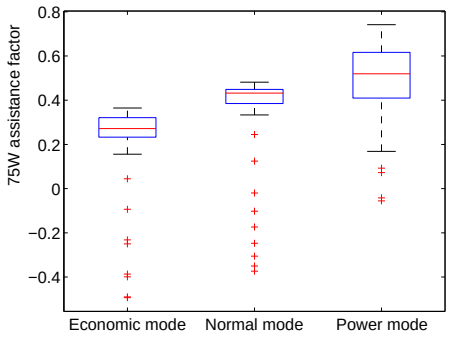

Figure 10.3: Boxplots of the $75W$ assistance factors of the 3 assistance modes of the Sparta Ion

All the assistance factors with 75 watt human power input, evaluated with a numeric step Δs (see the η_{100} calculation), represent a distribution of assistance factors. Instead of only comparing the average values ξ_{75}, it is more appropriate to compare the distributions of this $75W$ assistance factors. Therefore, the intersection of the two surfaces will be displayed as a boxplot. This is illustrated in figure 10.3 for the 3 assistance modes of a pedelec. The results of the wilcoxon hypothesis test (function *ranksum* in Matlab) between every two assistance modes is shown in table 10.1. P is a measure for the probability that the two modes have the same distribution. The conclusion here is that the 3 assistance modes are well distinguished. But the difference between the normal and power mode is smaller than the difference between the economic and the normal assistance mode.

Two modes	Probability P
Economic vs. Normal assistance mode	5.7e-018
Normal vs. Power assistance mode	6.7e-008
Economic vs. Power assistance mode	6.0e-019

Table 10.1: Results of the Wilcoxon hypothesis test on the boxplots of figure 10.3

10.1.3 100W climbing-ability

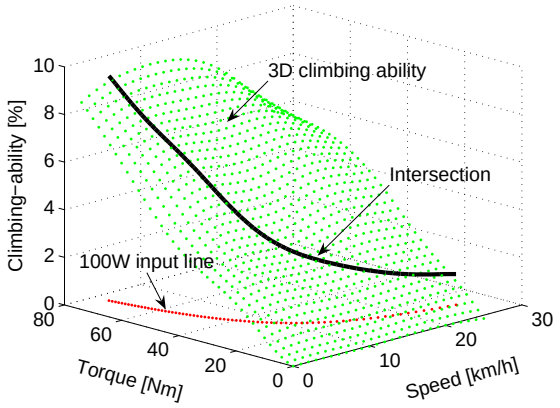

Figure 10.4: Calculation of the $100W$ climbing-ability

Another user-independent performance parameter, the $100W$ climbing-ability, is introduced to have a comprehensible comparison tool. Most users have no idea of the magnitudes of traction forces, but clearly understand the meaning of a slope percentage.
The comparison of the climbing-ability of pedelecs or pedelec assistance modes in a single arbitrary point of the operation area, will be too much influenced by the choice of that operation point. The average of the climbing-ability along the operation area is not really meaningful, because the climbing-ability is highly dependent on the cyclist's torque input. A solution is found in the averaging of the climbing-ability in all operation points with a human power input of $100W$.
Although the climbing-ability is depending on the weight of the user, there is decided not to consider this performance parameters as user-dependent. The total mass will be set to $100kg$ as a standard value. If necessary, the value can be changed by the graphical user interface described in chapter 12. The choice for $100W$ is based on the fact that for the weaker pedelec users, this might be the physical limit to climb a slope. In this way, the $100W$ climbing-ability is another measure for the maximum slope that can be climbed.

Also the $100W$ climbing-ability is the average of the intersection of 2 surfaces. This is graphically represented in figure 10.4:

- the surface represents the climbing-ability along the operation area,
- the lower line represents the operation points with $100W$ human input
- and the upper line is the projection of the former one in the surface.

The average of all the values of the upper line is called the $100W$ climbing-ability. The distribution of these values is used to compare different assistance levels.
An example of boxplot representations of these distributions is given in figure 10.5

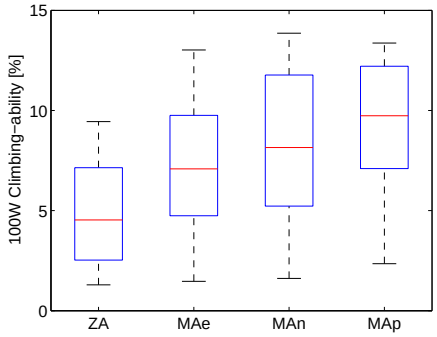

Figure 10.5: Boxplots of the distribution of the $100W$ climbing-abilities for the 4 assistance modes of the Sparta Ion

for the 4 motor assistance modes of one pedelec. The first boxplot is the one without motor assistance, the 3 others are motor assisted levels. The medians of the $100W$ climbing-ability are proportional to the assistance level. All the distributions are quite symmetrical, but the normal assistance level has the widest spreading.
Again a wilcoxon hypothesis test on the distributions of the $100W$ climbing-abilities can be used to quantify the resemblence of 2 assistance levels. This test is made available via the graphical user interface.

10.2 The user-dependent performance parameters

The market study brougth to light that there is not really a specific 'target group' for pedelec buyers (section 2.3.9). This means that pedelecs will be used by people with quite different expectations from their pedelec. The best pedelec buy for one rider will not necessarily be the best one for another rider. That's why the performance analysis cannot be totally be seperated from the way the pedelec will be used [51]. That's why a number of user-dependent performance parameters are introduced.
The behaviour of the pedelec driver will be analysed by *recording* a typical ride or by using a synthetical drive cycle. Both options are aplied in chapter 13.2 where

all the performance parameters for a number of test pedelecs are discussed. The determination of drive cycles will be discussed in chapter 11.
In this chapter the drive cycle is supposed to be known: the values for the speed and the percentage of slope are known at each moment in the drive cycle. An example of a drive cycle is given in figure 11.1.

10.2.1 The drive cycle efficiency

Although the tests learn that the mechanical efficiency of formula 8.3 varies little over the operation area, it is interesting to calcule the mechanical efficiency during a drive cycle. A global drive cycle efficiency as well as an instantaneous drive cycle efficiency are considered.

The global drive cycle efficiency

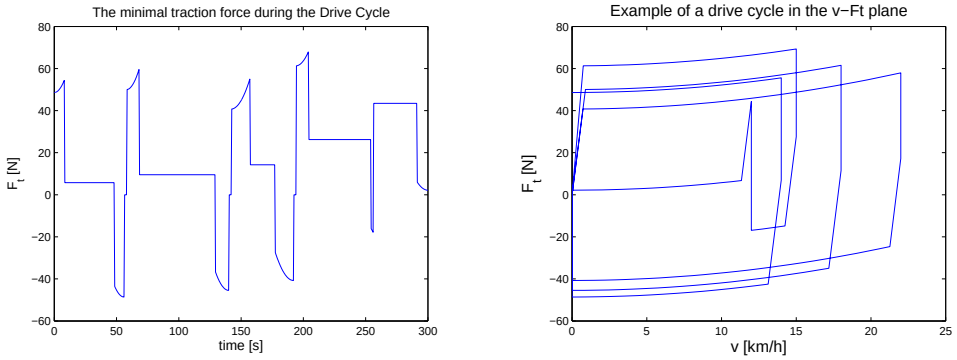

Figure 10.6: The minimal traction force as a function of time and speed during the drive cycle of figure 11.1

The global *drive cycle efficiency* η_{cycle} is defined as the quotient of the traction energy without motor assistance $W_{t_{ZA}}$ and the human input energy W_c at the pedal axis that is required to cover the drive cycle.

$$\eta_{cycle} = \frac{W_{t_{ZA}}}{W_c} \tag{10.4}$$

The required cyclist energy W_c is indirectly measurable via the heart rate, or by simultaneously logging a torque and speed sensor, but the traction energy $W_{t_{ZA}}$ (as defined in equation 6.13) is not easily measurable during cycling.
That makes the definition of equation 10.4 little useful. This problem was bypassed by using

- the bicycle model of section 6.4 to calculate the traction energy that is required to cover the drive cycle in *ideal circumstances*
- the (steady-state) LS-SVM torque model $\hat{T}_c(\bar{v}, \bar{F}_t)$ of section 8.2 to estimate the required cyclist energy

The *ideal circumstances* mentioned in the first item are accepted to be a pedelec ride

- without rolling resistance
- without internal mechanical losses
- with zero windspeed

In these *ideal circumstances* there is no difference between the propulsive force and the traction force (see 6.12). So, the *ideal* (or minimal) traction force $F_{t_{min}}$ required to cover the drive cycle with a lossless pedelec can be calculated as:

$$\vec{F}_{t_{min}} = \vec{F}_p = m_{tot}\frac{d\,\vec{v}}{dt} + \vec{F}_{air} + \vec{F}_{slope} \tag{10.5}$$

Thus, next to the inertial force, only the following forces have to be modelled:

- the air-resistance F_{air}
- the slope resistance F_{slope}

The slope resistance is calculated using equation 9.2, so a value for the total mass of the pedelec and the driver is required.
The air-resistance is modelled as

$$F_{air} = \frac{1}{2}c_d A \rho v_r^2 \tag{10.6}$$

where

- C_d = drag coefficient
- A = frontal area [m^2]
- ρ = density of air [kg/m^3]
- $v_r = v_{cycle} - v_{headwind}$ = velocity of the pedelec relative to the air [m/s]

Typical values for $C_d A$ were found in reference [52].
The default values for these parameters applied in this work are shown in table 10.2. It is possible to change them via the graphical user interface of section 12 if more precise measurements would be available.
Combining equations 9.2 and 10.6 with equation 10.5 for a given drive cycle results in a traction force as a time function $F_t(t)$ for this drive cycle. An example is shown in figure 10.6 for the drive cycle of figure 11.1. The traction force plotted versus the speed shows the same drive cycle in the $v - F_t$ plane. This is represented in figure 10.6b.

$\rho\,[kg/m^3]$	1.21
$v_{headwind}$ [m/s]	0
c_d [-]	0.9
A $[m^2]$	0.6
m_{tot} [kg]	100

Table 10.2: Default values for the calculation of $F_{t_{min}}$

The LS-SVM model for the cyclist torque $\hat{T}_c(\bar{v}, \bar{F}_t)$ derived from the measurements (see section 8.2) will be used to estimate the cyclist's torque $\hat{T}_c$ that is required to reach a point of the drive cycle in the $v - F_t$ plane.
So the time function $\hat{T}_c\,(t)$ will be derived from the steady state testbench measurements.
A problem of the $\hat{T}_c(\bar{v}, \bar{F}_t)$ LS-SVM model is the lack of information about the negative traction forces in braking situations. They cannot be measured by the load cell of the test application, and as a consequence not be transferred into a meaningfull negative torque for the pedelec.
For every two time moments t_1 and t_2 wherein between the traction force becomes negative, the integral of equation 10.7 represents the braking energy E_b that is available between t_1 and t_2.

$$E_b = \int_{t_1}^{t_2} |F_t(t)|\, v(t)dt \tag{10.7}$$

For the calculation of the efficiency during the drive cycle, these braking moments are neglected.
For the rest of the discussion, the drive cycle will be considered as the succession of only the positive sequences of the traction force. This modified drive cycle covers a time period T. The function $\hat{T}_c\,(t)$ is the projection of the modified drive cycle of figure 10.6b on the LS-SVM torque model. This is graphically presented in figure 10.7 for the drive cycle of figure 11.1.

So, if covering the drive cycle requires a time T, the efficiency of equation 10.4 may be written as a function of the instantaneous minimal traction force $F_{t_{min}}(t)$ and the instantaneous cyclist torque $\hat{T}_c$ (equation 10.8). The speed $v(t)$ is the instantaneous speed of the bicycle and $\omega(t)$ is the instantaneous angular speed of the pedal axis.

$$\eta_{cycle} = \frac{\int_0^T P_{t_{ZA}}(t)dt}{\int_0^T P_c(t)dt} = \frac{\int_0^T F_{t_{min}}(t)v(t)dt}{\int_0^T \hat{T}_c(t)\omega(t)dt} \tag{10.8}$$

This expression is directly applicable for all kinds of drive cycles and will be used to calculate the drive cycle efficiency η_{cycle}.

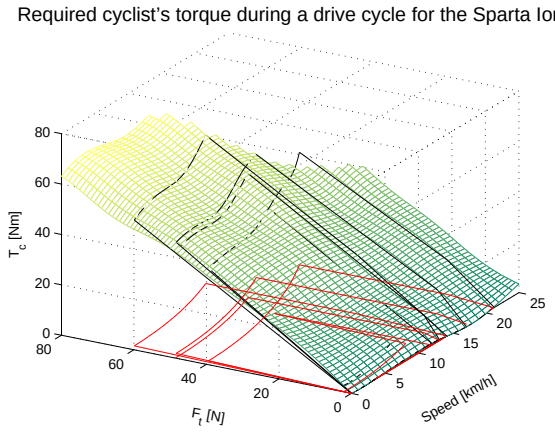

Figure 10.7: Projection of the drive cycle of figure 11.1 (neglecting the braking parts) on the 3D torque plot of the sparta Ion

The instantaneous drive cycle efficiency

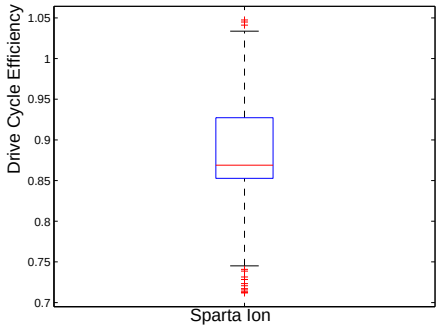

Figure 10.8: Boxplot of the distribution of the efficiency of the drive cycle from figure 11.1 for the Sparta Ion

Next to the global drive cycle efficiency η_{cycle}, also an instantaneous efficiency $\eta(t)$ could be determined. The efficiency at time t of the drive cycle with speed $v(t)$ and minimal traction force $F_{t_{min}}(t)$ becomes:

$$\eta(t) = \frac{P_{t_{ZA}}(t)}{P_c(t)} = \frac{F_{t_{min}}(t)v(t)}{\hat{T}_c(t)\omega(t)} = Z\frac{F_{t_{min}}(t)}{\hat{T}_c(t)} \tag{10.9}$$

This $\eta(t)$ function is evaluated at discrete time intervals with a time step Δt that is adjustable via the graphical user interface. The default value will be $\Delta t = 1s$. The

distribution of the η values can be presented in a boxplot to get an idea of the spreading. An example is given in figure 10.8. The outliers are the consequence of the numeric instability of the quotient 10.9 for smaller torques.

The comparison of *the drive cycle efficiencies* of two pedelecs will be performed by a wilcoxon test on the distribution of the instantaneous efficiencies. In this way a ranking can be made for the mechanical performances of the pedelecs for the given drive cycle.

10.2.2 The drive cycle assistance factor

In the same way as the *drive cycle efficiency* the *drive cycle assistance factor* will be introduced as a user-dependent performance parameter. First a global drive cycle assistance factor will be defined, followed by an expression for the instantaneous drive cycle assistance factor.

The global drive cycle assistance factor

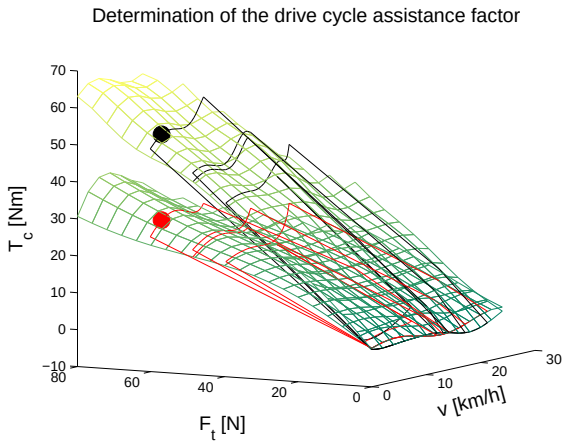

Figure 10.9: The determination of the drive cycle assistance factor. The curves in the surfaces represent the required cyclist torques during a drive cycle: $\hat{T}_{c_{MA}}(t)$ in the lower surface, $\hat{T}_{c_{ZA}}(t)$ in the upper surface

The global *drive cycle assistance factor* is defined as the quotient of the net contribution of the motor to the traction energy (=W_{tm}) and the total traction energy W_t that is required to cover the whole drive cycle.

$$\xi_{cycle} = \frac{W_{tm}}{W_t} \tag{10.10}$$

This assistance factor will be

- 1 : if the motor delivers all the traction energy
- 0 : if the cyclist delivers all the traction energy

The drive cycle assistance factor can be calculated for all the different power modes of a pedelec.
However, the determination of the drive cycle assistance factor by on-road measurement of the traction energy is difficult. Therefore the test bench measurements will be used to estimate the drive cycle assistance factor.
The determination of the motor traction W_{tm} by looking at a difference in traction force with and without motor power (as applied in section 8.4) is not applicable here, because the traction force is imposed by the drive cycle and thus the same while riding assisted or non-assisted. A difference is rather found at the level of the cyclist's efforts. The difference between the human energy need $W_{c_{ZA}}$ to cover the drive cycle without assistance power and the human energy need $W_{c_{MA}}$ to cover the drive cycle with motor power is a measure for the added motor power. It cannot be equated to the net motor traction energy W_{tm}, because the transmission losses are not considered. The difference $W_{c_{ZA}} - W_{c_{MA}}$ will be called the motor propulsion energy W_{pm}. η_1 is the efficiency of the conversion between propulsion and traction energy needs during the drive cycle.

$$W_{tm} = \eta_1 W_{pm} = \eta_1 \left(W_{c_{ZA}} - W_{c_{MA}}\right) \tag{10.11}$$

The energy $W_{c_{ZA}}$ delivered by the cyclist whenever the motor is switched off, equals the total propulsion energy required to cover the cycle. There should be noted again that this total propulsion energy differs from the traction energy W_t. The traction energy is what is left from the propulsion energy after the transmission losses. Considering a similar energy conversion as in equation 10.11 the total traction energy may be written as:

$$W_t = \eta_1 W_p = \eta_1 W_{c_{ZA}} \tag{10.12}$$

The calculation of the drive cycle assistance factor will be based on equation 10.13.

$$\xi_{cycle} = \frac{W_{tm}}{W_t} = \frac{W_{pm}}{W_p} = 1 - \frac{W_{c_{MA}}}{W_{c_{ZA}}} \tag{10.13}$$

The determination of the global drive cycle assistance factor ξ_{cycle} requires the knowledge of the angular speed of the pedals, and the instantaneous values for the cyclist torque with ($T_{c_{MA}}(t)$) and without ($T_{c_{ZA}}(t)$) assistance in order to calculate the cyclist energy needs W_c.
To get these time variables, the drive cycle is converted from a speed and slope percentage to a speed and minimal traction force as a function of time (see equation

10.5). Again the braking parts of the cycle will be excluded for the parameter determination, and the modified drive cycle from section 10.2.1 will be used.
The projection of the modified $v - F_t$ drive cycle on the LS-SVM torque model $\hat{T}_c(\bar{v}, \bar{F}_t)$ results in an estimate for the required cyclist torque as a function of time $\hat{T}_c(t)$. This is illustrated in figure 10.9 for two different assistance modes.
The practical formula for the estimation of the drive cycle assistance factor is given in equation 10.14.

$$\xi_{cycle} = 1 - \frac{\int_0^T \hat{T}_{c_{MA}} \omega(t) dt}{\int_0^T \hat{T}_{c_{ZA}} \omega(t) dt} \tag{10.14}$$

The instantaneous drive cycle assistance factor

The instantaneous *drive cycle assistance factor* is defined as the contribution of the motor to the traction power $P_{tm}(t)$ in proportion to the total available traction power $P_t(t)$.

$$\xi(t) = \frac{P_{tm}(t)}{P_t(t)} \tag{10.15}$$

It will appear to be more convenient to write this traction power in cyclist related quantities in the same way as for the global drive cycle assistance factor.

$$\xi(t) = 1 - \frac{\hat{T}_{c_{MA}}(t)}{\hat{T}_{c_{ZA}}(t)} \tag{10.16}$$

The factors $\hat{T}_c(t)$ in equation 10.16 represent the (steady-state) cyclist torques required to reach the operation point with speed $v(t)$ and traction force $F_t(t)$. The subscript MA means the case with motor power and the subscript ZA means the case without motor power.
The ratio in equation 10.16 is the quotient of the corresponding torques with and without motor power. As an example two corresponding torques are marked on figure 10.9 with a red (with motor power) and black (without motor power) point.
The $\xi(t)$ function is evaluated at discrete time intervals with a time step Δt that is adjustable via the graphical user interface. The default value is $\Delta t = 1s$.
As may be clear from equation 10.16 there might be numeric problems for the smaller input powers. That is why the calculation of $\xi(t)$ was not considered for cyclist powers less than 2W!
The (limited) distribution of the calculated ξ of a drive cycle can be presented in a boxplot to get an idea of the spreading of all ξ-values. An example is given in figure 10.10 for 3 different assistance modes of the same pedelec.
The distribution of $\xi(t)$ is used to compare the assistance factors for

- different assistance modes of the same pedelec

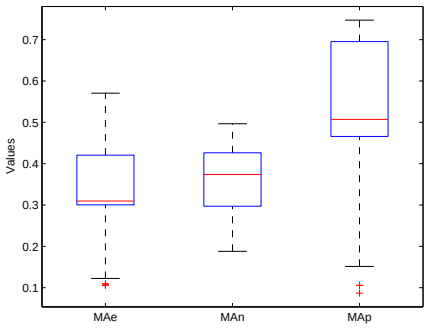

Figure 10.10: Boxplots of the distribution of the drive cycle assistance factor of the drive cycle from figure 11.1 for the Sparta Ion in its 3 assistance modes

- different pedelecs
- different drive cycles with the same pedelec

The comparison between two distributions will again be based on the wilcoxon test. Also the ranking of pedelec assistance behaviours along a drive cycle is now reduced to a merely mathematical procedure.

10.2.3 Human energy need during a drive cycle

While using *the drive cycle efficiency* η_{cycle} and *the drive cycle assistance factor* ξ_{cycle} as performance parameters, the information about the absolute energy requirements gets lost. However, the human energy need during a drive cycle with a pedelec in a given assistance mode $W_{c_{mode}}$ is implicitly used to calculate the ξ_{cycle}.

$$W_{c_{mode}} = \int_{cycle} T_{c_{mode}}(t)\omega(t)dt \tag{10.17}$$

The comparison between different assistance modes is better understandable on the basis of this absolute performance parameter $W_{c_{mode}}$, instead of using the assistance factor.
This value is therefore made available via the graphical user interface for all assistance modes to help to interprete the adequacy of a certain pedelec for a given drive cycle.

10.2.4 Motor energy need during a drive cycle

The determination of *the drive cycle assistance factor* ξ_{cycle} is based on the net contribution of the motor W_{tm} to the traction energy. The reason for that is the fact that

the testbench measurements are based on the traction force. The real required mechanical motor energy W_m will be higher because of the losses in the transmissions. This means that one shouldn't use the net motor energy to conclude something about the evolution of the battery state of charge. The relation between the net motor energy and the real motor energy is determined by the often complex drive train and will be called the motor transmission efficiency η_{mt}.

$$\eta_{mt} = \frac{W_{tm}}{W_m} \tag{10.18}$$

For pedelecs with the motor mounted near the bracket the efficiency of the motor power transmission will almost be the same as the efficiency for the human power transmission. The calculation of this last one is explained in equation 10.8. For such pedelecs there seemed to be no difference between the propulsion motor energy W_{pm} (defined in equation 10.11) and the mechanical energy of the motor W_m.
For hub motors, the motor power transmission will normally be more efficient because there is no chain transmission involved. Consequently there might be a small difference between W_{pm} and W_m.
Unfortunately, with todays available measurements, no further conclusions can be taken concerning this transmission efficiency.
Nevertheless, the motor energy need during a drive cycle W_m will be estimated in all cases as

$$W_m = \eta_{cycle} W_{pm} = \eta_{cycle} \left(W_{c_{ZA}} - W_{c_{MA}}\right) \tag{10.19}$$

$W_{c_{ZA}}$ and $W_{c_{MA}}$ in equation 10.19 are the required cyclist energy with and without motor assistance as defined in equation 10.13. A suggestion for a real measurement of this performance parameters is given in chapter 15.

10.2.5 Drive cycle battery range

The translation of the real motor energy need into a battery energy need assumes the knowledge of another efficiency η_{bm}. This is the efficiency of the transmission from electrical (battery) energy W_b to mechanical energy W_m.

$$\eta_{bm} = \frac{W_m}{W_b} \tag{10.20}$$

Until now, this efficiency is not measured on the testbench, but some information may be retrieved in the manufacturer data. Chapter 15 describes a way to add extra test facilities to perform an η_{bm} measurement. The often applied brushless DC motors lead all electric motor types in terms of efficiency. Values up to 97% (at rated power) are found in literature [53]. However, at no load conditions this efficiency may drop to 20% [54], , [55]. Knowing that the pedelec does not always work in the most performing operation point for these motors, a default average value of $\eta_{bm} = 0.6$ will

be used. This value is adaptable via the graphical user interface.

With this efficiency and the motor energy need, a rough estimate of the drive cycle radius D_{cycle} may be achieved. Therefore the energy capacity of the battery needs to be known. Although the amount of energy that can be extracted from a fully charged battery is difficult to specify in a single number (this highly depends on temperature, the rate of discharge, battery age, battery type,...), a fixed energy capacity W_{bat} is supposed. Assuming a depth of discharge DOD of 80%, the energy capacity may be estimated at

$$W_{bat} = 0.8 \cdot V_{bat}\,[V] \cdot CAP_{bat}\,[Ah] \tag{10.21}$$

The time between two charges of the battery or battery cycle time T_{bat} while continuously performing the drive cycle is calculated in equation 10.22.

$$T_{bat} = \frac{W_{bat}}{W_b} \cdot T_{cycle} \tag{10.22}$$

This battery cycle time may be transferred into a distance by using equation 10.23, where $v(t)$ is the periodic extension of the drive cycle speed with period T_{cycle}.

$$D_{cycle} = \int_0^{T_{bat}} v(t)dt \tag{10.23}$$

Because of the use of the steady-state measurements to draw conclusions for transient phenomena, the absolute battery ranges are a bit overestimated. But this performance parameter stays very interesting for comparison between pedelecs and/or drive cycles. A more suitable method to estimate the drive cycle range, is suggested in chapter 15.

10.3 Conclusions

In this chapter, a number of performance parameters were defined. These parameters are well defined combinations of different measurements that can be expressed as a single number. These parameters enable the ranking of different aspects of the pedelecs performances in a scientific way.
Two groups of performance parameters are distinguished: the user-independent performance parameters that are totally determined by the pedelec itself and the user-dependent performance parameters that may change by the way the cyclist is using the pedelec.

11

Towards a Standard Drive Cycle

The use of a standard drive cycle is very common in vehicle testing. By using such drive cycles, the fuel consumption and emissions of cars can be easily compared. These cycles simulate urban driving, out-of-town or highway driving. Some try to be as general as possible, others are even city specific (LA-4, New York City Cycle,...) [56]
In the European Union, the emission standard for petrol vehicles is based on the urban and sub-urban drive cycles ECE 15 and EUDC[58],[59], [60]. For electric scooters and smaller city-only electric vehicles, the SAE J227a-C and the ECE-47 are often used [56], [57].

Also for electric bicycles a drive cycle would be interesting. The comparison of the user-dependent performance parameters in chapter 13 will bring to light that the cycling behaviour seriously influences the battery range. The analysis of the user comments in section 2.4 shows that battery range is an important decisive argument for the users. As long as there is no standard drive cycle, the battery ranges specified by the manufacturers are not really scientifically meaningful.
The Dutch firm IDbike started the discussion about a standard drive cycle for pedelecs on their website [36] by introducing their own test cycle. This test drive cycle will be discussed as the first part of this chapter (section 11.1).
In the framework of this research, a microcontroller with additional flash memory is programmed to record the speed during cycling. These records resulted in some more realistic drive cycles that are used as an input for the performance analysis on the measured pedelecs (chapter 13). The measurement system for the speed logging is explained in section 11.2 of this chapter. The chapter is concluded with some remarks about the development of a standard drive cycle.

11.1 The IDbike drive cycle

11.1.1 Description of the IDbike drive cycle

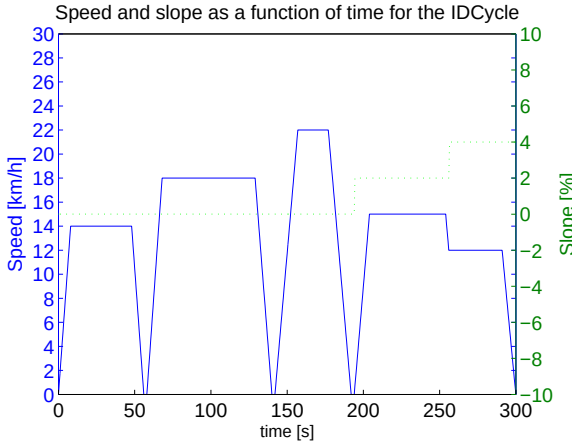

Figure 11.1: Representation of the 'IDcycle': The bicycle speed and percentage of slope as a function of time

The IDbike drive cycle (referred to as the 'IDcycle') is a synthetic drive cycle. The drive cycle is designed with the aim to include all possible real life difficulties within a limited cycle time: different constant speeds, different accelerations and decelerations, a few start/stops, headwind and/or slope loads,...

The 'IDcycle' is graphically represented at figure 11.1 and is described as follows [36]:
"The bicycle fastly accelerates to $14km/h$ and keeps this speed for 40 seconds. After a stop it accelerates to $18km/h$ and keeps this speed for 60 seconds. It stops again and accelerates slowly to $22km/h$ and keeps this speed for 20 seconds. After a last stop an extra brake load is applied, simulating a slope of 2%. The bicycle accelerates to $15km/h$ and stays at this speed for 50 seconds. Then the brake load is increased to a slope of 4%. After 35 seconds the bicycle decelerates and stops. The total distance of the 'IDcycle' is 1050 meters and the average speed is $13.5km/h$."

11.1.2 Analysis of the IDbike drive cycle

In this work the 'IDcycle' is used to calculate and compare some user-dependent performance parameters (chapters 10 and 13). Different qualities of the drive cycle are represented in figure 11.2:

- The *Speed Duration Curve* of figure 11.2a shows the monotonous diagram of

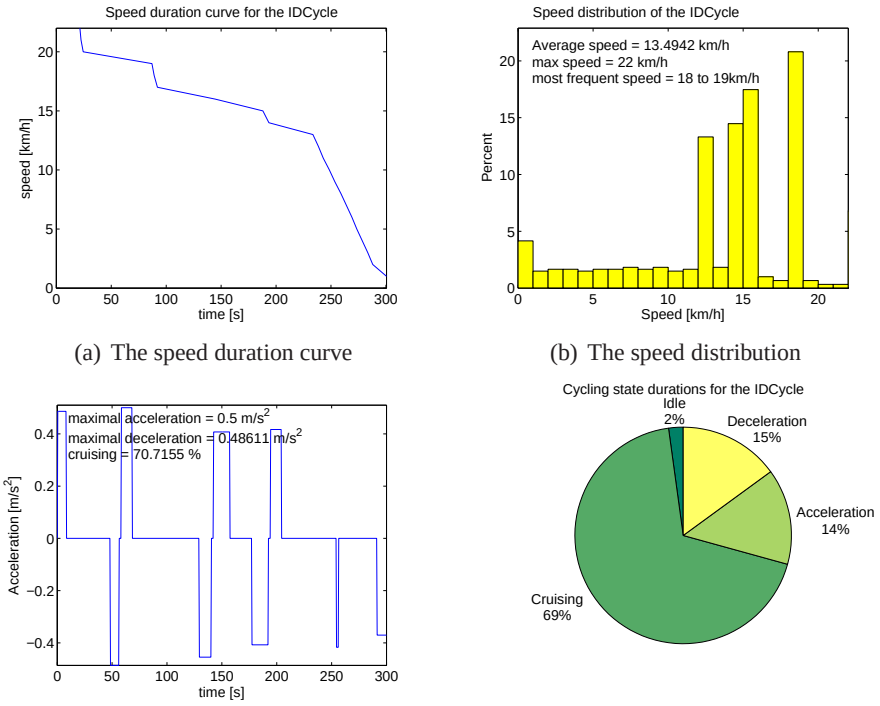

(a) The speed duration curve

(b) The speed distribution

(c) The acceleration plot

(d) The state plot

Figure 11.2: Extra plot options for the 'IDcycle' of figure 11.1

the speed distribution. For every speed on the y-axis, one can read how long the cyclist is riding above this speed on the x-axis.

- The *Weibull Distribution* of figure 11.2b shows for every speed interval on the x-axis which percentage of the time the cyclist is riding at a speed within this interval. The average speed, the maximum speed and the most frequent speed interval are displayed as text in the figure window.

- The *Acceleration Plot* of figure 11.2c plots the acceleration versus the time. The maximum values for the acceleration and decelaration are displayed as text in the figure window.

- The *State Plot* of figure 11.2d shows a pie with the percentages of the time that the cyclist is cruising, accelerating, decelerating and standing still.

All these plottypes can be automatically generated with the graphical interface of chapter 12.

11.2 Recording drive cycles

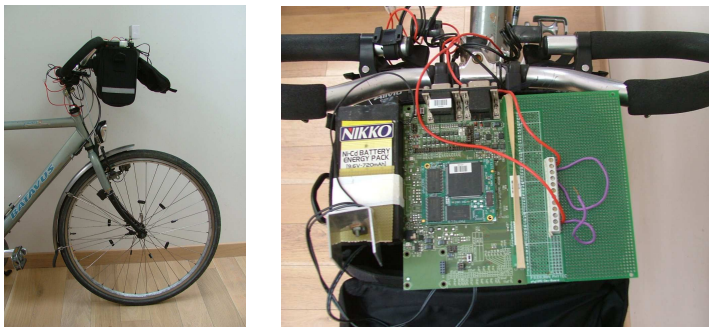

Figure 11.3: On-road speed logging system

An on-road speed logging system is developed with available and cheap equipment, because

- gathering information about the driving behaviour of cyclists in different circumstances is a first step to develop a standard cycle.
- in this work the performance is analysed by means of user-dependent performance parameters (chapter 10) which requires a realistic drive cycle of the user as an input.

A picture of the on-road speed logging system is shown in figure 11.3. The left picture shows the speed sensing magnets and the connection of the reed contact to the microcontroller. The right picture zooms on the microcontroller and its stabilized battery power supply.

11.2.1 The speed sensors

Nine magnets are equidistantly mounted in the frontwheel of the measurement bicycle. A reed contact of a common bicycle computer is connected to the bicycle's front fork. The reed contact gets its power from a $5V$ PWM-output of a microcontroller with duty cycle kept permanently at 100%. Every time a magnet passes by the reed contact, a counter (referred to as counter 1) is increased by 1.

11.2.2 The microcontroller

The phyCore-167 16-bit single-chip microcontroller with $f_{cpu} = 20Mhz$ is programmed to log the speed of the bicycle. There are 2 different ways to calculate the speed using the pulses caused by the speed sensors:

- measuring the time between two pulses

- or measuring the number of pulses in a fixed time interval

The easiest way to program is the second one. The fixed interval is determined by a second counter (counter 2). Counter 2 generates an interrupt at overflow every $838.86ms$ [1]. The major drawback of this system is the rather high minimal discrete speed step Δv. This smallest detectable speed step Δv is calculated in equation 11.1. Therefore the wheel perimeter of the test bicycle is required. A single rotation of the frontwheel of the test bicycle represents $2.2m$.

$$\Delta v = \frac{1}{838.86} pulses/ms = \frac{\frac{1}{9}2.2}{0.83886} m/s = 0.29m/s = 1.0km/h \qquad (11.1)$$

11.2.3 The flash memory

When the interrupt of counter 2 is given, the microcontroller writes the value (in pulses/s) into an AMD flash memory. In order to keep the driver informed about the state of the measurement equipment a LED is lighted everytime the data transfer to the flash memory takes place. A great advantage of using flash memory is appeared to be the non-volatile property, preventing the erasing of data when the power supply is interrupted.

11.2.4 The power supply

The standard phyCore-167 is delivered with a grid power supply. There is need for a conversion to battery power to make the log system portable. For this reason a stabilized power supply is designed using the battery and charger of a $9V$ electric drill.

11.2.5 Example of a recorded cycle

The systematic logging of the cycling behaviour of different user groups is now possible but is not yet included in this work. Only one measured drive cycle will be discussed here to show the possibilities of the log system. This drive cycle will be referred to as the 'Commutercycle'. The speed and slope of this cycle as a function of time is represented in figure 11.4. The difference between this cycle and the synthetic 'IDcycle' is already clear from this figure, but can be furtherly quantified by the comparison of the plots of figure 11.5 with those of figure 11.2:

- The maximum and average speed of the 'Commutercycle' is about 13% higher than the maximum and average speed of the 'IDcycle'.
- The speed distribution is much more continuous
- The acceleration and deceleration maxima are almost twice as high
- There is much less cruising time in the recorded cycle

[1] This value is obtained by counting at a clock speed of f_{cpu}/256

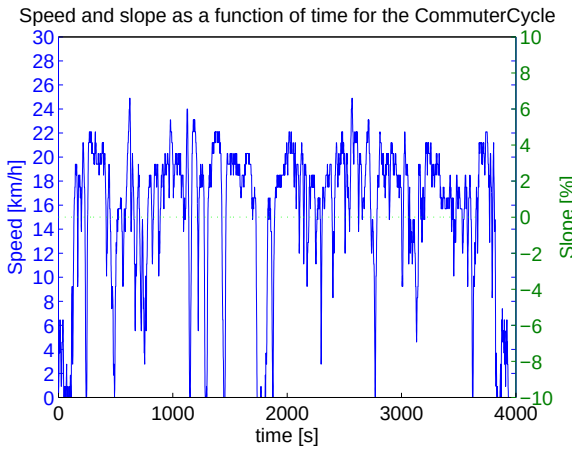

Figure 11.4: Representation of the 'Commutercycle': The bicycle speed and percentage of slope as a function of time

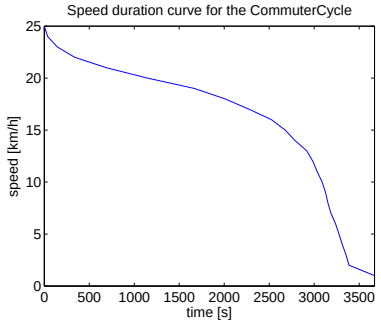

(a) The speed duration curve

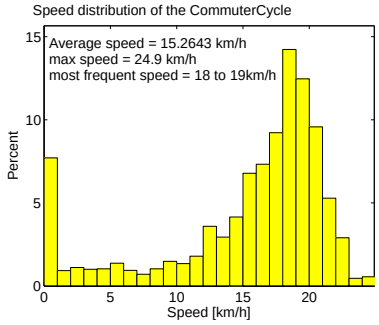

(b) The speed distribution

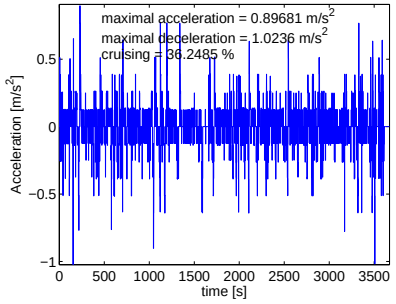

(c) The acceleration plot

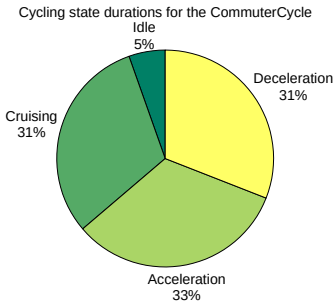

(d) The state plot

Figure 11.5: Extra plot options for the 'Commutercycle' of figure 11.4

- The cycle states cruising, deceleration and acceleration are equally distributed in time (this phenomenon is noticed in most of the recorded cycles)

11.3 Developing a standard drive cycle

The results of the user-dependent performance parameters in chapter 13 clearly show the dependency of the pedelec's performance on the used drive cycle. The development of a standard drive cycle for pedelecs should be discussed among researchers, consumer organisations and manufucturers and is out of the scope of this work. The two drive cycles discussed in the previous sections already learn that the definition of a standard drive cycle for pedelecs will always be a bit arbitrary. Moreover, the proposal of a standard requires much more road measurements. Not only speed measurements are valuable but also the cyclist's torque should be measured to analyse the cycling behaviour on the road.

12

A Graphical User Interface for the Pedelec's Performance Analysis

The characterisation of a pedelec with the developed test installation of section 5 happens in several steps:

1. The measuring of the pedelec
2. The LS-SVM modelling
3. The creation of the performance plots
4. The calculation of the performance parameters
5. The comparison with other pedelecs

The first step is rather time consuming. Plenty of measurements have to be taken for every assistance mode. The record of the cyclist torque, the pedelec speed and the traction force in one operation point takes about 20 seconds. The availabitity of a second battery is recommended to be able to measure without reload breaks. All together, the measurement step quickly takes some hours.
The time for the other steps is kept under control by the introduction of a graphical user interface (GUI) including all the tools for the steps 2 until 5. This chapter will describe the most important functions of the user interface and is written to serve as a user manual.

12.1 Set-up of the GUI

The GUI is programmed in Matlab mainly because there is a *LS-SVM toolbox* available for this numerical computing environment. This toolbox is required for the in-

tended pedelec performance analysis. It can be downloaded for free from `http://www.esat.kuleuven.ac.be/sista/lssvmlab/`.
A *pedelec toolbox* is developed with all the function files and required manipulations for the measurement data. These both toolboxes should be stored in the 'matlabroot/toolbox' path in order to let the GUI work properly.
The GUI is set-up around 5 programfiles or m-files, preferably executed in the given order.

1. **Models_Creation.m** for the creation of the LS-SVM models
2. **Performance_Plots.m** for the creation of the performance plots
3. **DriveCycle.m** for the creation and analysis of a user defined drive cycle
4. **Performance_Parameters.m** for the calculation of the performance parameters
5. **Comparison.m** for the comparison of the performance of different pedelecs

These files may be stored in an arbitrary working directory. The pedelec toolbox and the complete GUI for the pedelec's performance analysis are freely available at `http://www.mathworks.com/matlabcentral/fileexchange`[1] or may be obtained by mailing to *jancappelle@hotmail.com*.

12.2 The creation of the LS-SVM pedelec models

Opening *Models_Creation.m* results in the window of figure 12.1. The window has four fields: the two first fields are reserved to enter the essential measurement and pedelec data, the last two to edit model related information.

12.2.1 The 'Files and Folders' field

The measurement data sets of the pedelec are stored in Excel-files via the Labview DAQ described in section 5.4.6. These files should contain 3 columns:

- Column 1: the speed measurements in m/s
- Column 2: the torque measurements in Nm
- Column 3: the force measurements in N

The measurement data of different assistance modes are stored in different files. The 'datafile' field enables the user to enter the datafile location on the computer and the number of the Excel sheet containing the measurements.

Once the models are created, a lot of data will be stored in a matlab file 'pedelec.mat' in the folder entered in the 'Destination folder'-field.
The 'Pedelec.mat' file may contain up to 8 objects. The structure of this file and its objects are represented in figure 12.2. The object structures are explained in the next sections.

[1] Note that the GUI and the pedelec toolbox is developed for Matlab 7.1 or higher

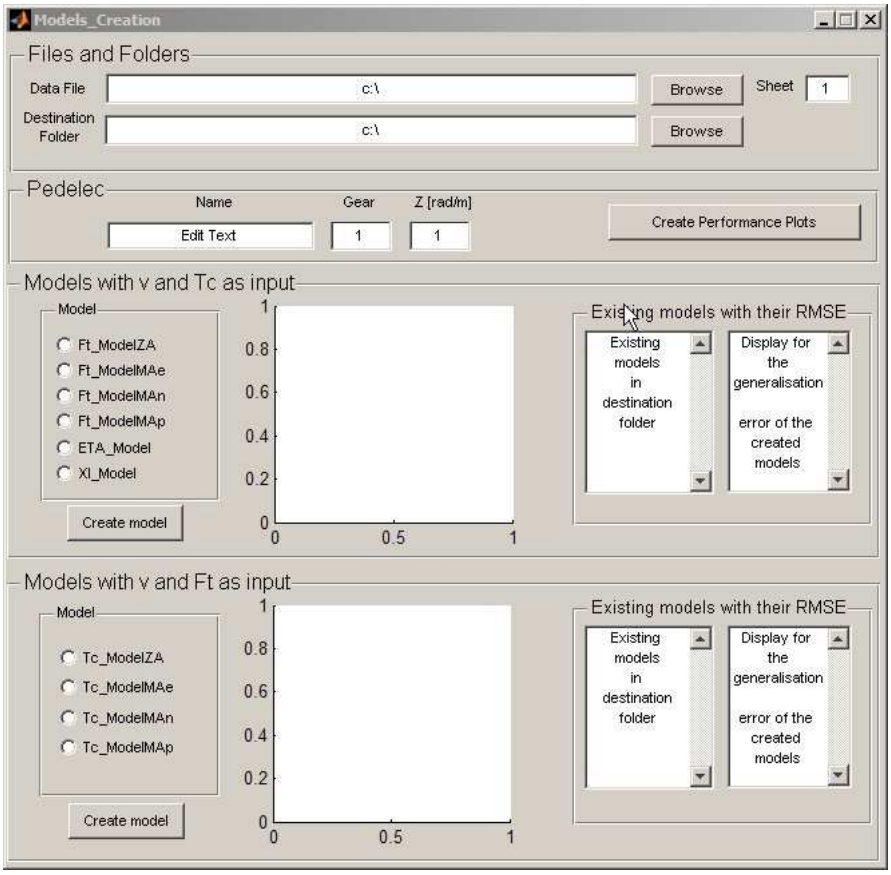

Figure 12.1: Screenshot of the GUI for the creation of the LS-SVM models

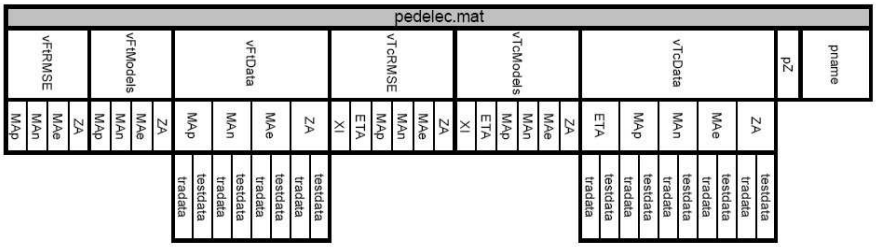

Figure 12.2: Structure of the 'pedelec.mat'-file

12.2.2 The 'pedelec' field

In this field the name, the gearnumber and the transmission ratio Z of the recorded pedelec should be entered. These data are also stored in the 'pedelec.mat'-file when-

ever a model is created.

- The *'pname'-object* (figure 12.2) of this file is a row matrix of two strings: the pedelecname and the gearnumber.
- The *'pZ'-object* is the transmission ratio stored as a string.

Pushing the 'Create Perfomance Plots'-button sends the user to the GUI for the creation of the performance plots of section 12.3. This only makes sense if the required models are already calculated. These model calculations are controlled by the 'Models'-field

12.2.3 The 'Models' fields

There are two 'Models' fields available. The first field enables the user to create all the models where the speed v and the cyclist torque T_c serves as an input. The second field helps to create the models where the speed v and the traction force F_t serve as input variables.
The creation of the LS-SVM models is based on the existing LS-SVM toolbox. The LS-SVM models structure is given in table 12.1. But for this application, the main interest is the calculation of new data points. The syntax for this interpolation is found in equation 12.1.

$$Y_{new} = simlssvm(model, X_{new}) \tag{12.1}$$

X_{new} represents the new input and Y_{new} the resulting output quantities.
Before pushing the 'Create model'-button of the first 'Models'-field, a model choice has to be made:

- Choose the *Ft_ModelZA* and/or *ETA_model* LS-SVM models if the input datafile contains measurement data without assistance power.
- Choose the *Ft_ModelMAe*, *Ft_ModelMAn*, *Ft_ModelMAp* LS-SVM models if the input file contains measurement data with economic, normal or power assistance respectively.
- Choose the *XI_model* when at least the *Ft_ModelZA* and one assisted model Ft_ModelMAx is already calculated.

The name giving as well as more details of all these models are found in chapter 8.
If one is interested in the torque models, the 'Create model'-button of the second 'Models'-field has to be used. Again, the choice of 1 out of 4 torque models has to be made first. This choice depends on the selected measurement datafile.

A push on the 'Create model'-button has 3 major results:

1. A first warning dialog box informs about models that possibly could be found in the destination folder. A second dialog box warns for the duration of the models creation (several minutes per model on a slow computer). If the user

Field	Content	Field	Content
type	'f'	x_delays	0
implementation	'CMEX'	y_delays	0
x_dim	2	steps	1
y_dim	1	latent	'no'
nb_data	149	duration	0.0951
preprocess	'preprocess'	code	'original'
prestatus	'ok'	codetype	'none'
xtrain	[149x2 double]	pre_xscheme	'cc'
ytrain	[149x1 double]	pre_yscheme	'c'
selector	[1x149 double]	pre_xmean	[13.7457 52.9800]
gam	1.7225e+003	pre_xstd	[8.7502 35.9091]
kernel_type	'RBF_kernel'	pre_ymean	27.5396
kernel_pars	3.1728	pre_ystd	16.5099
cga_max_itr	149	status	'changed'
cga_eps	1.0000e-015	cga_startvalues	[]
cga_fi_bound	1.0000e-015	alpha	[149x1 double]
cga_show	0	b	-0.0069

Table 12.1: An example of a LS-SVM model construction

still decides to go on, **the model creation** will start. The axes in the middle of the 'Models'-field will show the state of the LS-SVM model creation. If the state of the LS-SVM calculation is opening in a new window, just close the window and the right axes will take over.

2. After the creation of the models, **the calculation of the RMSE values** from the testdata applied to the corresponding model is executed following the rules of chapter 8. These RMSE values and the corresponding short model name (ZA, MAe, MAn, MAp, XI, ETA) are displayed in the 2 RMSE columns within the 'Models'-field. Because the creation of a model is based on a random split up of the input data in testdata and trainingsdata, the RMSE may differ if calculated more than once. When the user judges the displayed RMSE value to be too high, a recalculation of the same model might lower this value. If still not satisfying, more data points should be taken to refine the model, or more accurate measurements should be taken!

3. **The 'pedelec.mat'-file is updated**:

   - The created models of the first field will be stored as subobjects of the 'vTcModels'-object[2]. The *'vTcModels'-object* may be filled with 5 possible LS-SVM models and 1 *XI_model* as may be clear from figure 12.2.

[2]The names of the model-objects are based on the input (x,y) variables of their 3D presentation: e.g. vTc for $\hat{F}(v, Tc)$.

The created models of the second field will be stored as subobjects of the 'vFtModels'-object of the 'pedelec.mat'-file (figure 12.2). The *'vFtModels'-object* may be filled with 4 possible LS-SVM models.

- The RMSE values are stored as part of the *'vTcRMSE'-object* or the *'vFtRMSE'-object* depending on the model type.
- The applied training and testdata are stored as part of the *'vTcData'-object* or the *'vFtData'-object* depending on the model type.

12.3 The creation of the performance plots

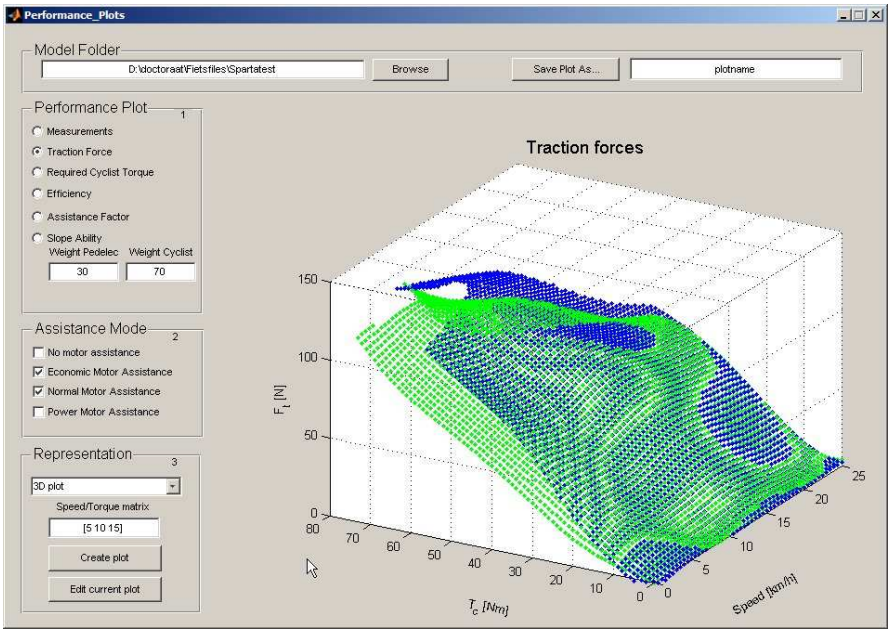

Figure 12.3: Screenshot of the GUI for the visualisation of the performance plots

Chapter 9 describes the different ways of presenting the pedelec models using performance plots. These performance plots are easily created, displayed and saved with the 'Performance_Plots.m'-file. Running this m-file opens the graphical user interface of figure 12.3. Five main fields with their own functionalities may be recognized:

1. In the *'Model Folder'-field* the path to the folder with the 'pedelec.mat'-file of interest has to be filled in first. Browsing as well as typing the pathname is possible. If the user wants to save the performance plot, an eps-file of the performance plot is saved in the pedelec folder when pushing the 'Save Plot As...'-button. In the 'plotname'-field, the desired name of this eps-file may be typed.

2. The *'Performance Plot'-field* enables the user to switch between the different performance plots. The radio buttons assure exclusive selection.

   - Choose 'Measurements' to select the measurement data splitted up between trainings- and testdata.
   - Choose 'Traction force' to select the $\hat{F}_t(\bar{v}, \bar{T}_c)$ LS-SVM model
   - Choose 'Required Cyclist Torque' to select the $\hat{T}_c(\bar{v}, \bar{F}_t)$ LS-SVM model
   - Choose 'Efficiency' to select the $\hat{\eta}_t(\bar{v}, \bar{T}_c)$ LS-SVM model
   - Choose 'Assistance Factor' to select the $\hat{\xi}_t(\bar{v}, \bar{T}_c)$ model
   - Fill in the weights of the pedelec and the cyclist and choose 'Slopeabibity' to select the maximal slope that can be overcome by a given torque and speed.

3. The desired assistance mode or modes may be selected in the *'Assistance Mode'-field*.

4. The way of presenting the models may also be changed: The popup-menu in the *'Representation'-field* allows 3D-plots, contourplots, slices of constant speed or slices of constant torque. For the slice plots, the number of slices is adaptable by giving the values of the constant torques or constant speeds as a matrix $[a_1\ a_2\ ..\ a_n]$.

5. A push on the 'Create plot'-button is required every time a new selection has been made. Then a plot of the selection is displayed in the *'Axes'-field*. If one would like to edit the plot, a new editable figure window will be opened after a push on the 'Edit current plot'-button.

If 'weird' combinations are selected, or if some data is missing a warning dialog box appears.

12.4 The creation and analysis of a drive cycle

A number of performance parameters are labelled as 'user-dependent'. They are explained in chapter 10. The calculation of these user-dependent performance parameters requires data about a drive cycle, the environment, the driver and his position on the bicycle. These data may be entered via a new graphical user interface 'DriveCycle.m' which is shown in figure 12.4. This GUI allows the calculation and visualisation of the different forces and the energy consumption during the cycle coverage. After running this file, all relevant drive cycle data are stored in one 'cycledata.mat'-file.

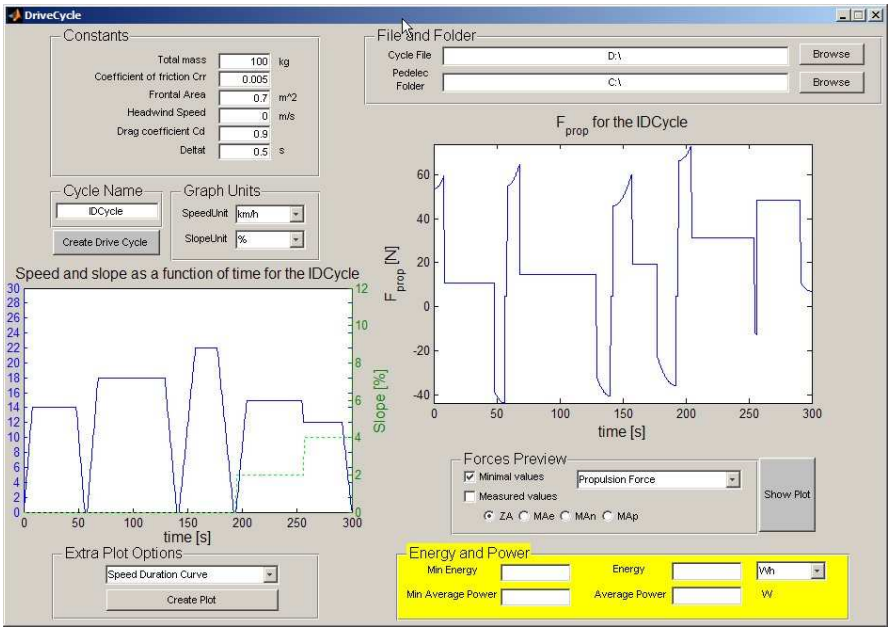

Figure 12.4: The graphical user interface to create and analyze drive cycles

12.4.1 The input fields

File and Folder

The user may introduce his own cycling trip (= 'drive cycle') to compare the performances of different pedelecs to cover his trip.
The base format for entering a drive cycle in the graphical user interface is an Excel file with 3 columns including in column:

1. the time in seconds (start by $t = 0$),
2. the speed in km/h,
3. the percent slope.

At least, each change in the percent slope or acceleration requires a new row entry in the Excel file. A possible Excel file for the drive cycle of figure 11.1 is given in table 12.2.
The absolute pathname to this Excel file has to be entered in the 'Cycle File'-field. This may happen by typing or browsing.
In this GUI there is also a built-in tool to analyse the 'drive cycle' behaviour of a particular pedelec. Therefore the directory of the folder where the concerning 'pedelec.mat'-file (section 12.2) is stored has to be entered in the 'Pedelec Folder'-field. Again, both typing and browsing are possible.

%Time [s]	%Speed [km/h]	%Slope [%]
0	0	0
8	14	0
48	14	0
56	0	0
58	0	0
68	18	0
129	18	0
140	0	0
142	0	0
157	22	0
177	22	0
192	0	0
194	0	2
204	15	2
254	15	2
256	12	4
291	12	4
300	0	4

Table 12.2: An example of a drive cycle entry for the GUI

Constants

The 'Constants'-field enables the user to enter information that may be helpful to estimate the forces during the drive cycle.

- *The total mass* m_{tot} of the bicycle, the cyclist and, if any, the luggage.
- *The coefficient of friction* C_{rr} between the pedelec and the road surface.
- *The frontal area* of the cyclist and his bicycle.
- *The headwind speed*
- *The drag coefficient* C_d
- *Deltat* is the time step which will be used to linearly interpolate the rows of the drive cycle Excel-file. So an estimate of the percent slope and speed is obtained for all moments between the time entries of the first and the last row of the file.

The total mass and the coefficient of friction are required to estimate the rolling resistance during the drive cycle. The dynamic rolling resistance may be modelled by equation 12.2 where g represents the gravitational acceleration and α the angle of the slope.

$$F_{roll} = C_{rr} \cdot m_{tot} \cdot g \cdot cos\alpha \tag{12.2}$$

The frontal area, the headwind speed and the drag coefficient are required to estimate the air resistance using equation 10.6. The default value for the coefficient of friction will be 0.005 as proposed in reference [61]. The other default values were already specified in table 10.2.

Cycle Name

In the 'Cycle Name'-field a name may be entered for the drive cycle. This name will appear in the title of the created plots.

Graph Units

The units for the speed and the slope applied in the plots can be adjusted in the 'Graph Units'-fields. The speed may be displayed in km/h or m/s, the slope in degrees or as a percentage.

12.4.2 The creation of a drive Cycle

The 'Create Drive Cycle'-button

If all the input fields are checked, the 'Create Drive Cycle'-button may be pushed. This results in

- the *visualisation of the drive cycle* in the left axes-field, which means that the slope as well as the speed will be displayed as a function of time
- the *calculation of the resisting forces* as time functions
- the *creation of a 'Cycleforces'-object* (see next section)
- the *saving of the 'Cycleforces'-object* in a cycledata.mat file in the folder of the input drive cycle Excel-file.

The structure of a 'Cycleforces'-object

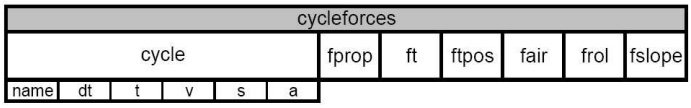

Figure 12.5: The structure of a 'Cycleforces'-object

Information that is essential to calculate the user-dependent performance parameters (with the m-file described in section 12.5) is stored in the 'cycledata.mat'-file as a 'Cycleforces'-object with 7 subobjects. This is represented in figure 12.5.

- The *'cycle'-subobject* includes:
  - the $name$ of the cycle
  - the applied interpolation step dt
  - all times t going from zero to the total cycling time with time step dt
  - the values of the speed v at the moments t
  - the values of the slope s at the moments t

  - the values of the acceleration a at the moments t

- The *propulsion force* $fprop$ at each moment t, calculated with equation 6.12, but considering a bicycle without internal mechanical losses
- The *minimal traction force* ft at each moment t, equals the $F_{t_{min}}$ from equation 10.5
- The *minimal traction force* $ftpos$ at each moment t equals the previous item, but ignores the negative (or braking) parts
- The *air resistance* $fair$ at each moment t, using equation 10.6
- The *rolling resistance* $frol$ at each moment t, using equation 12.2
- The *slope resistance* $fslope$ at each moment t, using equation 9.1

12.4.3 Forces Preview

The axes-field at the right side of the GUI will be used to plot the forces and torques as a function of time.
When the 'Minimal values'-checkbox is checked while pushing the 'Show Plot'-button, the plot selected in the pop-up menu will be displayed. These 'Minimal values'-plots are all based on the coverage of the drive cycle with a lossless bicycle. The options are

- the *Propulsion Force* to see $fprop$
- the *Traction Force on testbench* to see $ftmin$
- the *Rolling, Slope or Air Resistance*
- and the *Required Cyclist Torque*

The *Required Cyclist Torque* represents the torque that should be delivered by the (dummy) cyclist on the testbench to reach the speed and traction force of the drive cycle with a lossless non-assisted pedelec.
When the 'Measured values'-checkbox is checked, this *Required Cyclist Torque* option of the pop-up menu is the only one that makes sense! In this case, the torque is calculated using the data from the 'pedelec.mat'-file that are found in the given pedelec folder. Here, also another choice has to be made by the user.

- checking *ZA* will display the cyclist torque that should be delivered by the cyclist with the pedelec without motor assistance
- checking *MAe* will display the cyclist torque with low motor assistance
- checking *MAn* will display the cyclist torque with normal motor assistance
- checking *MAp* will display the cyclist torque with high motor assistance

12.4.4 Energy and power

By pushing the 'Show Plot'-button while the 'Required Cyclist Torque' is selected, also the 'Energy and power'-field will be edited.
Here, the user may read *the human energy* and *average human power* that is required to cover the drive cycle

- with a lossless bicycle if the 'Minimal values'-checkbox is checked
- with the pedelec from the entered 'pedelec.mat'-file in the indicated assistance mode if the 'Measured values'-checkbox is checked

The units for the displayed energies may be switched between watthour [Wh] and joule [J] by a pop-up menu.

12.4.5 Extra Plot Options

The analysis of the cycling behaviour using the road measurements of chapter 11 and also the comparison between different drive cycles is facilitated by means of the extra plot options in this GUI.
Choosing an option of the pop-up menu will open a new figure window when the 'Create Plot'-button is pushed. The next plot options are available:

- The speed duration curve
- The weibull distribution
- The acceleration plot
- The state plot
- The drive cycle plot (opens the left-axes field in a new figure window that is easily editable by the user)

The meaning and some examples of these plots are already discussed in chapter 11.

12.5 Calculation of the performance parameters

The objective performance analysis described in chapter 10 requires many data manipulations. An automation of these manipulations is recommended. By running the 'Performance_Parameters.m'-file, the graphical user interface of figure 12.6 will open. This GUI allows the user to calculate the user-independent as well as the user-dependent parameters.
Both parameter types require the input of a 'pedelec.mat'-file that may be developed by the 'Models_Creation.m' GUI of section 12.2. The directory where this file is stored has to be entered in the 'Pedelec Folder'-field. Typing as well as browsing is possible. The calculation of the user-dependent parameters also requires drive cycle data. The directory of a 'cycledata.mat'-file developed by the 'DriveCycle.m'-GUI of section 12.4 has to be entered in the 'Drive Cycle Folder'-field.

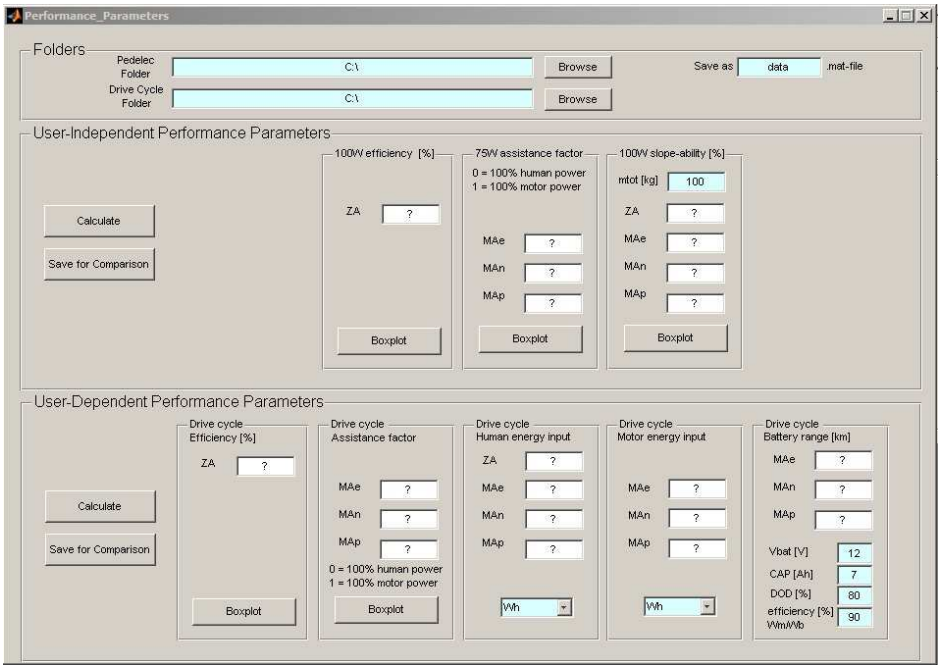

Figure 12.6: Screenshot of the GUI for the calculation of the performance parameters

12.5.1 The user-independent performance parameters

The 'Calculate'-button

A push on the 'Calculate'-button in the 'User-Indepent Performance Parameters'-field results in the calculation of

- the $100W$ efficiency (ETA)
- the $75W$ assistance factors (XI)
- the $100W$ climbing-(or slope-) abilities (SA)

as explained in chapter 10 for the pedelec described in the entered 'pedelec.mat'-file. The abbreviations between brackets are used to refer to the corresponding parameters in the '*data*.mat'-file that will be introduced in the next section. The calculation of the climbing-ability requires an input for the total mass of the cyclist, the pedelec and the luggage. The default value is $100kg$
The user-independent parameters are displayed for all assistance modes that are found in the 'pedelec.mat'-file. The names given in the 'Models_Creation.m' (section 12.2) determine which fields that are available in this file. Maximum 4 modes may be displayed: A non-assisted mode (ZA), an economic mode (MAe), a normal mode (MAn) and a power mode (MAp). If there are less assistance modes available, not all the fields will be filled.

The 'Boxplot'-buttons

There are many points of the operation area that represent $100W$ or $75W$ input. The values that appear in the '?'-fields are the averages of all these points for the corresponding performance parameters as explained in chapter 10. The distribution of these points may be displayed in a boxplot by pushing the corresponding 'boxplot'-button. This representation enables the user to quantify the differences in efficiency, motor assistance or climbing-ability for the different power modes from the considered pedelec. This could be done by a simple comparison between the average values, but by preference, a comparison should be based on the distributions of the performance parameter. This is discussed in more detail in chapter 10. The values that appear between each two boxplots are the results of the wilcoxon hypothesis tests applied on the two adjacent assistance modes. The smaller this number, the smaller the change that both data samples are coming from equally distributed models, and so the smaller the change that both assistance modes are equal.

12.5.2 The user-dependent performance parameters

The 'Calculate'-button

The calculation of the user-dependent performance parameters requires the input of the cycling behaviour of the user. So, a push on the 'Calculate'-button in the 'User-Indepent Performance Parameters'-field will only fill in the '?'-fields if a 'cycledata.mat'-file is entered in the 'Drive Cycle Folder'-field. The fields to be filled are

- the drive cycle efficiency (ETA)
- the drive cycle assistance factor (XI)
- the required human energy input to cover the drive cycle (HEI)
- the required motor energy input to cover the drive cycle
- the drive cycle battery range (BR)

The quantities of energy may be expressed in joules or watthours, as indicated by the pop-up menus. The number of fields that will be filled depends on the number of assistance modes that are available in the 'pedelec.mat'-file as is earlier explained for the user-dependent performance parameters. The calculation of the drive cycle battery range requires the following input data:

- the battery voltage ($24V$)
- the battery capacity ($7Ah$)
- the allowed Depth of Discharge (80%)
- the efficiency of the energy conversion (60%)

The default values are given between brackets but may be changed by filling in the corresponding fields of the GUI.

The 'Boxplot'-buttons

The distributions of the efficiency and the assistance factor along the drive cycle may be expressed in a boxplot by pushing the corresponding 'boxplot'-button. If more assistance modes are available, the results of the wilcoxon hypothesis tests are displayed between each two adjacent assistance modes. The smaller the result, the more probable the hypothesis that both assistance modes differ.

12.5.3 Saving the parameters

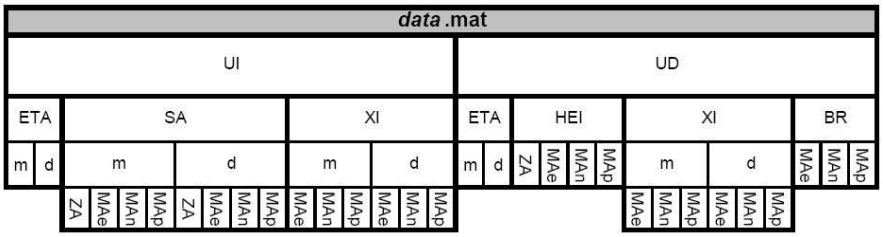

Figure 12.7: Structure of the saved performance parameters

Only momentarily representing the performance parameters lead to a lot of manual datatransfer if the comparison between two different pedelecs is required. This can be avoided by saving all the performance parameters in a new '*data*.mat-file'. The average values as wel as the distributions are saved. The name of the '*data*.mat-file' is editable via the 'Save as'-field in the upper right corner of the GUI (figure 12.6. It is recommended to choose a name that refers to the pedelec as well as to the drive cycle applied for the calculation of the user dependent performance parameters.

The structure of this saved results of the performance analysis is given in figure 12.7. The '*data*.mat-file' contains 2 major objects, the user-independent (UI) performance parameters and the user-dependent (UD) performance parameters. Each performance parameter consists of the average value (m) as well as its distribution (d), except for the human energy input (HEI) and the battery range (BR). The lowest layer distinguishes between the different assistance levels. This '*data*.mat-file' will serve as an input for the 'Comparison.m'-file of section 12.6.

Example

The values can be recalled by the standard Matlab commands. The Matlab commands that will recall the list of values (d) of all assistance factor (XI) along a drive cycle (UD) in normal assistance mode (MAn) is given as an example.

load data.mat
UD.XI.d.MAn

The first line only loads the stored data-file. The second line searches the values in the structure of figure 12.7.

12.6 Comparison of the performance of different pedelecs

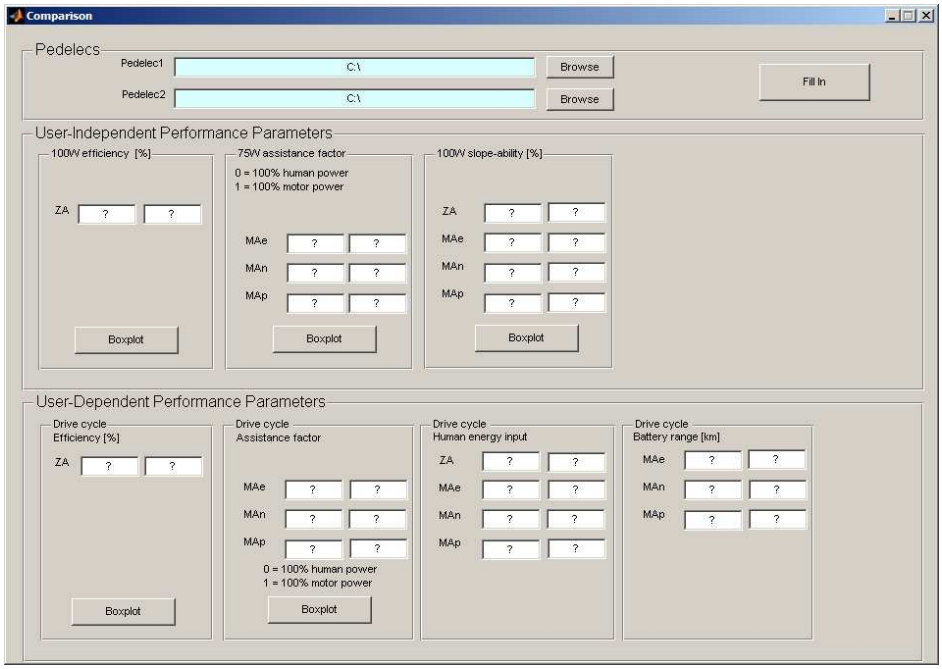

Figure 12.8: Screenshot of the GUI for the comparison of different pedelecs

Not only a comparison between the different assistance modes of one pedelec is interesting. Also the difference in the performance of different pedelecs, or different gears of the same pedelec, or the different behaviour for different drive cycles with the same pedelec, or the influence of different tyre pressures,... are interesting to investigate.
The previous section reports how the calculated performance parameters are stored in a single '*data*.mat'-file. Because of this structure, the comparison of two pedelecs is reduced to the comparison between 2 of these files. The graphical user interface 'Comparison.m' enables this comparison based as well on the average values as on the complete distributions. The method is described below, practical results of various comparisons are given in chapter 13.

12.6.1 Average values

There are 3 main fields in the 'Comparison.m'-GUI:

- The *'Pedelecs'-field* where the 2 '*data*.mat'-files (see figure 12.7) for the intended comparison have to be entered.
- The field of the *User-Independent Performance Parameters* where the $100W$ efficiency, the $75W$ assistance factor and the $100W$ climbing-ability will be displayed
- The field of the *User-Dependent Performance Parameters* where the drive cycle efficiency, the drive cycle assistance factor, the human energy input and the battery range will be displayed.

A push on the 'Fill in'-Button shows all available performance parameters. The left columns represent the values for the first pedelec of the *'Pedelecs'-field*, the right columns the second pedelec.

12.6.2 Boxplots

The 'Boxplot'-buttons under some of the performance parameters enable the user to compare the distributions of these performance parameters by means of the boxplot representation. For every available assistance mode, a new figure window is opened containing two boxplots, the left one represents the first pedelec, the right one, the second pedelec. Again, the wilcoxon hypothesis test is performed on the parameters of both pedelecs, and the result is shown in each figure window. A value near 1 raises the change that both performance parameters are equal, a value near 0 means that the parameters distributions differ.

12.7 Conclusion

A lot of manipulations are required on the data from the testbench measurements before the performance plots and performance parameters of a pedelec can be derived. These data manipulations are automated by means of the five Matlab programs introduced in this chapter. Each of these programs have a simple graphical user interface for data input and output. Next to the performance analysis of a single pedelec, also comparisons between different pedelecs are automated.

13
Performance Analysis Results

The objective performance analysis method described in part II of this book, is applied to different pedelecs. This chapter reports about the measurement of these pedelecs on the designed test bench.
The tests are not only executed to get an idea of the performance of these pedelecs, but also to refine and optimize the construction of the testbench and the corresponding performance analysis method. That is the reason why the spreading of the measurements is not always optimized for the finally intended performance analysis. With an optimal spreading of the trainingsdata, the testdata errors on the regression models are expected to be lower.
This chapter will mainly focus on the calculated performance parameters. The performance analysis by means of performance plots is preferably executed directly with the graphical user interface of chapter 12 and thus hard to discuss in a textbook.

13.1 Pedelec tests

Up to now 6 different pedelecs are measured and analysed, they are all given in table 13.1 with their recorded gearnumber, transmission ratios Z and the available assistance modes. The last column shows the short name that will be used to indicate the pedelec in the test results of the next sections.
The Sachs Elo-bike is measured in different gears and is used to discuss the influence of the gearnumber on the assistance (see also section 5.8).
From the Sparta Ion, two different pedelecs with different motor assistance programs are put at the disposal by the manufacturer. The first one (labelled as ‘Sparta Ion 1’) has no gears, the second one (‘Sparta Ion 2’) is equipped with a Shimano Nexave 7

Pedelec	Gear number	Z $[m/rad]$	Assistance Modes	Short Name
L'avenir pre-scoot MERIDA	2	0.679	MAn	MER
Yamaha PAS easy	2	0.654	MAe-MAp	PAS
SACHS Elo-bike touring	1	0.506	MAn	$SA1$
	2	0.674	MAn	$SA2$
	3	0.897	MAn	$SA3$
Swiss FLYER F6	2-4	0.700	MAn	FLY
Sparta ION 1	1	0.827	MAe-MAn-MAp	$IO1$
Sparta ION 2	5	0.783	MAe-MAn-MAp	$IO2$

Table 13.1: Tested pedelecs

gear apparatus. To measure the last one, its transmission ratio was set similar to the first one.

13.2 Performance Plot Results

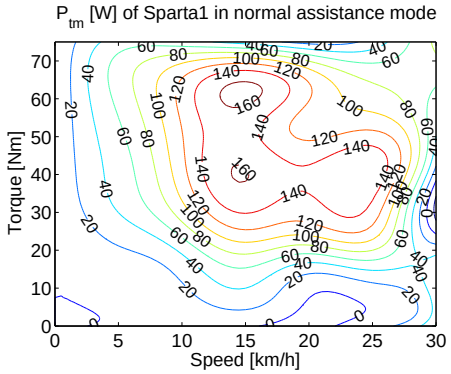

Figure 13.1: Absolute contribution (expressed in watts) of the motor to the traction power for the Sparta Ion

The performance analysis by means of the performance plots is fast and easy with the graphical user interface (see chapter 12). The dynamic production of different plottypes and slices learns a lot about the behaviour of the pedelecs. However the representation of all possible plots for all test pedelecs would lead to too much figures in this book.
It is nevertheless interesting to have a look at the contourplots for the assistance factor of all tested pedelecs that are given in Appendix C. They give a good idea of the applied control strategy for the different motor assistance modes.

Some things attract attention:

- Looking at the operation point were the assistance factor reaches a maximum, many different control strategies are discovered:
  - Maximum assistance for small speeds and high torques for the Merida and Yamaha PAS.
  - Maximum assistance extended for small torques and low speed for the Sachs.
  - Maximum assistance for higher speeds and lower torques for the Sparta Ion pedelecs.

- The Merida, the Yamaha PAS and the Sachs in 3^{rd} gear provide motor assistance almost independently from the input torque. The Sparta Ion and Swiss Flyer introduce a torque dependency.

- The Merida and Yamaha PAS decrease the assistance level very fast with speed.

- The Flyer also seemed to stop assisting for speeds above 17km/h. This might be due to an internal error of the controller during the tests. This error was only discovered when the tested Flyer was put again on the road. A reset of the controller could solve the problem, but so far the measurements are not yet retaken. *So, for the further analysis of the test results, the Flyer is left out of consideration!*

- The assistance values for small torques of all pedelecs are rather high because of the numeric instability of the calculation method in this region.

- The Sachs in 3rd gear assists up to higher speeds than the lower gears.

- The Sparta Ion also assists for speeds above 25km/h. This is contrary to the pedelec speed limit used in the preliminary standard prEN15194 which is discussed in section 1.5.4. A more detailed look on this fact is given in figure 13.1. The assistance cuts off at around 30km/h, which is 20% over the permitted speed limit.

Anyway, the contourplots of the assistance factors show that the effective assistance level is a result of the interaction between the pre-programmed controller, the measurement techniques for speed and/or torque, and the behaviour of the pedelec/cyclist/road system.
The comparison of the assistance levels of all the tested pedelecs is furtherly investigated in the next sections on the performance parameter basis.

	MER	PAS	$SA1$	$SA2$	$SA3$	$IO1$	$IO2$
$\eta\,(100W)$ [%]							
ZA	73±8	81±6	87±5	95±7	88±9	94±7	100±5
$\xi\,(75W)$							
MAe	-	0.38±0.03	-	-	-	0.3±0.04	0.28±0.04
MAn	0.48±0.08	0.52±0.04	0.44±0.03	0.43±0.06	0.47±0.08	0.39±0.04	0.39±0.06
MAp	-	-	-	-	-	0.52±0.06	0.48±0.07
$SA\,(100W)$ [%]							
ZA	4.6±0.5	5±0.3	6.6±0.6	5.8±0.5	4.4±0.3	4.9±0.2	5.3±0.4
MAe	-	8.9±0.5	-	-	-	7.1±0.3	7.4±0.4
MAn	9.9±1.1	13±0.6	14±1.1	11±1.1	8.6±0.7	8.2±0.2	8.5±0.5
MAp	-	-	-	-	-	9.3±0.4	10±0.5

Table 13.2: Results for the user-independent performance parameters of all tested pedelecs

13.3 The user-independent performance parameters

13.3.1 The Average Values and the RMSE

Table 13.2 shows the average values of the user-independent performance parameters for all pedelecs of table 13.1: the $100W$ efficiency (η), the $75W$ assistance factor (ξ) and the $100W$ climbing-ability (SA). The assistance modes to which the values belong are displayed in the first column. The values for the efficiencies are only available without motor power (ZA), the assistance factor and climbing-abilities may be available in different assistance modes (MAe, MAn, MAp).
Chapter 8 explains how an idea of the accurracy of the regression models is obtained by using the RMSE on a serie of testdata applied to the models. The results for these RMSE are also given in table 13.1 [1].

A graphical representation of the average values (as central spots) and the errorbars of $\pm 1\sigma$ (as grey bars) for the user-independent performance parameters is given in figure 13.2. If more than one assistance mode is available, more than one bar is shown in the pedelec column. This is the case for the Yamaha PAS and the Sparta Ions.
Some conclusions drawn out of these figures are collected below:

- The Merida and the YamahaPAS have a significant lower efficiency than the other pedelecs at $100W$ human power input.
- The pedelecs with a hub motor (Sachs Elo-bike and Sparta Ion) have a greater mechanical efficiency.
- The assistance factors for most pedelecs are slightly below 0.5. This means that a bit more than 50% of the traction power is coming from the cyclist's efforts.
- The different assistance modes of the YamahaPAS as well as those of the Sparta Ions are well distinguished for a human input power of $75W$.

[1] The RMSE values for the climbing-ability (SA) are derived from the RSME values of the traction force models using the conversion of equation 9.2 with a (default) total mass of $100kg$.

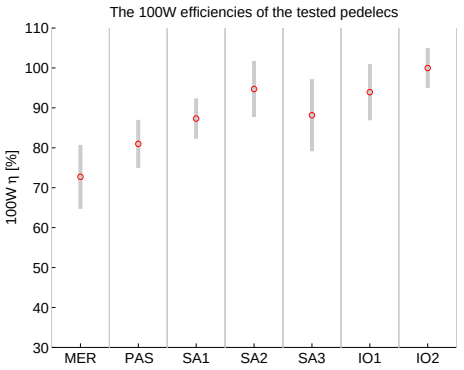

(a) The $100W$ efficiency

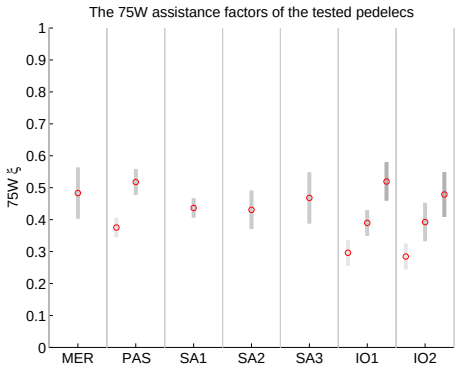

(b) The $75W$ assistance factor

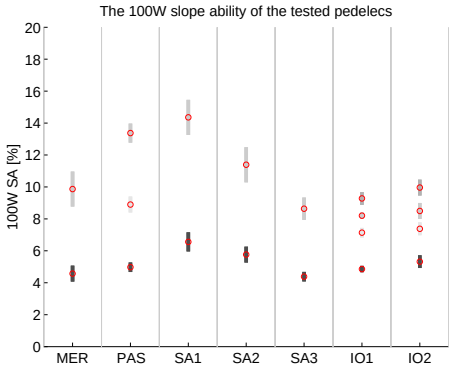

(c) The $100W$ climbing-ability without (black) and with (greyscales) motor power

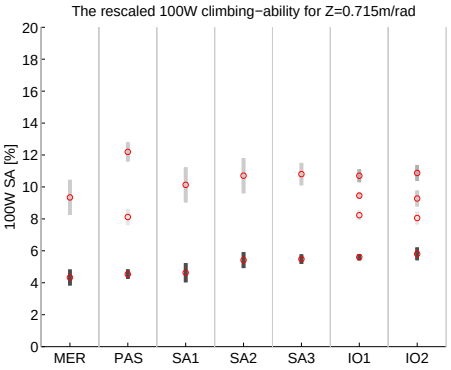

(d) The rescaled (for $Z = 0.715$) $100W$ climbing-ability without (black) and with (greyscales) motor power

Figure 13.2: The average values and the RMSE errorbars for the user-independent performance parameters of the pedelecs from table 13.1.

- All pedelecs double their climbing-ability by adding motor power. The YamahaPAS almost triples the climbing-ability by applying its highest assistance mode.
- The Sachs Elo-bike in first gear may overcome a percent slope of 14% with a human power input of $100W$!
- Remark that the climbing-ability is (logically) gradually decreasing by increasing gearnumber. The climbing ability for all bicycles is therefore rescaled to a transmission ratio of $Z = 0.715m/rad$ (the average of the measured pedelec) resulting in figure 13.2(d).
- The predictability of the models for the testdata can be approved by a more

aimed test program for the pedelecs. The spreading of the measurements in the operation area of the cyclist is not always well considered during the tests (read the suggestions for future measurements in chapter 15).

13.3.2 The distributions

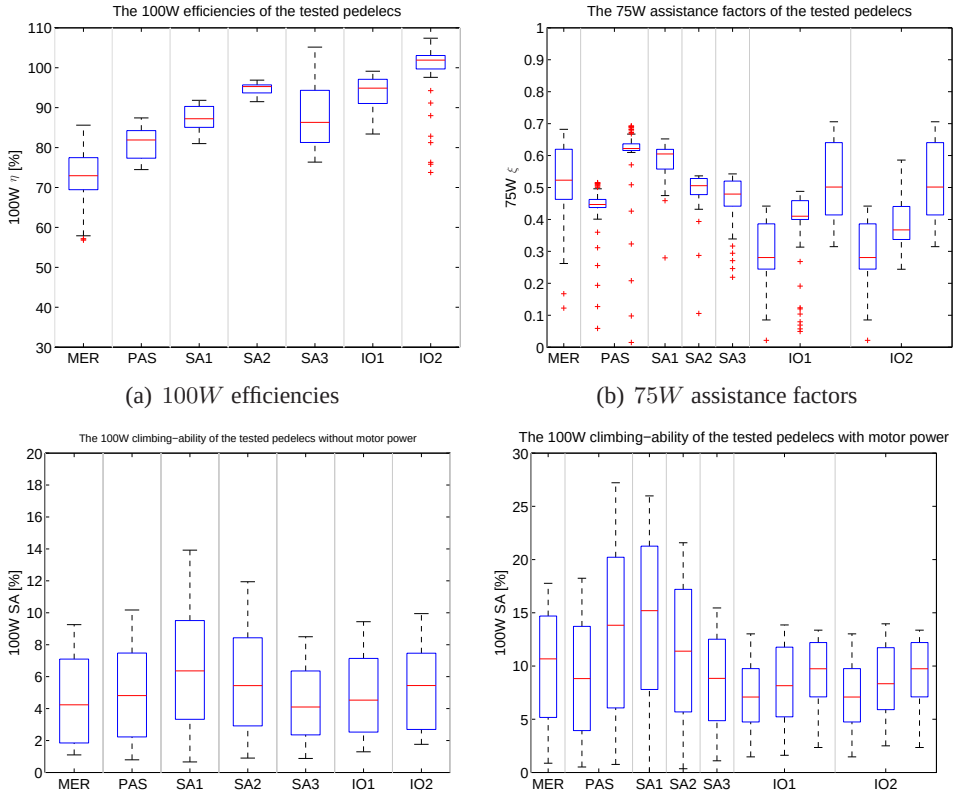

(a) $100W$ efficiencies

(b) $75W$ assistance factors

(c) $100W$ climbing-ability without motor power

(d) $100W$ climbing-ability with motor power

Figure 13.3: The boxplots of the distributions of the user-independent performance parameters for the pedelecs of table 13.1

Chapter 10 indicated already that a comparison between the average values of the performance parameters is only a part of the performance analysis. Two average values of a performance parameter can be the same, while the behaviour of the pedelec is completely different over the operation area. The $100W$ efficiency, the $75W$ assistance factor as well as the $100W$ climbing-ability are obtained by considering well-defined parts of the regression models. The representation of the distribution of these constant power parts tells how much the performance parameters are changing

with a constant power input.
The boxplots representing the distributions of the user independent performance parameters of the considered pedelecs are given in figure 13.3.

The analysis of these figures lead to the following conclusions:

- A lot of outliers appear for the 100W efficiency and the 75W assistance factors because both performance parameters are the quotient of two power measurements. This quotient is numerically less stable when the nominator gets smaller.
- The larger distance between the upper and lower quartiles of the efficiency distributions for the Sachs3 measurements is unexpected, because the efficiency is supposed to be quite stable over the operation area. Only a slight drop with higher speeds is expected. Again, the unstable behaviour of the quotient calculation of two powers may be the cause of this problem.
- The distance between the upper and lower quartiles of the assistance factor and the climbing-ability is explicable by the role of the controller, a different torque and speed input may result in a different motor assistance and so a different climbing-ability and assistance factor.
- The distributions seems to be quite symmetrical. The median and average values will be close to each other.

13.4 The user-dependent performance parameters

The assistance levels seem to fluctuate a lot over the operation area as shown in the former section. To show the impact of these fluctuations on the driving experience, the behaviour of the cyclist has to be introduced by means of a drive cycle. The instruments that are used in this work are the user dependent performance parameters of chapter 10:

- The drive cycle efficiency
- The drive cycle assistance factor
- The human energy need to cover the drive cycle
- The motor energy need to cover the drive cycle
- The drive cycle battery range

The user-dependent performance parameters are calculated for 2 different drive cycles:

- The ‘IDcycle’, which is the drive cycle of figure 11.1. It is a synthetic cycle of 300s with a few slopes introduced.

- The ‘CommuterCycle’ introduced in section 11.2.5 as a recorded commuting cycle of 3670s without slopes.

The difference in the speed distributions of both drive cycles are given in figures 11.2 and 11.5. The average values as well as the distributions for the drive cycle efficiency and the drive cycle assistance factor, are given in the next two paragraphs. The energy needs and the battery ranges are just single values where no distribution has to be considered. These values are discussed in the next paragraph.

13.4.1 The average values

This section shows figures of the average values of the user dependent performance parameters of all pedelecs of table 13.1.
Three things will be considered:

- The mutual differences between the different pedelecs
- The deviation of the user dependent parameters from their user independent equivalent
- The variation of the user dependent parameters with the driving behaviour

The drive cycle efficiency

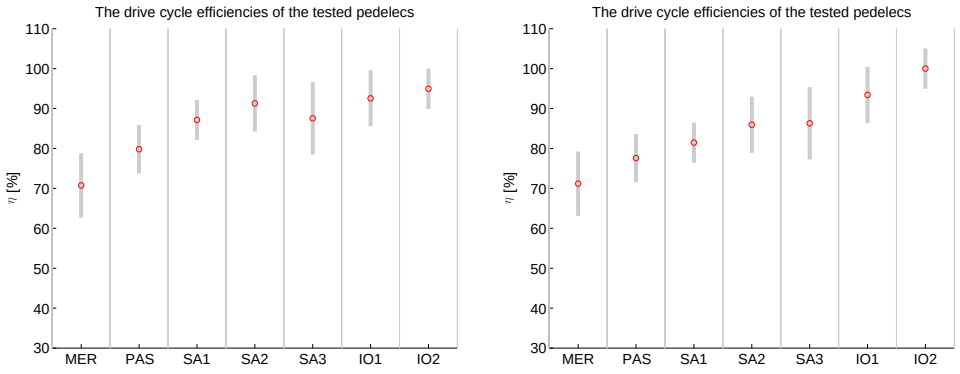

(a) The ‘IDcycle’ efficiency (b) The ‘CommuterCycle’ efficiency

Figure 13.4: The average values and the RMSE errorbars for 2 different drive cycle efficiencies of the pedelecs from table 13.1.

The drive cycle efficiencies of the pedelecs from table 13.1 for both drive cycles are represented in figure 13.4. The central spots represent the average values of the drive cycle efficiencies. The grey bars are $\pm 1\sigma$ errorbars.
The average values does not differ too much from the $100W$ efficiencies that are given in figure 13.2a. This corresponds with the idea that the mechanical efficiency

is rather constant over the operation area. Although the global mechanical efficiency average over all pedelecs still changes from

- 89% for the $100W$ efficiency over
- 86% for the 'IDcycle' efficiency to
- 83% for the 'CommuterCycle' efficiency.

Mainly the first two gears of the Sachs ($SA1$ and $SA2$) differ significantly between figures 13.2a, 13.4a and 13.4b.

The drive cycle assistance factor

Much more variation is noticed when the drive cycle assistance factors are considered. The drive cycle assistance factors of the pedelecs from table 13.1 for both drive cycles are represented in figure 13.5 with their average values and $\pm 1\sigma$ errorbars. If more spots are drawn for one pedelec, the left most represents the smallest assistance level, the right most the highest assistance level.

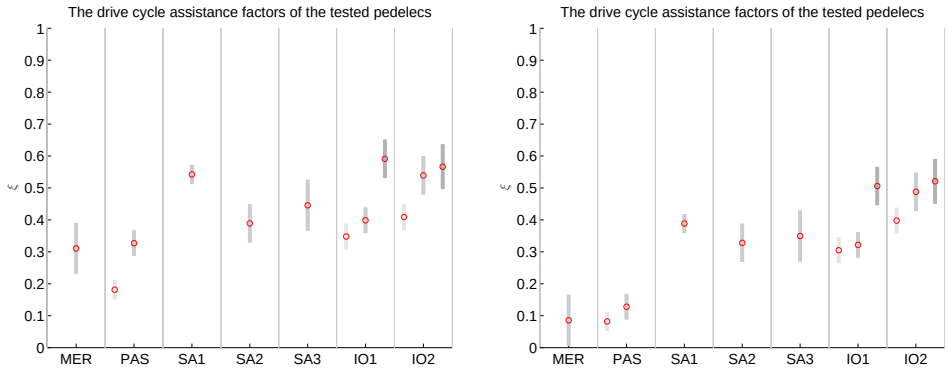

(a) The 'IDcycle' assistance factor (b) The 'CommuterCycle' assistance factor

Figure 13.5: The average values and the RMSE errorbars for 2 different drive cycle assistance factors of the pedelecs from table 13.1.

The drive cycle assistance factors of the different pedelecs are ranging from 0.1 to 0.6.
The global assistance factor average over all pedelecs changes from

- 0.41 for the $75W$ assistance factor over
- 0.40 for the 'IDcycle' assistance factor to
- 0.30 for the 'CommuterCycle' assistance factor.

The reason for the big difference between the 2 drive cycle assistance factors is explained by the higher speeds of the 'CommuterCycle'. The Merida and the Yamaha PAS are hardly assisting above 15 km/h.
The 3 power modes of the Sparta Ion 1 are well distinguished for the (user independent) $75W$ assistance factor, but there is hardly some difference left between the economical and the normal assistance mode for the 'CommuterCycle'.
The Sachs in its 1^{st} gear has an assistance factor over 50% in figure 13.5a and seems to fit perfectly for the hilly 'IDcycle'.
These facts clearly show that for the same pedelec one user could experience a comfortable motor assistance, while another user would legitimately judge that the assistance is too low.

The human and motor energy needs

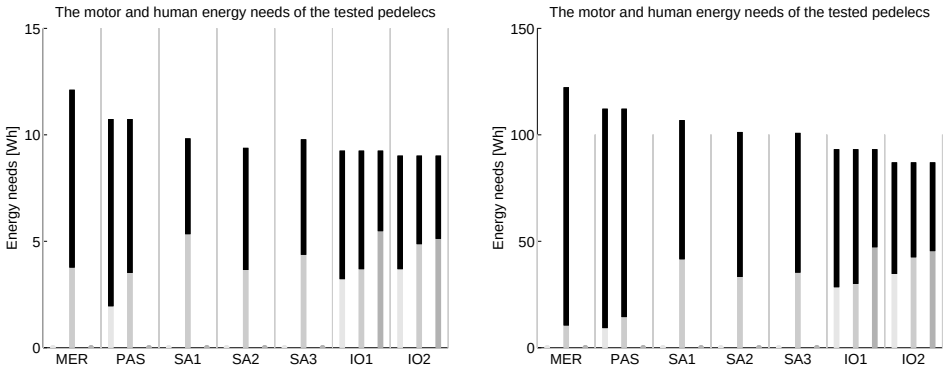

(a) to cover the 'IDcycle' (b) to cover the 'CommuterCycle' assistance

Figure 13.6: The human (black) and motor energy (greyscales) needs to cover 2 different drive cycles with the pedelecs from table 13.1 in the available assistance modes

The same conclusions as above can be drawn if one looks at the absolute amounts of human and motor energy that are required to cover the drive cycles. The black parts of figure 13.6 represent the human energy needs, the grey parts the motor energy. If more bars are drawn for one pedelec, the left most represents the smallest assistance level, the right most the highest level.

The battery range

Because the motor and human energy needs are depending on the total cycle time, the battery range as defined in chapter 10 might be a better instrument to compare the energy consumption during cycling.

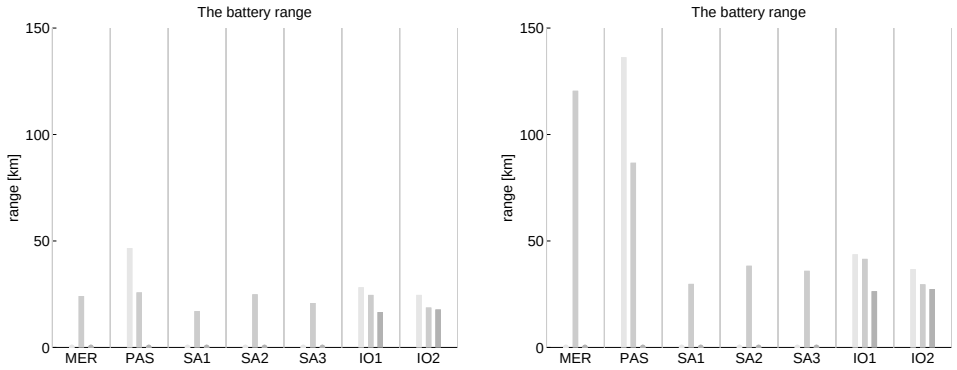

(a) The 'IDcycle' battery range

(b) The 'CommuterCycle' battery range

Figure 13.7: The battery range for 2 different drive cycles for the pedelecs from table 13.1.

The battery ranges are derived from static measurements and does not include the start currents of the motor. For the figure 13.7 a $24V$, $7Ah$ battery with a DOD of 80% is used, the motor efficiency is accepted to be 60%. The intention of this static battery range is to offer a single comprehensible quantity to compare different pedelecs, rather than trying to model the real battery range.

The values for the Merida and the YamahaPAS exceed the $100km$ for the 'CommuterCycle', because the motor is hardly assisting for the higher speeds in this drive cycle. The variation with driving behaviour is extremely clear for the Yamaha PAS and the Merida. Remark also that no gear changing is considered in these experiments.

13.4.2 The distributions

The drive cycle efficiency and the drive cycle assistance factor are time varying quantities because the cyclist moves the pedelec to different points in the operation area during cycling. This is already shown in figure 10.6. The distribution of these user dependent parameters are represented in boxplots in figure 13.8.
The distance between the quartiles is larger for the user dependent performance parameters of figure 13.8 than for the user independent performance parameters of figure 13.3. Also more outliers appear:
The fixed human power inputs used to calculate the user independent parameters are situated in the middle of the operation area where a lot of data points were taken. The positions in the operation area during the drive cycle are much more spread (figure 10.6) and may lead to the inclusion of more numerically unstable small power quotient. This is also the reason why some of the boxplots are not completely representable in the expected range.

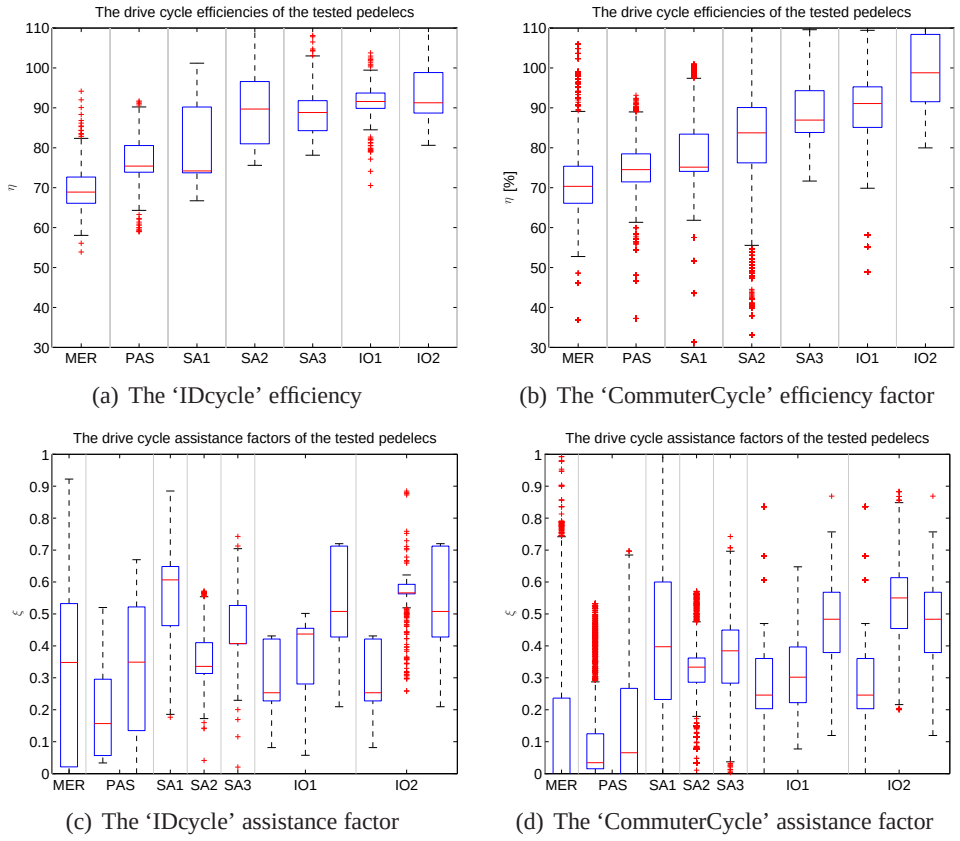

(a) The 'IDcycle' efficiency

(b) The 'CommuterCycle' efficiency factor

(c) The 'IDcycle' assistance factor

(d) The 'CommuterCycle' assistance factor

Figure 13.8: The boxplots of the distributions of the drive cycle efficiencies and the drive cycle assistance factors for different drive cycles for the pedelecs from table 13.1

For the 'IDcycle' assistance factor, the distributions are less symmetrical which might be due to the presence of slopes and thus higher torques in this drive cycle.

13.5 Conclusions of the performance analysis

In this chapter the first pedelec test results of the testbench are presented. These first measurements came along with the developing process of the test method. After each of these measurements the measurement method was slightly changed and optimized. This optimizing process is now finished and from now on, the systematic testing of pedelecs can be started. However, these first test results already show that:

- The pedelec performance analysis (based on the testbench measurements and charted by means of the performance plots and performance parameters) is able to uncover the differences in control strategy of the different manufacturers.

- Some pedelecs have really bad mechanical efficiencies, and are in that way hard to ride without assistance.
- Sometimes the observed differences are inherent to the implemented control strategy, sometimes the interaction of the pedelec/cyclist/road system caused extra differences.
- The user-independent 75W assistance factors are for all measured pedelecs lying between 43% and 52%. But the user-dependent drive cycle assistance factors have a much wider range (10% - 60%). So different ways of use may result in very different experienced driving comforts.
- The introduction of the user dependent performance parameters is interesting to see the influence of the cycling behaviour on the motor assistance. The cycling behaviour extremely influences the battery range and is certainly a manipulative argument for manufacturers to convince the potential client.
- A well-planned spreading of the measurements in the operation area is required to obtain a substantial decrease in the RMSE values.

Part III

Conclusions and suggestions for future research

14

Conclusions of the performance analysis

This work intended the performance analysis of PEDal ELectric Cycles approached from two different points of view. The first approach to the performance analysis was a subjective one: *How does the cycling community appreciate bicycles with an electric assistance motor?* The second approach was an objective one. *How to quantify the performance of a pedelec in a technical way?*

Many answers on the first question were found in part I of this book. The information was gathered by a poll of test persons that lended a pedelec for a limited period and an inquiry of the bicycle dealer shops.
After the tests, one can say that pedelecs are well appreciated by the users as well as the dealers. However, the mainly positive feedback was somehow shaded by a lot of remarks:
Users as well as dealers would like to see

- lighter pedelecs
- a higher battery autonomy
- cheaper pedelecs
- more robust pedelecs
- and pedelecs with a nicer design

There also seemed to be an image problem: while younger people pointed at the elder people as typical pedelec users, the elder people often still found the physical effort on a pedelec too heavy.
Another drawback of the pedelec was not found in the technology itself, but in the lack of cycling infrastructure along the road. With a good infrastructure the test

persons were able to realize substantial time gains while using the pedelec for commuting.
The politicians should give priority to the development of cycling infrastructure in cities like Brussels. So much the more, because the pedelec was experienced as suitable for commuting as well as shopping and leisure.
The market analysis also brought to light that a lot of brands are available at the dealershops, but there is certainly place for more native products. Although 10.000 pedelecs were sold in Flanders in 2005, few dealers are actively promoting the pedelec. There is still some work to be left for the manufacturers to remove the bad experiences of the dealers with the first generation pedelecs and convince the dealers of todays pedelec product quality.

In part II of this book, a technical method is developed to analyse the performance of a pedelec. Performance plots and performance parameters are defined and calculated based on a limited number of testbench measurements. With these parameters a ranking of performances is possible. Six pedelecs were already put on the testbench to show the possibilities of the developed performance analysis tool:

- A ranking of the measured pedelecs is possible based on different aspects (=performance parameters)

- The objective performance analysis is able to uncover the differences in control strategy of the different manufacturers.

- The complaints about the weight and bad mechanical construction of the test persons can be affirmed by the low measured mechanical efficiency of some pedelecs.

- The user-independent 75W assistance factors are for all measured pedelecs lying between 43% and 52%. But the user-dependent drive cycle assistance factors have a much wider range (10% - 60%). So different ways of use may result in very different experienced driving comforts. This partly declares why the answers of the test persons were sometimes very contradictory.

- The introduction of the user dependent performance parameters clearly quantifies the influence of the cycling behaviour on the motor assistance and battery autonomy. As long as there is no standard drive cycle, the battery autonomy stays a manipulative argument for manufacturers to convince the potential client. The unrealistic high battery autonomies in the manufacturer's data sheet unfortunately contributes to the bad image of the pedelec that are mentioned by some dealers.

- Now that the optimizing process of the measurement method is finished, the systematic testing of pedelecs can be started.

Linking the objective and subjective approaches of the performance analysis is not always easy and was not the major intention of this work. The inquiries of the subjective approach in this work focussed on the global appreciation of pedelecs by the cycling community. The subjective approach contains a broad spectrum of judgement criteria. Next to a good assistance level and great battery autonomy, the users also like to have a comfortable seat, a good-looking pedelec, a cheap pedelec, a practical pedelec,... The objective analysis, on the other hand, is focussed on the modelling of the motor and pedelec behaviour during cycling.
It would only be possible to link the testbench measurements of a single pedelec to the comments given by the users of that pedelec if a substantial number of test persons should comment the same pedelecs in a very structured way. Subjective differentiation between pedelecs would require a different experimental design, and would be very time consuming. Fortunately, some consumer organisations recently started this kind of research and published the first results [62],[63].

15
Suggestions for Future Research

The appreciation of pedelecs by their users is investigated in chapter 2 on the basis of a lending service that ran from 2000 until 2003. The pedelec and battery technology has evolved a lot in the last years. The organisation of a new lending service with newer pedelec types could be interesting to see which inconveniences that are already solved and which annoyances still exist.
The Flemish pedelec dealers poll of chapter 3 dates from 2005. Entering a bigger dealer shop today without noticing the presence of an electric two-wheeler gets rare. In may 2007, a publicity flyer for pedelecs was distributed in the letterboxes of the houses in Ghent city by a local bicycle dealer shop. These facts show that new efforts have been made by the manufacturers as well as the dealers to promote the pedelec. The collection of new sales figures would be interesting to follow the evolution of the pedelec's prices and popularity.

The objective performance analysis of pedelecs in part II of this book focusses on the amount of traction power that is added by the motor in the operation area. This is certainly not the only item that determines whether the users like or dislike their pedelec. The subjective analysis already mentions a lot of other important aspects (price, driving comfort,...) that also could be involved in the performance analysis.
For the existing performance analysis a number of improvements are suggested below:

- A well-balanced spreading of the measurements in the operation area of the cyclist will raise the predictability qualities of the models.
- Further automation of the test bench measurements will reduce the characterisation time. In this way the pedelec could be entirely measured with one bat-

tery charge. The automated balancing of the pedelec on the bench is already successful for a fixed operation point, but has to be extended for the whole operation area. This could enable a single person to perform the test bench measurements instead of the two persons that are required today.

- The performance analysis is based on steady state measurements. If one wants to measure the real drive cycle behaviour, the simultaneous measurement of speed and torque is required as is expressed by equation 6.8.

- The feedback of the speed and torque signals to the control system of the test bench would enable the imposition of a real drive cycle on the pedelec. Therefore an adaptation of the data acquisition is required. In this way the real drive cycle battery range could be measured. Another advantage of the feedback is the possibility to calculate the traction forces $F_{t_{ZA}}$ and $F_{t_{MA}}$ at exactly the same speed and cyclist torque. This would increase the accuracy of the assistance factor model.

- Another extension of the data acquisition could be the logging of the battery and motor power. So, the efficiency of the power transmissions and the power losses could be described more precisely.

- The development of a standard drive cycle for pedelecs requires the systematic logging of the cycling behaviour of different user groups. This can be done with the test equipment of chapter 11 and the analysis tools of the GUI of chapter 12.

Appendices

A

EMC measurements on the Yamaha Easy

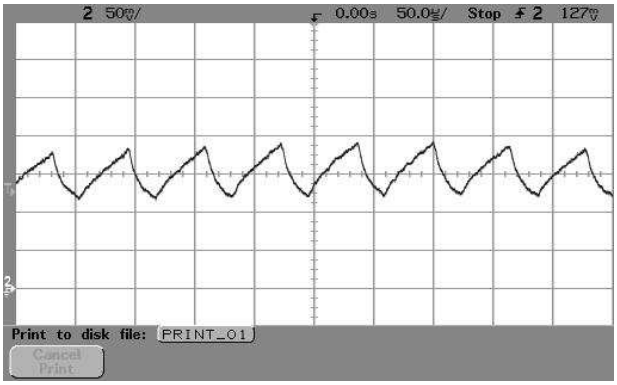

Figure A.1: Motor current of the Yamaha Easy when easily pedalling in the 3° gear delivering a small torque

During the lending service of section 2 a complaint is received about an EMC conflict between the Yamaha Easy pedelec and the Brussels Police communication infrastructure. In the EMC laboratory of KaHo Sint-Lieven Ghent the EMC radiation of the Yamaha drive system is measured with an EMC probe with frequency band from 0-30Mhz. Therefore one person is riding the pedelec on a roller system, while another one handles the probe. The pedelec radiation is situated in the frequency band of 0-5Mhz. No considerable radiation is found in the 150-175 Mhz frequency band that is used by the local police services.
A closer view on the applied frequencies is obtained by using a DC probe (bandwidth

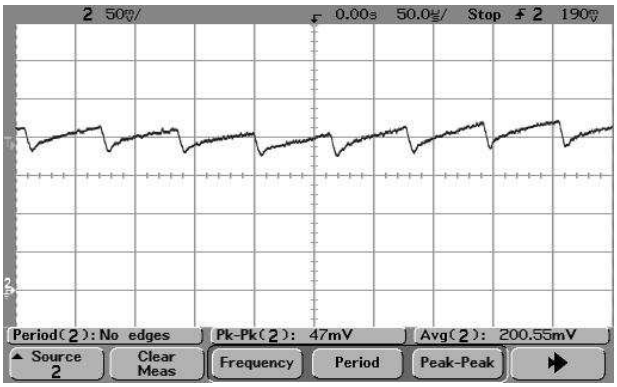

Figure A.2: Motor current of the Yamaha Easy when easily pedalling in the 3° *gear delivering a higher torque*

100kHz, resolution 100mV/A) on one of the supply cables from the battery.
The switching frequency of the DC-DC convertor appears to be 15,7 kHz in the 4° gear. The signal captured by the probe is visualized on an oscilloscope. Figure A.1 is the current signal when the cyclist is easily pedalling in the 3° gear. The average value is 1,27A and the estimated frequency 16,4 kHz. The current of figure A.2 is recorded at the same pedalling frequency and in the same gear, but with a higher cyclist torque. Here an average current of 2,0A is measured and a switching frequency of 15,4kHz. These measurements lead to the conclusion that an interference between the pedelec and the communication system is highly improbable. And more general, it learnt that EMC problems are not a big issue for pedelecs.

B

The Standard Questionnaire of the Pedelec Lending Service

Personal data

Sex M ☐ F ☐ Date of birth_____
Height _____ Weight _____
Optional
First name _____ Name _____
Address _____ Postcode/City _____
Phone _____ E-mail _____

Appreciation of the pedelec

A.0 Used Pedelec:_____
Begin Date_____
Duration of the Test Period:_____

A.1 Did the pedelec replace another means of transportation during the test period? Y ☐ N ☐
If yes, cross the first column boxes with the means and the other column boxes with the displacement reasons.

☐ Public transport:	☐ Commuting	☐ Shopping	☐ Leisure	☐ Other_____
☐ Car:	☐ Commuting	☐ Shopping	☐ Leisure	☐ Other_____
☐ Motorcycle:	☐ Commuting	☐ Shopping	☐ Leisure	☐ Other_____
☐ Bicycle:	☐ Commuting	☐ Shopping	☐ Leisure	☐ Other_____
☐ Walking:	☐ Commuting	☐ Shopping	☐ Leisure	☐ Other_____
☐ Other:	☐ Commuting	☐ Shopping	☐ Leisure	☐ Other_____

A.2 Did you realize a time gain by using the pedelec for commuting?

Y ☐ N ☐

If yes, what was this average time gain?_____

A.3 Did you make new trips that you would not have made without the availability of a pedelec?

Y ☐ N ☐

A.4 How did you appreciate the pedelec? *	5	4	3	2	1
The user-friendlyness of the assistance					
The weight of the pedelec					
The ease of charging					
Assistance on slopes					
The battery range					
The weight of the pedelec					
The quality/reliability					

* 5=totally satisfactory, 1=totally unsatisfactory

A.5 Did you use your conventional bicycle more often after the test?

Y ☐ N ☐

A.6 Did you experience a lack of cycling infrastructure like

cycle tracks? Y ☐ N ☐

bicycle sheds? Y ☐ N ☐

A.7 Who is, according to you, the most typical pedelec user?

_____

A.8 Are you prepared to buy a pedelec?

Y ☐ N ☐

A.9 Did you already buy a pedelec?

Y ☐ N ☐

A.10 Do you think that €1000 is a fair price for a pedelec?

Y ☐ N ☐

Remarks:_____
_____
_____
_____
_____

C

Contourplots of the Tested Pedelecs

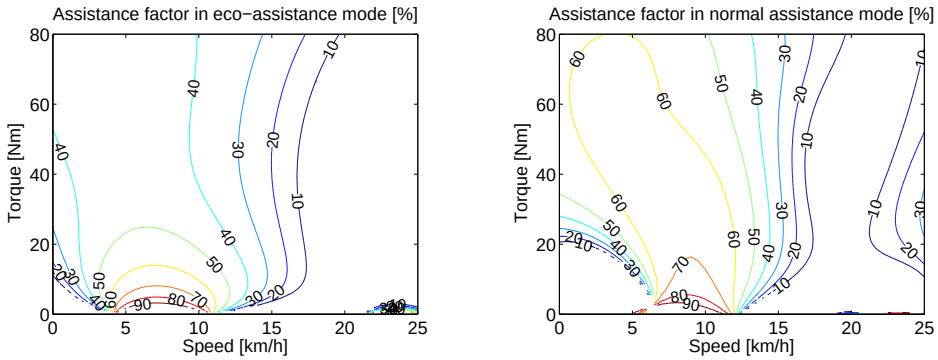

(a) YamahaPAS MAe

(b) YamahaPAS MAn

Figure C.1: Contourplots of the assistance factors for the Yamaha PAS

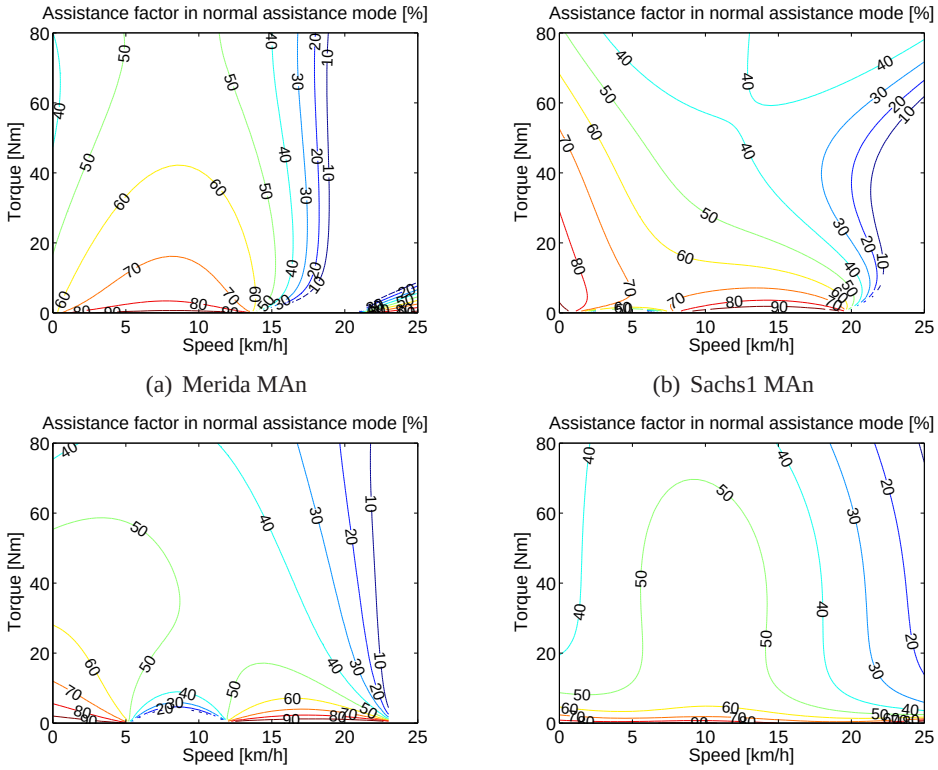

(a) Merida MAn

(b) Sachs1 MAn

(c) Sachs2 MAn

(d) Sachs3 MAn

Figure C.2: Contourplots of the assistance factors for the Merida, and the Sachs Elo-bike in its 3 gears

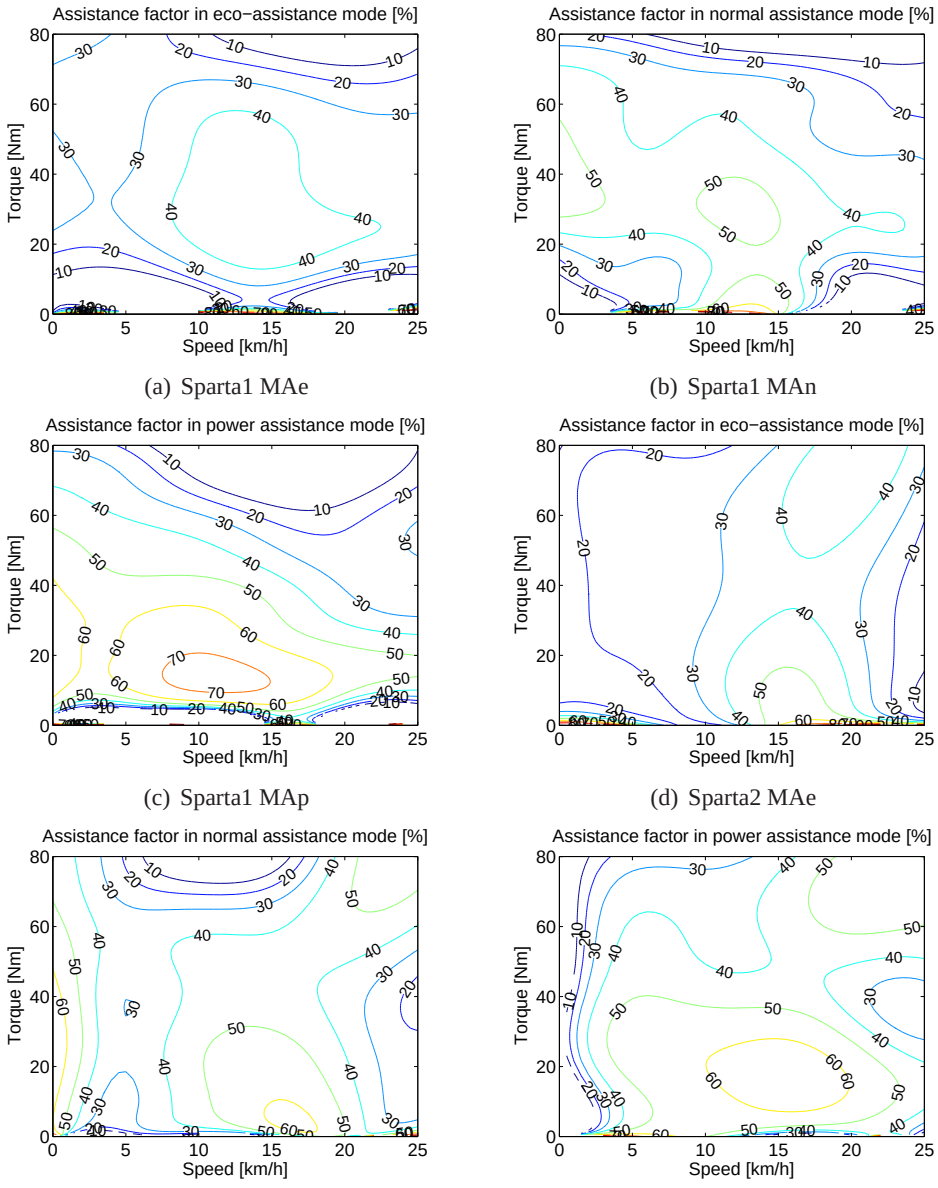

(a) Sparta1 MAe

(b) Sparta1 MAn

(c) Sparta1 MAp

(d) Sparta2 MAe

(e) Sparta2 MAn

(f) Sparta2 MAp

Figure C.3: Contourplots of the assistance factors for the 2 Sparta ION pedelecs

References

[1] Directorate-General of the European Commission for Energy and Transport. *Consumers in Europe - Facts and figures*. Office for Official Publications of the European Communities, ISBN 92-894-1400-6, 1° edition, 2001. [$Cited$ $08/01/2008$], Available at `http://epp.eurostat.ec.europa.eu/cache/ITY_OFFPUB/KS-39-01-134/EN/KS-39-01-134-EN.PDF`.

[2] Hans Strelow. *Passenger transport in the European Union*. Eurostat, Statistics in focus, 2006. [$Cited$ $08/01/2008$], Available at `http://epp.eurostat.ec.europa.eu/cache/ITY_OFFPUB/KS-NZ-06-009/EN/KS-NZ-06-009-EN.PDF`.

[3] Luc Cappelle. *Autorijden, daar heb ik geen tijd voor...* bvba Verraes, Ostenstraat 32, 8930 Menen, 1990.

[4] Douglas Self. *The museum of retrotechnology*. [$Cited$ $08/01/2008$], Available at `http://www.dself.dsl.pipex.com/MUSEUM/TRANSPORT/steambike/steambike.htm`, 1998.

[5] G. Donald Adams. *Collecting and restoring antique bicycles*. Pedaling History, Burgwardt Bicycle Museum, ISBN 0-9649537-1-4, 2° edition, 1996.

[6] Hannes Neupert. *Das Powerbike*. Delius Klasing, ISBN 3895951234, moby dick edition, 1997.

[7] John van de Kerkhof. *De nederlandse solex website*. [$Cited$ $08/01/2008$], Available at `http://www.solex.nl`.

[8] Ad Sekeris. *Spartamet: onderdelenMETshop*. [$Cited$ $08/01/2008$], Available at `http://www.spartamet.org`, 2006.

[9] Alan A. Parker. *The electric powered assisted bicycle; a clean vehicle to reduce oil dependence and enhance the mobility of the elderly*. The New Zealand Society for Sustainability Engineering and Science, 2004. [$Cited$ $08/01/2008$], Available at `http://www.nzsses.auckland.ac.nz/conference/2004/Session5`.

[10] Tim Blumenthal. *Annual Report 2005*. Bikes Belong Coalition, 2005. [$Cited$ $08/01/2008$], Available at `http://www.bikesbelong.org/files/BB_Annual_Report_2005.pdf`.

[11] Patrick D'haese. *Stijgende Fietsverkoop*. $[Cited\ 08/01/2008]$, Available at `http://www.fietsersbond.be/Index.asp?pageurl=/Archief/StijgendeFietsverkoopAug2003.asp`, 2003.

[12] Cyril Rosman. *Elektrische fiets ook voor jonkies van 40*. $[Cited\ 30/06/2007]$, Available at `http://www.bndestem.nl/economie/article181856.ece`, 2006. BN DeStem.

[13] Ed Benjamin. *Handbook on the light electric vehicle business*. CycleElectric International Consulting Group, 2005. $[Cited\ 08/01/2008]$, Available at `http://www.cycleelectric.com/en/downloads.php`.

[14] Steve Christini. *All wheel drive mountainbikes*. $[Cited\ 08/01/2008]$, Available at `http://www.christini.com`, 1990.

[15] Ed Benjamin. *Light Electric Vehicle propulsion*. CycleElectric International Consulting Group, 2005. $[Cited\ 08/01/2008]$, Available at `http://www.cycleelectric.com/en/downloads.php`.

[16] EU council. *Council Directive 92/61/EEC of 30 June 1992 relating to the type-approval of two or three-wheel motor vehicles*. EU Enterprise and Industry, 1992.

[17] Peter Van den Bossche. *The electric vehicle: raising the standards*. Phd thesis, Faculty of Applied Sciences , *Vrije Universiteit Brussel*, 2003.

[18] H.R. 727 EH. *Low-speed electric bicycles Safety Act*. The Senate and House of Representatives of the United States of America, 2001. $[Cited\ 08/01/2008]$, Available at `http://www.cycleelectric.com/rsc/Chinese727.pdf`.

[19] Cock P. Rose G. *Encouraging E-bike use: the need for regulatory reform in Australia*. Working Paper ITS-WP-03-19, Institute of Transport Studies, 2003.

[20] European Communities. *The community's range of tools*. $[Cited\ 30/06/2007]$, Available at `http://europa.eu`, 1995.

[21] Ton Vermie. *E-tour Final Report*. Public Works, Environmental Policy Department, Rotterdam, Netherlands, 2003. $[Cited\ 16/03/2008]$, Available at `http://etecmc10.vub.ac.be/publications/etourfinal.pdf`.

[22] EU council. *Directive 2002/24/EC of the European Parliament and of the Council of 18 March 2002 relating to the type-approval of two or three-wheel motor vehicles and repealing Council Directive 92/61/EEC*. EU Enterprise and Industry, 2002.

[23] Annick Roetynck. *E-bike and Pedelec Legislation in the European Union*. Pedelec and E-Bike 2001 Global Congress, Taipeh, Taiwan, 2001.

[24] ExtraEnergy. *First Fast Pedelec Legal in the EU*. $[Cited\ 08/01/2008]$, Available at `http://www.extraenergy.org`, 2004.

[25] Technical Committee CEN/TC 333. *prEN 15194, Cycles - Electrically power assisted cycles - EPAC bicycle*. $[Cited\ 08/01/2008]$, Available at `http://cyclurba.fr/velo/image/Projet%20de%20Norme%20VAE.pdf`, 2005.

[26] National institute of statistics. *Fietsen of niet fietsen? Fietsgebruik in België*. Groupe de Recherche sur les Transports des Facultés Universitaires Notre-Dame de la Paix, 2002. $[Cited\ 08/01/2008]$, Available at `http://www.statbel.fgov.be/press/fl031_nl.asp`.

[27] IBSR Miguel Vertriest. *Réalisation des pistes cyclables marquées*. Vademecum vélo en Région de Bruxelles-Capitale, 2007. $[Cited\ 08/01/2008]$, Available at `http://www.velo.irisnet.be/download/vademecum_marquages.pdf`.

[28] Statbel. *Mobiliteit in de Europese Unie : Koning Auto regeert*. 2002.

[29] Fietsersbond VZW. *Enquête fietsfonds - kwaliteit fietsen*. 2002. $[Cited\ 08/01/2008]$, Available at `http://www.fietsersbond.be`.

[30] Ed Benjamin. *Market Size for Two Wheelers*. CycleElectric International Consulting Group, 2002. $[Cited\ 08/01/2008]$, Available at `http://www.cycleelectric.com/en/downloads.php`.

[31] Fietsersbond VZW. *Fietsenhandelaars in Vlaanderen en Brussel*. $[Cited\ 08/01/2008]$, Available at `http://www.fietsersbond.be/Index.asp?pageurl=./Adressen/FietsHandelSelect.asp`.

[32] GfK Panel Services Benelux. *Verkoopcijfers elektrische fietsen in Nederland*. Fietsenmonitor 2005, 2005.

[33] Philippe Lataire. *Electrically assisted bicycles: demonstration, characterisation, healthbenefit*. Revue E-tijdschrift, 119^e jaargang(99):p32–39, 3/2003.

[34] Bas De Geus. *Cycling to work, Psychosocial and environmental factors associated with cycling and the effect of cycling on fitness and health indexes in an untrained working population*. PhD, Vrije Universiteit Brussel, Faculty of Physical Education and Physiotherapy, pages p45–p61, 2007.

[35] W.G. Cochran. *Sampling techniques*. New York, Wiley, (3), 1977.

[36] Bas d'Herripon. *De IDbike test cyclus*. $[Cited\ 08/01/2008]$, Available at `http://www.IDbike.com/test.htm`, 1999.

[37] Nico Smets and Dimitri Goehals. *Testbank voor elektrische fietsen*. Master thesis, pages 225–233, 2000. *ETEC, Vrije Universiteit Brussel*.

[38] Jean-Marc Timmermans. *Testbank voor elektrische fietsen*. Master thesis, 2003. *ETEC, Vrije Universiteit Brussel*.

[39] Claude Genzling. *Le vrai recordman de l'heure, c'est Bracke !* le Cycle, (99), 1984.

[40] David Gordon Wilson. *Bicycling Science*. Massachussets Institute of Technology, ISBN 0-262-73154-1, 3° edition, 2004.

[41] N.R. Draper and H. Smith. *Applied regression analysis*. New York: Wiley, ISBN 0-471-17082-8, 3° edition, 1998.

[42] Wolfgang Hardle. *Applied Nonparametric Regression*. Cambridge University Press, ISBN 0-521-42950-1, 1990.

[43] Jos De Brabanter. *LS-SVM regression modelling and its applications*. Phd thesis, ESAT/SISTA, *Katholieke universiteit leuven*, 2004.

[44] G. Campa, Davini Massimo, and M. Innocenti. *MvTools: Multivariable System Toolbox*. IEEE International Symposium on Computer Aided Control System Design, Anchorage, AK, USA, (9), 2000.

[45] T. Hastie, R. Tibshirani, and J. H. Friedman. *The Elements of Statistical Learning*. Springer, ISBN 0387952845, 1° edition, 2003.

[46] J.A.K. Suykens, T. Van Gestel, J. De Brabanter, B. De Moor, and J. Vandewalle. *Least Squares Support Vector Machines*. World Scientific, Singapore, ISBN 981-238-151-1, 2002.

[47] J. Mercer. *Functions of positive and negative type and their connection with the theory of integral equations*. Philos. Trans. Roy. Soc., London 1909.

[48] James B. Spicer. *Effects of Frictional Losses on Bicycle Chain Drive Efficiency*. Journal of Mechanical Design, 123(4):p598–605, 2001.

[49] L.J.F. Hermans. *Voortbewegen op eigen kracht*. kennislink, 2003. $[Cited\ 08/01/2008]$, Available at `http://www.kennislink.nl/web/show?id=105669`.

[50] P-J. Laurent, P. Sablonniere, and L. L. Schumaker. *Curve and Surface Design*. Vanderbilt University Press, Saint-Malo, 1999.

[51] Annette Muetze and Ying Chin Tan. *Modeling and Analysis of the Technical Performance of DC-Motor Electric Bicycle Drives Based on Bicycle Road Test Data*. IEEE International IEMDC apos, 2:p1574–1581, 2007. Electric Machines & Drives Conference.

[52] Rainer Pivit. *Measuring Aerodynamic Drag*. Radfahren, (2):p47–49, 1990.

[53] V. S. Ramsden. *Design of an in-wheel motor for a solar-powered electric vehicle*. 8th International Conference on Electrical Machines and Drives, IEEE, Cambridge 1997.

[54] *Motor info*. $[Cited\ 08/01/2008]$, Available at `http://www.users.bigpond.com/solarbbq/cheapdiybike.htm`.

[55] Klaus Gössel, Helmut Grüneberg, and Manfred Glöckner. *Contribution to Future Oriented Electric Drive Technology for Light Vehicles e.g. Bikes, Trikes, Wheel Chairs*. 18th International Battery, Hybrid and Fuel Cell Electric Vehicle Symposium and Exhibition, Berlin, october 2001.

[56] *Electric Vehicle Modelling*. $[Cited\ 08/01/2008]$, Available at `http://www.mechanicalengineering.cc/mechanical-engineering-archives/194-Electric-Vehicle-Modelling.html`.

[57] Rudolf Rijkeboer, Dion Bremmers, Zissis Samaras, and Leonidas Ntziachristos. *Particulate matter regulation for two-stroke two-wheelers: Necessity or haphazard legislation*. 2th International Symposium, Transport and Air Pollution, 39(13):2483–2490, 2005.

[58] *ECE-15 drive cycle*. $[Cited\ 08/01/2008]$, Available at `http://www.dieselnet.com/standards/cycles/ece_eudc.html`.

[59] Joeri Van Mierlo. *Simulation software for comparison and design of electric, hybrid and internal combustion vehicles with respect to energy, emissions and performances*. Phd thesis, Faculty of Applied Sciences , *Vrije Universiteit Brussel*, 2000.

[60] K. Jonasson, M. Alakla, and Rolf Egnell. *Comparative Study of Petrol- and Diesel Hybrid Topologies vs Directly Diesel Driven Vehicle*. EVS-20, November 2003. Long Beach, California.

[61] John Lafford. *Rolling resistance test results*. $[Cited\ 08/01/2008]$, Available at `http://www.users.globalnet.co.uk/~hadland/lafford.htm`.

[62] Hedwig Berendsen. *Elektrisch scoort goed*. Tweewieler, pages p26–30, april 2007.

[63] Extra Energy. *Testreport 2006*. 2006. $[Cited\ 16/03/2008]$, Available at `http://www.ExtraEnergy.com`.

List of Publications

[1] Ph. Lataire, J.-M. Timmermans, G. Maggetto, P. Van den Bossche, and J. Cappelle. *Electrically assisted bicycles*, volume 8-1. International Journal of Assistive Robotics and Mechatronics, January 2007. p3-9.

[2] J. Cappelle, Ph. Lataire, G. Maggetto, R. Meeusen, and F. Kempenaers. *Characterisation of Electric Bicycles Performances*. The 19^{th} International Battery, Hybrid and Fuel Cell Electric Vehicle Symposium, October 2002. Busan, Korea.

[3] Ph. Lataire, J.-M. Timmermans, J. Cappelle, and G. Maggetto. *Electrically assisted bicycles: demonstration, characterisation, healthbenefit*, volume 119^{e} jaargang. 3/2003.

[4] J. Cappelle, Ph. Lataire, G. Maggetto, and P. Van den Bossche. *Electrically Assisted Cycling around the World*. The 20^{th} International Battery, Hybrid and Fuel Cell Electric Vehicle Symposium, November 2003. Long Beach, California.

[5] J.-M. Timmermans, J. Cappelle, and Ph. Lataire. *De elektrische fiets als duurzame mobiliteit in steden*. Lloyd, intermodaal transport en verkeer, december 2003. p4.

[6] J. Cappelle, Ph. Lataire, and J.-M. Timmermans. *Personalized testing method for E-PACs*. The 21^{th} International Battery, Hybrid and Fuel Cell Electric Vehicle Symposium and Exhibition, april 2005. Monaco.

[7] J. Cappelle, J.-M. Timmermans, Ph. Lataire, J. Van Mierlo, and G. Maggetto. *The pedelec market in Flanders: The position of the bicycle dealers*. The 22^{th} International Battery, Hybrid and Fuel Cell Electric Vehicle Symposium and Exhibition, October 2006. Yokohama, Japan.

[8] J.-M. Timmermans, J. Mattheys, J. Cappelle, Ph. Lataire, J. Van Mierlo, G. Maggetto, and P. Van den Bossche. *New electric postman helper: from user requirements to technical design parameters*. The 22^{th} International Battery, Hybrid and Fuel Cell Electric Vehicle Symposium, October 2006. Yokohama, Japan.

[9] J. Cappelle, J.-M. Timmermans, Ph. Lataire, J. Van Mierlo, and G. Maggetto. *The pedelec market in Flanders*. 2^{nd} European Ele-Drive Transportation Conference, May 2007. Brussels, Belgium.

[10] Ph. Lataire, J.-M. Timmermans, G. Maggetto, J. Cappelle, and P. Van den Bossche. *Electrically assisted bicycles*. Proceedings of the 3^{rd} COE Workshop on Human Adaptive Mechatronics (HAM), March 2006.